Renal macrophages promote Shiga toxin-induced Hemolytic Uremic Syndrome through TNFα and CXCR2-dependent neutrophil recruitment

Inaugural-Dissertation zur Erlangung des Doktorgrades

Dr. rer. nat.

der Fakultät für Biologie
an der

Universität Duisburg-Essen

Vorgelegt von

Julia Klara Katharina Lill
geborene Volke
aus Essen

Februar 2021

Die der vorliegenden Arbeit zugrunde liegenden Experimente wurden am Institut für Experimentelle Immunologie und Bildgebung in der Arbeitsgruppe Immundynamik der Universität Duisburg-Essen durchgeführt.

1. Gutachter: * Prof. Dr. rer. nat. Daniel R. Engel
2. Gutachter: * Prof. Dr. rer. nat. Sven Brandau
3. Gutachter: * Prof. Dr. med. Thomas Miethke

Vorsitzender des Prüfungsausschusses: * Prof. Dr. rer. nat. Wiebke Hansen

Tag der mündlichen Prüfung: # 10.5.2021

---

*, # Ist nicht vom/n Doktoranden/in auszufüllen

DOI: 10.17185/duepublico/74476
URN: urn:nbn:de:hbz:465-20220719-140441-6

Table of Content

I. List of abbreviations

°C	Degrees Celsius
µg	Microgram(s)
µl	Microliter(s)
µm	Micrometer(s)
µM	Micromolar
αCSF1R	Antibody against CSF1R
AF	Alexa Fluor®
aHUS	Atypical HUS
APC	Allophycocyanin (fluorochrome)
APC-Cy7	Allophycocyanin conjugated to Cyanine 7 dye (fluorochrome)
Approx.	Approximately
BM	Bone marrow
BSA	Bovine serum albumin
BUN	Blood urea nitrogen
BV	Brilliant™ Violet
C-kit	Tyrosine-protein kinase KIT
CD	Cluster of differentiation
CNS	Central nervous system
CSF1	Colony-stimulating factor 1
CSF1R	Colony-stimulating factor 1 receptor
CUBIC	Clear, unobstructed brain imaging cocktails
CXCL1/2	C-X-C motif chemokine 1/2
CXCR2	C-X-C chemokine receptor type 2
d	Day(s)
DAPI	4’,6-Diamidin-2-phenylindol
DC	Dendritic cell
ddH_2O	Double-deionized water
DDSA	2-Dodecenylsuccinic-acid
dH_2O	Deionized water
DMP	2,4,6-Tris-aminomethyl-phenol
DMSO	Dimethyl sulfoxide
E	Embryonic age (in days)

E. coli	*Escherichia coli*
EDTA	Ethylenediaminetetraacetic acid
EHEC	Enterohaemorrhagic *o0o9E. coli*
EMP	Erythron-myeloid progenitor
EpCAM	Epithelial cell adhesion molecule
Epon	Epoxipropyl ether of glycerol
FCS	Fetal calf serum
FMO	Fluorescence minus one
FSC	Forward scatter
g	Gram(s)
G	Gauge
GA	Glutaraldehyde
Gb_3	Globotriaosylceramide
GBM	Glomerular basement membrane
GFB	Glomerular filtration barrier
GFP	Green fluorescent protein
GFR	Glomerular filtration rate
GMOF	Geometric mean of fluorescence
GN	Glomerulonephritis
h	Hour(s)
HSC	Hematopoietic stem cell
IC_{50}	Half maximal inhibitor concentration
IFN	Interferon
IL	Interleukin
IHC	Immunohistochemistry
ip	intraperitoneal
iv	intravenous
IC_{50}	Half maximal inhibitory concentration
IL	Interleukin
IMCES	Imaging Center Essen
l	Liter(s)
LMP	Lympho-myeloid progenitor
loxP	Locus of X-over P1
LPS	Lipopolysaccharide

Ly6C /G	Lymphocyte antigen 6 complex
Lyz2	Lysozyme C-2
M	Molar
Mac-1	Macrophage-1 antigen
mg	Milligram(s)
MHC II	Major histocompatibility complex II
min	Minute(s)
ml	Milliliter(s)
mm	Millimeter(s)
mM	Millimol(s)
µmol	Micromol
MNA	Methylnadic anhydride
MP	Macrophage
MTT	3-(4,5-dimethylthiazol-2-yl)-2,5-diphenyltetrazolium bromide
n/a	Not applicable
NETs	Neutrophil extracellular traps
nm	Nanometer(s)
ON	Overnight
PBS	Phosphate-buffered saline
PBT	Phosphate-buffered saline supplemented with 0.05% Triton-X 100
PE	Phycoerythrin (fluorochrome)
PECAM-1	Platelet endothelial cell adhesion molecule
PerCP-Cy5.5	Peridinin-chlorophyll-protein complex conjugated to Cy5.5 dye (fluorochrome)
PFA	Paraformaldehyde
pg	Picogram (s)
pH	Power of hydrogen
R	Receptor
ROS	Reactive oxygen species
rpm	Revolutions per minute
RPMI	Roswell Park Memorial Institute
RT	Room temperature
s	Second(s)

SEM	Standard error of mean
SSC	Sideward scatter
sTNF	Soluble TNF
Stx	Shiga toxin
TBS	Tris-buffered saline
TEM	Transmission electron microscopy
Th1/2	T helper 1/2
TLR	Toll-like receptor
TMA	Thrombotic microangiopathy
TNFα	Tumor necrosis factor α
Tris	Tris(hydroxymethyl)aminomethane
vs.	Versus
YS	Yolk sac

II. Abstract

Enterohaemorrhagic *Escherichia coli* (EHEC) is a major cause for worldwide epidemics linked to significant organ damage and high mortality. One of the EHEC-associated diseases is hemolytic uremic syndrome (HUS); a rare but devastating disease characterized by microangiopathic hemolytic anemia, thrombocytopenia and acute kidney injury. While the main cause of HUS is due to ingestion of the Shiga toxin-producing *E. coli* (STEC), an effective therapeutic intervention is yet to be determined. Several studies have identified neutrophil recruitment to be crucial in both the promotion of STEC-HUS severity and mediation of endothelial injury. Nevertheless, the mechanisms leading to this leukocyte activation and recruitment remain elusive. Additionally, the role of macrophages in STEC-HUS is not fully understood, even though they are the predominant leukocyte population in the healthy kidney.

In our study, we elucidated the role of resident kidney macrophages in a preclinical STEC-HUS model and showed a phenotypic and functional macrophage change after disease induction, which promoted neutrophil recruitment. Macrophages produced the inflammatory cytokine tumor necrosis factor α (TNFα) and inhibition of this molecule significantly reduced kidney injury. Furthermore, direct targeting of macrophages via their depletion by the colony-stimulating factor receptor 1 (CSF1R) reduced local TNFα levels and significantly decreased disease severity. In detail, macrophage depletion did not only diminish endothelial damage and thrombocytopenia, but additionally activation of thrombocytes and neutrophils. By microscopy, we showed that recruited neutrophils mainly infiltrated the renal cortex in response to STEC-HUS. Macrophage depletion significantly reduced renal neutrophil infiltration and renal levels of neutrophil-attracting C-X-C motif chemokine 1 and 2 (CXCL1 and CXCL2). Intravital microscopy validated that inhibition of CXCR2, the receptor of CXCL1 and CXCL2, significantly attenuates cortical neutrophil recruitment. In addition, CXCR2 inhibition reduced kidney injury thereby emphasizing the role of renal neutrophil recruitment for STEC-HUS severity.

In conclusion, our study demonstrates the pathological role of macrophages in STEC-HUS upon activation and subsequent production of proinflammatory cytokines, which lead to the CXCR2-dependent recruitment of neutrophils contributing to kidney injury. In addition, this study identifies inhibition of TNFα, CXCR2 or direct targeting of macrophages via CSF1R as promising therapeutic approaches to inhibit macrophage-dependent inflammation and kidney injury.

III. Zusammenfassung

Enterohämorrhagische *E. coli* Bakterien verursachen weltweit schwere Epidemien, in denen die Betroffenen schwere Organschädigungen erleiden, die zum Tode führen können. Eine seltene, aber schwere Erkrankungen ist das Hämolytisch-Urämische Syndrom (HUS). Als typische HUS-Symptome gelten mikroangiopatische hämolytische Anämie, Thrombozytopenie und akute Nierenschäden. HUS wird hauptsächlich durch die Aufnahme von Shiga toxin-produzierenden *E. coli* (STEC) verursacht und ist aktuell nicht zu therapieren.

Es wurde bereits erforscht, dass neutrophile Granulozyten (kurz: Neutrophile) STEC-HUS begünstigen und Endothelschäden vermitteln. Dennoch ist der genaue Mechanismus, der zur Aktivierung der Neutrophilen und ihrer Rekrutierung führt nicht erforscht. Des Weiteren ist die Rolle von Makrophagen in STEC-HUS nicht vollständig geklärt, obwohl sie die häufigsten Leukozyten in der gesunden Niere sind.

In dieser Studie wurde ein präklinisches STEC-HUS Model verwendet um die Rolle der residenten Nierenmakrophagen und den Mechanismus der Neutrophilenwanderung zu erforschen. Es konnten gezeigt werden, dass diese Zellen sich nach Krankheitsinduktion funktionell und phänotypisch verändern. Makrophagen produzierten das inflammatorische Zytokin Tumor Nekrose Faktor α (TNFα), dessen Inhibition den Nierenschaden signifikant reduzierte. Ebenfalls verbesserte die direkte Depletion der Makrophagen über den Kolonie-stimulierenden Faktor 1 Rezeptor (CSF1R) den Nierenschaden und senkte die lokalen TNFα-Level. Die Makrophagen-Depletion verminderte nicht nur die Endothelschäden und die krankheitstypische Thrombozytopenie, sondern reduzierte ebenfalls die Aktivierung der Thrombozyten und Neutrophilen. Mikroskopisch konnte gezeigt werden, dass die Neutrophilen in STEC-HUS-erkrankten Mäusen hauptsächlich den Nierenkortex infiltrierten. Diese Infiltrate, wie auch die lokale CXCL1- und CXCL2-Expression, wurden durch die Depletion der Makrophagen signifikant reduziert. Außerdem konnte mittels intravitaler Mikroskopie validiert werden, dass die Inhibition von CXCR2, dem Rezeptor für CXCL1 und CXCL2, die Rekrutierung der Neutrophilen in den Nierenkortex signifikant verminderte. Zusätzlich reduzierte die pharmakologische CXCR2-Inhibition den Nierenschaden und betont somit die Rolle der rekrutierten Neutrophilen zusätzlich für die Entwicklung des STEC-HUS.

Zusammenfassend belegt diese Studie eine zentrale Rolle der Makrophagen in STEC-HUS, da ihre Aktivierung einhergehend mit einer Zytokinproduktion Neutrophile

via CXCR2 rekrutiert und so die Niere schädigt. Außerdem wurde die Inhibition von TNFα, CXCR2 sowie Makrophagen als mögliche Therapiestrategien identifiziert um die Makrophagen-vermittelte Entzündung und den einhergehenden Nierenschaden in STEC-HUS zu vermindern.

IV. Aim of the thesis

STEC-HUS is the leading cause for kidney failure in children (Salvadori and Bertoni, 2013) and numerous outbreaks have been reported in the recent decades with mortality rates ranging from 5 -9 % of reported cases, i.e. 2011 in Northern Germany (Frank et al., 2011a; Garg et al., 2003). These incidences highlight the need of an effective therapy demanding for a more comprehensive understanding of the disease mechanism. Previous studies have identified neutrophils recruited to renal glomeruli as crucial mediators for kidney injury (Fernandez et al., 2006; Gomez et al., 2013; Ramos et al., 2016), but the detailed cues leading to such neutrophil recruitment have not been elucidated completely. The aim of this study was to investigate the immunological mechanisms, with a strong focus on resident macrophages as these cells are involved in renal neutrophil recruitment in other kidney diseases. Clarifying the underlying molecular mechanisms, the overarching objective of this study was to identify novel targets for STEC-HUS therapy, finally reducing disease burden and the need for supportive care.

1. Introduction

1.1. The immune system defends the host against pathogens

All organisms are exposed to a variety of invading pathogens including bacteria, viruses, fungi and parasites on a daily base. During evolution, a complex defense system, namely the immune systems, has been developed to ensure host protection with the key ability to distinguish self- from foreign substances.

In humans, the first line of defense is composed of several mechanical defense mechanisms that hamper host invasion. The skin and mucosal membranes equipped with cilia and anti-bacterial surfactants are important physical barriers. Once the pathogen has breached this mechanical barrier, different cells, i.e. cells of the immune system, target the pathogen with effector responses to ensure host safety. Circulating immune cells, also termed leukocytes, are crucial in fighting spreading pathogens. In addition to patrol the circulation, some leukocytes extravasate into peripheral tissues to maintain tissue homeostasis. Upon extravasation, these cells can differentiate into tissue-resident cells, such as macrophages or dendritic cells.

The immune system is subdivided into the innate and the adaptive branch. Adaptive immunity, also termed specific immunity, is composed of antigen-presenting cells, like macrophages and dendritic cells (DCs) that capture and present antigens. The lymphocytes, namely B and T cells can be involved in direct pathogen neutralization or set up an immunological memory. To memorize specific pathogens and mount a more efficient immune response in subsequent encounters, lymphocytes produce antibodies and develop into memory cells. Conclusively, adaptive immunity is slow but flexible and long-lasting.

In contrast, innate immunity, termed unspecific or inborn immunity, is evolutionarily the oldest form of defense (Janeway's immunobiology, chapter 16, K.P. Murphy, C.Weaver, C. Janeway, 9th edition, 2017, Garland Science). As indicated in the name, it defends the body against a vast majority of pathogens by initiating a rapid and broad immune response. The innate immune system consists of granulocytes (collective term for eosinophils, basophils and neutrophils), monocytes/macrophages, natural killer cells, macrophages and dendritic cells. Dendritic cells and macrophages link the innate to the adaptive immunity and are therefore allocated to both immune systems.

Leukocytes, central for innate and adaptive immunity, are generated in hematopoietic tissues, namely the spleen and liver in the fetus and the red bone

marrow (BM) in adults (Taschenatlas Physiologie, Chapter 4, S. Silbernagl, A. Despopoulos, W.-R. Gay, 7. Auflage, 2007, Thieme). During hematopoiesis, not only leukocytes but also erythrocytes and thrombocytes originate from a common pluripotent progenitor, the hematopoietic stem cell (HSC) (Figure 1).

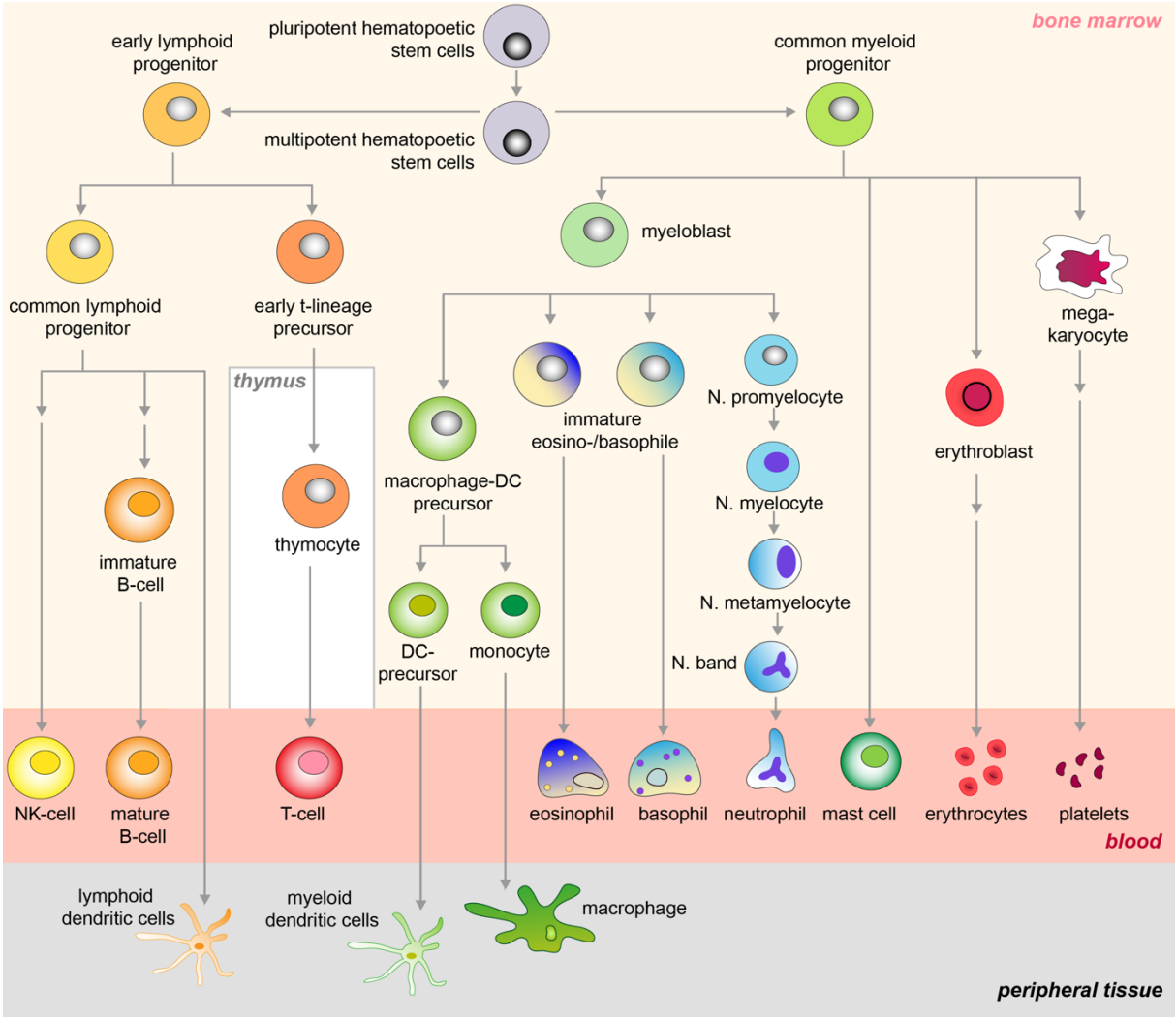

Figure 1: Hematopoiesis
The scheme illustrates the development of blood cells from a common pluripotent hematopoietic progenitor. The generation of the different lymphocytes, leukocytes, erythrocytes and platelets is depicted. The figure was generated based on Janeway's immunobiology, K.P. Murphy, C. Weaver, C. Janeway, 9th edition, 2017, Garland Science , Fogg et al., 2006; Liu et al., 2009
DC: dendritic cell, N: neutrophil, NK: natural killer

In addition to the cellular components, several organisms, such as vertebrates, are equipped with the humoral complement system. Since its initial discovery, awarded with a Nobel prize in 1919, it is allocated to innate immunity as it mediates microbial lysis. More recent discoveries have changed such allocation and the humoral complement system is now identified as a linker of innate and adaptive immunity due its additional role in antibody-mediated pathogen killing (Carroll, 2008).

1.1.2. Neutrophils constitute the first line of defense

Elie Metchnikoff, a Russian zoologist, had first described phagocytic cells in 1883. He observed accumulation of migrating cells in an experiment where he pierced starfish larvae with rose thorns. Metchnikoff differentiated the accumulating cells into macro- and microphages, the latter now referred to as neutrophils, according to the particle size the corresponding cells engulfed. In 1908, Metchnikoff was awarded a shared Nobel Prize in Medicine/Physiology for his discovery (Cavaillon, 2011) and based on his research he is frequently referred to as “father of innate immunity, cellular and modern immunology” (Gordon, 2008).

Phagocytosis (from greek: *phagein* meaning “to eat”, and *cytos*, meaning “cell”), is a central defense mechanism of neutrophils and the innate immune system in general, by which invading microorganisms are engulfed and digested. Neutrophils, also termed polymorphonuclear leukocytes due to their segmented nucleus, are classified as professional phagocytes (Rabinovitch, 1995). They are a specific type of granulocytes, which are characterized by their neutrally stained granules. Neutrophils originate from several precursor cells, which mature in the bone marrow (Figure 1) and approximately 5-10 $x10^{10}$ neutrophils are produced daily in an adolescent human in steady state (Dancey et al., 1976). Once released into circulation, neutrophils are the most abundant innate immune cells, which are rapidly recruited to inflamed tissues, thereby constituting the first line of cellular defense (Kolaczkowska and Kubes, 2013). The cues for neutrophil activation and subsequent recruitment can be derived from the pathogens themselves, resident tissue macrophages or other stimuli from the host immune system (Ley et al., 2018). Commonly, the expression of CD11b on the surface of neutrophils is considered as a neutrophil activation marker as it is enhanced in inflammatory milieus (Hyun et al., 2009). Moreover, CD11b primes circulating neutrophils for transmigration into inflamed tissues and is central in the neutrophil recruitment cascade (Kolaczkowska and Kubes, 2013; Zhang et al., 2006).

After neutrophil activation, they extravasate into the tissues and migrate towards the inflammatory site. Neutrophil chemotaxis is mediated by cell-membrane bounded G protein-coupled receptors that sense local chemokine gradients and allow the neutrophil to migrate towards the infection site. CXCR2 is the central chemokine receptor on murine neutrophils as it binds CXCL1, 2, 5, 6 and 7 (Sadik et al., 2011). Moreover, CXCR2 is upregulated on the surface of neutrophils as they are released into the blood from the BM and finally extravasate into tissues (Miyabe et al., 2017).

Once at the inflammation site, neutrophils are equipped with versatile defense mechanisms to ensure host protection (Borregaard, 2010). In addition to phagocytosis, neutrophils can secrete antimicrobial molecules from their granules, produce reactive oxygen species (ROS) and emit their DNA (formation of neutrophil extracellular traps (NETs)) to kill invading pathogens (Brinkmann et al., 2004; Cassatella, 1999). Not only such aggressive armamentarium, but also their high abundance, rapid migration and accumulation at site of infections require tight regulation of neutrophils (Ley et al., 2018).

It has long been thought that terminally differentiated neutrophils egress the bone marrow on a “one-way killing mission” patrolling the circulation for approximately 5-8 hours before they a cleared from the circulation (Athens et al., 1961; Mauer et al., 1960). Nevertheless, this dogma regarding the lifecycle and function of neutrophils is more complex as assumed initially. In addition to the bone marrow, marginated pools of neutrophils have been identified in the spleen, liver and lung that have been attributed with different functions and were classified as independent neutrophil subpopulations (Deniset et al., 2017; Doerschuk et al., 1987; Puga et al., 2011; Yipp et al., 2017). Even though neutrophils egress the bone marrow in a fully functional state, they still adapt and react to environmental cues in the circulation or later in peripheral tissues. Moreover, numerous recent investigations have proven that the lifespan of circulating neutrophils has previously been highly underestimated and can vary largely. Some studies have demonstrated neutrophils to live in the circulation for 5 days and exhibit 3-4 fold increased lifetimes in tissues (Pillay et al., 2010; Summers et al., 2010). Recent investigations have not only challenged the dogma regarding the lifecycle of neutrophils but also the function of neutrophils (Casanova-Acebes et al., 2018; Liew and Kubes, 2019; Wang et al., 2017).

Overshooting immune reactions driven by neutrophils promote diseases such as sepsis, fibrosis or cancer progression (Ley et al., 2018). Neutrophils often contribute to pathogenesis by degranulation that does not only neutralize invading pathogens, but also harms the surrounding host tissue. In these cases, ROS and NETs were frequently identified as detrimental cues (Gupta and Kaplan, 2016; Ley et al., 2018). Recently, the release of ROS and NETs has been shown to underly a circadian rhythm fluctuating during the day (Adrover et al., 2020).

1.1.3. Macrophages maintain host homeostasis

Similar to neutrophils, macrophages have initially been described by Metchnikoff due to their ability to phagocytose big particles (from greek: *makrós*, meaning “large”, and *phagein*, meaning “to eat”). Apart from pathogen neutralization, this process mounts an adaptive immune response, induced by antigen processing and presentation. In addition, phagocytosis is important to ensure tissue homeostasis by removal of dead cells (Parnaik et al., 2000). Together with neutrophils and DCs, macrophages are determined as professional phagocytes (Rabinovitch, 1995). Given by the common bone marrow precursor, the myeloblast (Figure 1), these three individual cell populations share some functions.

Tissue-resident macrophages are one of the most abundant leukocyte populations found throughout the entire body (Mowat et al., 2017). Apart from their function as “professional” phagocytes, they are not only immunological sentinels to detect and fight infections, but also central in tissue homeostasis and remodeling (Geissmann et al., 2010). Macrophages are, in many regards, very heterogeneous: their origin, function and expression profile vary extensively. To provide a comprehensive overview, the following chapter will start by providing general information and later specific details on renal macrophages.

1.1.3.1. Different precursors give rise to macrophages in distinct tissues

Although the origin of macrophages during development is still under debate, the availability of numerous methods such as fate mapping in genetically modified mice, parabiosis and adoptive transfer experiments have substantially expanded our current knowledge. Initially, as unique source of tissue-resident macrophages BM-derived circulating monocytes were suggested to invade tissues and give rise to macrophages. This dogma remained *state-of-the-art* for decades after being described in 1972 by van Furth *et al.* as the mononuclear phagocyte system (van Furth et al., 1972). However, BM-derived monocytes only minimally contribute to maintenance of tissue macrophages in steady state as the vast majority of tissues are seeded with macrophages prior to definitive (BM-originated) hematopoiesis and retain their population independent of local proliferation (Hashimoto et al., 2013; Honold and Nahrendorf, 2018; Hume et al., 2002). In this new concept of macrophage origin, the dermis, gut and heart represent exceptions as they are continuously replenished by circulating monocytes and thus the old dogma still holds true for these specific organs

(Bain et al., 2014; Molawi et al., 2014; Tamoutounour et al., 2013). Other tissue macrophage populations mostly originate from embryonic precursors that seed the peripheral tissues prior to birth. After tissue seeding, these cells maintain their pool by local self-renewal independent of circulating precursors (Hashimoto et al., 2013; Merad et al., 2002; Yona et al., 2013). However, in case this initial fetal-derived macrophage population is damaged or even lost, experimentally induced by irradiation or other environmental cues, the macrophage population can be replenished by BM-derived monocytes from the circulation (Scott et al., 2016).

HSCs are formed during fetal development and macrophage ontogeny occurs simultaneously

Before establishment of the general definitive hematopoiesis, several transient events occur during fetal development, which lead to production of HSCs that are derived from the yolk sac (YS) or the fetal liver. These cells give rise to BM-independent macrophage populations that persist until adulthood (Figure 2, modified according to (Hoeffel and Ginhoux, 2015)). The initial fetal hematopoiesis giving rise to HSCs is divided into a primitive, transient definitive and definitive phase (Bertrand et al., 2005). In parallel to this initial fetal hematopoiesis, different macrophage populations seed the tissues and are partially replenished during fetal development.

Primitive hematopoiesis: During primitive hematopoiesis, the first progenitor cells are formed in the YS blood islands of mice at the embryonic age of 7.5 days (E7.5) (Palis et al., 1999). Therein produced cells are termed erythro-myeloid progenitors (EMPs) and are characterized by the expression of the tyrosine-protein kinase KIT (C-kit or CD117), CD41 and later during their development by stimulation of the colony-stimulating factor 1 receptor (CSF1R). C-kit is a receptor tyrosine kinase type III binding to the stem cell factor (Hoeffel et al., 2015). CSF1R, a tyrosine-protein kinase, is the cell-surface bound receptor for interleukin-34 (IL-34) and CSF1. It is crucial for survival, proliferation and differentiation of hematopoietic precursor cells, especially for monocytes and macrophages (Stanley and Chitu, 2014). These $CSF1R^+$ EMPs (Figure ***2***, shown in green) infiltrate the fetal liver and other peripheral tissues as soon as the circulatory system is developed (McGrath et al., 2003). Thereby a primitive YS-derived macrophage population develops (Figure 2, shown in green) that gives rise to microglia, which are not replenished during adulthood (Ginhoux et al., 2010). A small percentage of these YS-derived macrophages was found in versatile organs of adult mice (Schulz et al., 2012). Their development is modulated by CSF1R, and blocking

CSF1R during embryogenesis can result in complete depletion of the YS-derived macrophage population (Hoeffel et al., 2015). Hoeffel *et al.* showed that the population of tissue-resident macrophages was repopulated to normal levels in absence of CSF1R signaling until birth, thereby demonstrating that CSF1R-independent macrophage replenishment exists (Hoeffel et al., 2015). However, usage of a *Csf1r*-GFP reporter mouse has validated that many macrophages in numerous tissues are positive for the CSF1R in adults (Hume, 2008). Conclusively, these studies highlight that CSF1R signaling is central in macrophage development but can be subverted to ensure host protection.

Transient definitive hematopoiesis: Simultaneous to the development of the circulatory system, at E8.5 the hemogenic endothelium of the YS produces late EMPs, characterized by the expression of transcription factor C-Myb. C-Myb is central for later fetal hematopoiesis, as c-Myb-deficient mice become strongly anemic by day 15 of gestation (Mucenski et al., 1991). These C-Myb$^+$ EMPs (Figure 2, shown in light blue) migrate to the fetal liver and give rise to fetal monocytes, which are in turn transported via the circulation to peripheral tissues (Naito et al., 1990). The previously established population of primitive macrophages is continuously replenished in the vast majority of tissues, excluding for example the brain, by infiltrating fetal monocytes, which in turn locally differentiate into macrophages (Figure 2, shown in light blue). Later during development (E9.0), the additionally generated hemogenic endothelium gives rise to lympho-myeloid progenitors (LMPs), which initiates the last step of fetal macrophage development. The seeding of LMPs in the fetal liver give rise to late fetal monocytes (Figure 2, shown in rose). These late monocytes contribute to the generation of the tissue-resident macrophage population as long as the fetal liver is responsible for hematopoiesis.

Definitive hematopoiesis: Finally, HSCs are generated by the hemogenic endothelium of the aorta-gonad mesonephros regions and seed the fetal liver (Kieusseian et al., 2012). The first HSCs develop five weeks after gastrulation in humans (Tavian et al., 2001). All cells produced by the YS or hemogenic endothelium during fetal hematopoiesis migrate to the fetal liver and contribute to definitive hematopoiesis. Once the BM takes over (E17.0), the adult form of hematopoiesis is established. Hematopoietic potential is given to the BM upon infiltration of the HSCs (Figure 2, shown in purple).

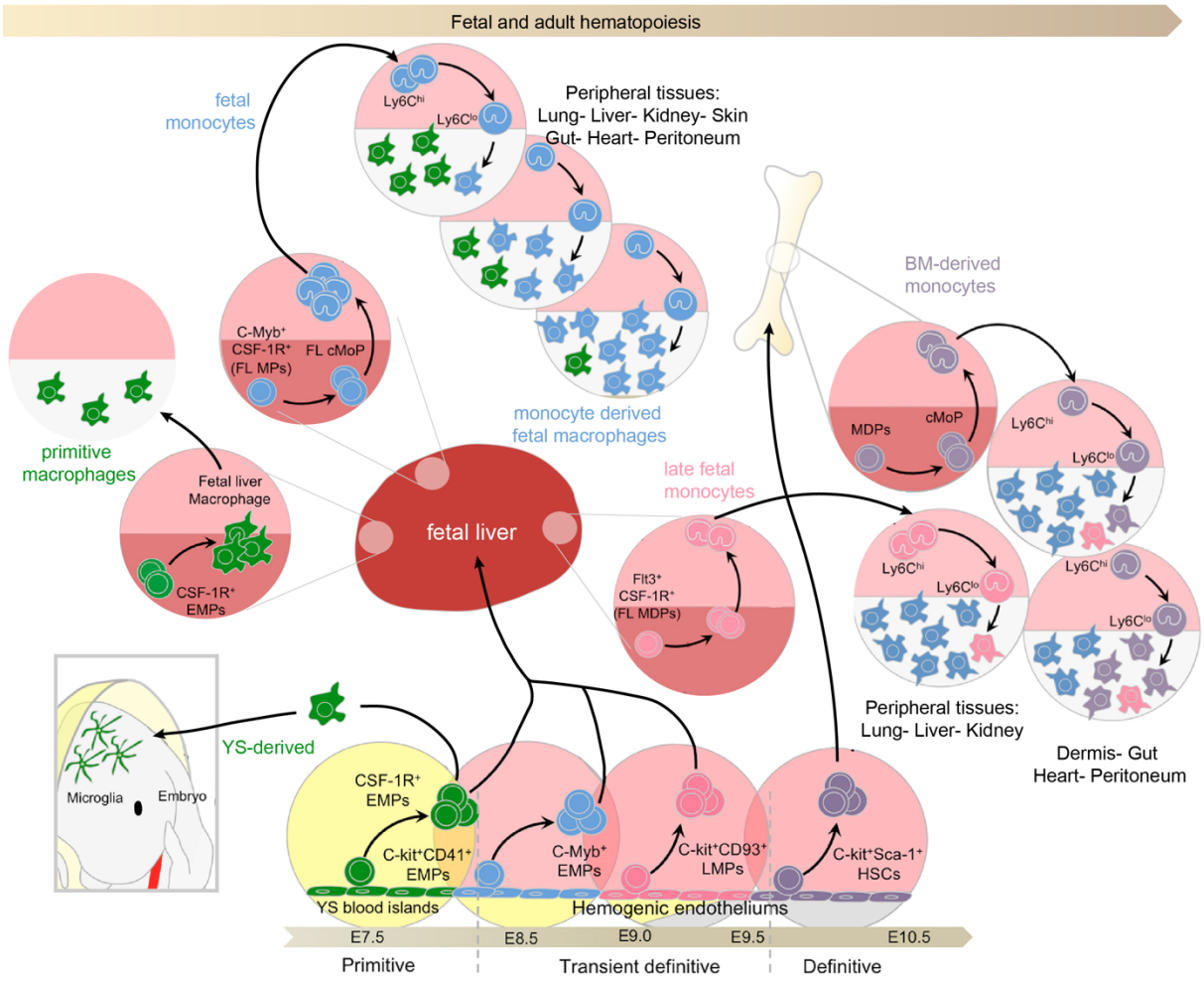

Figure 2: Fetal and adult hematopoiesis

The scheme summarizes the transient waves leading to the production of hematopoietic cells during fetal development and the subsequent ontogeny of the versatile monocyte and macrophage populations. Figure adapted from Hoeffel and Ginhoux 2015

CSF1R: colony-stimulating factor 1 receptor, cMoP: common monocyte precursor, E: embryonic age (in days), EMPs: erythro-myeloid progenitors, FL: fetal liver, HSC: hematopoietic stem cells, LMPs: lympho-myeloid progenitors, MDPs: macrophage/ dendritic cell progenitor, YS: yolk sac

Importantly, all research conducted on the ontogeny of macrophages was performed in mice with findings considered to be applicable to humans, but this has not been verified yet. The understanding of how macrophages originate is crucial to designing novel intervention strategies targeting the macrophage population.

1.1.3.2. Macrophage subtypes are classified according to their function and phenotype

Different concepts for the understanding of macrophage differentiation were introduced in the last few decades and macrophages were classified according to their phenotype and function. The activation or polarization of macrophages describes the induction of a distinct pattern regarding gene and protein expression in response to a stimulus by the microenvironment. The scientific community sought for a commonly used terminology of these versatile activation states, since the diverse outcomes of macrophage activation are involved in the clinical manifestation of numerous diseases (Murray et al., 2014).

In 1992, the concept of “classical” vs. “alternatively activated” macrophages was introduced by Stein *et al.* (Stein et al., 1992). Both macrophage states exhibit an activated phenotype, but with a distinct metabolic program, thereby promoting inflammation (upon classical activation) or tissue repair (upon alternative activation). The previously known “classically activated” macrophage was activated via lipopolysaccharides (LPS) or Interferon-γ (IFN-γ), a T helper (Th) cell1-derived cytokine, classifying them as proinflammatory cells. Alternatively, IL-4, a Th2 derived cytokine, was described to upregulate major histocompatibility class II antigens (MHCII), leading to enhanced antigen presentation. Moreover, IL-4 activation inhibited the production of proinflammatory cytokines such as TNFα. (Stein et al., 1992).

Eight years later, the differentiation concept of M1 and M2-like macrophages was introduced (Mills et al., 2000). This new concept proposed that the same stimuli, namely IFN-γ and LPS, resulted in different outcomes *in vitro,* depending on the origin of macrophages (C57BL/6 (Th1) or Balb/c (Th2)). The Th1-derived macrophages produced nitric oxide, whereas the Th2-derived macrophages upregulated arginine metabolism. These different responses were found to exist independently of lymphocytes, as they were also observed in T/B-cell deficient animals (Mills et al., 2000). The concept of M1/M2 was later further subdivided, thereby incorporating the idea of activation on a spectrum and not in just two states (Edwards et al., 2006; Martinez and Gordon, 2014; Stout et al., 2005). The idea of a spectrum model has further been extended by a transcriptomic study on human macrophages that identified at least nine distinct macrophage activation patterns (Xue et al., 2014).

Since their introduction, the concept of M1/M2 and classical vs. alternative activation have frequently been incorrectly merged or referred to as the same (Orecchioni et al., 2019). The merging led to the most common differentiation of an inflammatory-

(classically activated and M1) and a more immunoregulatory macrophage population (alternatively activated and M2), associated with tissue repair, wound healing and fibrosis (Nahrendorf and Swirski, 2016).

In 2014, the classical concept of the two-dimensional *in vitro* classification of M1/M2 or classical vs. alternative activation was revised (Murray et al., 2014). Accordingly, the new classification was based on the stimuli, which induced a certain metabolic program and function. However, this novel concept was limited to the stimuli provided *in vitro*. Thus, the simplicity of the model might not be applicable to complex *in vivo* situations with multitude of molecules expressed during homeostasis and inflammation.

Nevertheless, these concepts insufficiently describe the enormous heterogeneity of macrophages (Nahrendorf and Swirski, 2016). Thus, macrophages are highly plastic cells that can exhibit very distinct metabolic programs and functions determined by their local microenvironment. Currently, macrophages are classified in a network model based on their function (Nahrendorf and Swirski, 2016). It is important to note that each macrophage population exhibits not only tissue-specific but also a shared gene-expression signature, determined by the tissue of origin (Gautier et al., 2012; Okabe and Medzhitov, 2014). Furthermore, it has been shown that transplantation of specific tissue macrophages into other tissues induces genetic adaptation (Lavin et al., 2014). Analysis of these alterations revealed that the transplanted macrophages adopted the phenotype of the recipient’s tissue-resident macrophages, thereby highlighting that the local microenvironment reprograms macrophages and thereby governs the heterogeneity of macrophages (Lavin et al., 2014). Conclusively, it has to be acknowledged that macrophages are highly heterogenous and the role of microenvironmental cues for their functional and phenotypical state is central, thereby highlighting how well macrophages sense their local environment.

1.1.3.3. Colony-stimulating factor 1 regulates macrophage proliferation, differentiation and survival

One of the signaling mechanisms of the tissue microenvironment that strongly affect the macrophage phenotype and their function is the colony-stimulating factor (CSF) 1. It is also termed macrophage-CSF (M-CSF) and was first described in the 1980's as the essential regulator of macrophage homeostasis. Together with the granulocyte/macrophage CSF (GM-CSF, CSF2) and the granulocyte CSF (G-CSF, CSF3), it resembles the family of CSFs, which were originally described as hematopoietic-cell growth factors, but were later shown to additionally regulate mature myeloid cells (Hamilton, 2008). In initial experiments, CSF1 has been shown to differentiate hematopoietic precursor cells into macrophage colonies (Stanley et al., 1978; Stanley et al., 1976). Among other functions, such as regulation of the production of oocytes in the female reproductive tract, osteoclast production and differentiation of neuronal progenitor cells (Lloyd et al., 2009; Stanley and Chitu, 2014), the unique role of CSF1-signaling for the differentiation of macrophages from monocytes, macrophage survival and proliferation is well established (Chitu and Stanley, 2006; Pollard, 2009). Central for the establishment of this concept were experiments conducted on CSF1-deficient op/op mice, which revealed detrimental effect on macrophage development and differentiation (Wiktor-Jedrzejczak et al., 1990; Wiktor-Jedrzejczak et al., 1992).

Subsequent to the description of CSF1, its cell-surface bound binding partner, the CSF1 receptor (CSF1R, CD115), was identified and a cell intrinsic tyrosine-kinase activity was discovered downstream of this receptor (Yeung et al., 1987). In addition to CSF1, IL-34 was later identified as additional CSF1R ligand with redundant effects on monocyte and macrophage differentiation and survival (Chihara et al., 2010; Wei et al., 2010). However, the role of IL-34 differs regarding polarization effects on macrophages and the generation of Langerhans cells and microglia (Boulakirba et al., 2018; Nandi et al., 2012; Wang et al., 2012). Based on the common phenotypes induced by CSF1-deficient and CSF1R-deficient mice, it can be concluded that CSF1 can uniquely signal via its corresponding receptor (Dai et al., 2002). In contrast, IL-34 can further signal via an alternative receptor.

Among others, CSF1R is expressed at low levels on HSCs (Sarrazin et al., 2009), whereas it is highly abundant on monocytes, myeloid DCs and tissue macrophages (Byrne et al., 1981; Lenzo et al., 2012; MacDonald et al., 2005). The expression of CSF1R is gradually increasing during the differentiation of these mononuclear

phagocytes and regulates their survival, proliferation, differentiation and chemotaxis (Bartelmez and Stanley, 1985; Tushinski et al., 1982). To orchestrate this broad set of functions, numerous downstream signaling pathways are stimulated by CSF1R activation, such as the PI3K-AKT and the AMPK pathway – both central for macrophage differentiation (Jacquel et al., 2012; Stanley and Chitu, 2014). In addition to maintain macrophage homeostasis, which critically contributes to host protection by wound healing, immunosuppression and the initiation of immune responses, CSF1-signaling is involved in inflammatory diseases, autoimmunity, bone disease and especially cancer (Goswami et al., 2005; Hamilton, 2008; Hume and MacDonald, 2012; Lin et al., 2001). In line with these observations, it was hypothesized that CSF1 participates in a cytokine network, which allows the communication of myeloid cells and surrounding tissue cells in inflammation (Hamilton, 1993). Moreover, the increased number of macrophages in certain inflammations, such as rheumatoid arthritis, is based on increased levels of CSF1 extending macrophage survival. Based on this hypothesis of a cytokine network, it was assumed that CSF1-inhibition might decrease proinflammatory cytokines and thereby dampen detrimental inflammation. In different experimental models of rheumatoid arthritis, CSF1R-blockage reduced circulating cytokines, typical disease hallmarks such as joint swelling and finally inflammation (Garcia et al., 2016). Moreover, different strategies inhibiting the CSF1R-signaling have made their way into clinical trials as potent therapy candidates not only for rheumatoid arthritis, but also lupus erythematosus and diverse solid cancers (Cannarile et al., 2017; Korkosz et al., 2012; Masek-Hammerman et al., 2016). Two strategies to block CSF1R-signaling are established: inhibitors targeting the tyrosine kinase activation of the CSF1R or blocking of ligand-receptor interaction thereby abolishing receptor activation and subsequent downstream signaling (Hume and MacDonald, 2012). Very recently, a small molecule tyrosine kinase inhibitor targeting the CSF1R, named Pexidartinib, has been approved for the treatment of symptomatic tenosynovial giant cell tumor (Lamb, 2019). Pexidartinib targets tumor-associated macrophages (TAMs), which suppress host-immunity in the local cancer environment and thereby ensure cancer protection (Noy and Pollard, 2014).

In summary, CSF1R-signaling is pivotal to macrophage homeostasis and targeting CSF1 has already been proven as a promising therapeutic approach in different macrophage-driven diseases.

1.1.3.4. Macrophages control neutrophil responses

Numerous tissues harbor networks of resident macrophages that function as local sentinels by sensing threats and alerting the host by secretion of inflammatory mediators. These macrophage-derived mediators, such as cytokines, can activate the endothelium, which binds circulating leukocytes. In particular, highly immunoreactive neutrophils bind to activated endothelium and cytokines facilitate their transmigration guiding these cells to the site of infection. The neutrophil chemoattractants CXCL1, CXCL2, IL-1α or monocyte chemoattractant protein-1 are induced in macrophages after recognition of pathogen-associated microbial patterns (PAMPs) or damage-associated molecular patterns (DAMPs) by toll-like receptors (TLR) (Barry et al., 2013; Beck-Schimmer et al., 2005; De Filippo et al., 2008). Once in the tissue, neutrophil survival is regulated by macrophages via secretion of IL-1β, Tumor necrosis factor α (TNFα), G-CSF and GM-CSF (Kobayashi et al., 2005; Takano et al., 2009). After neutrophils have conducted their effector function in the tissue, macrophages mediate the resolution of the inflammation and phagocytose neutrophils (Odaka et al., 2003). In various organisms and disease settings this macrophage-neutrophil crosstalk has been validated to crucially maintain host defense (Abtin et al., 2014; Kim and Luster, 2015; Schiwon et al., 2014; Takano et al., 2009). After initiating inflammation, neutrophils can orchestrate a feedback loop via the secretion of chemoattractants that further recruit monocytes/macrophages into the inflamed tissue (Chertov et al., 1997; Soehnlein et al., 2008). In summary, macrophages are local regulators that shape a pro- or anti-inflammatory microenvironment.

1.1.3.5. The proinflammatory cytokine TNFα is a key regulator in inflammation

Additional to extend the life span of extravasated neutrophils in tissues, TNF-signaling regulates numerous inflammatory processes. TNFα was discovered in 1975 and, as the name indicates, the molecule induced necrosis in tumor cell lines (Carswell et al., 1975). TNFα is a transmembrane protein (also termed pro-TNF) expressed on the cellular surface prior to cleavage by a specific metalloprotease (Black et al., 1997). After cleavage, the soluble TNF (sTNF) is released, which can act at distant sites throughout the body. The pro-TNF and the sTNF are both recognized by the membrane-bound TNF receptors 1 and 2 (TNFR1 and TNFR2). Additionally, a soluble TNFR exists, capable of neutralizing TNF and thus reducing the local cytokine

concentration. The expression of these TNFRs is regulated by other cytokines, especially interferons (Aggarwal et al., 1985).

In addition to macrophages, monocytes, NK-cells, endothelial cells, fibroblasts and activated T-cells were determined as major cellular sources of TNFα (English et al., 1991; Kelker et al., 1985; Sedger and McDermott, 2014). Even though TNFα is involved in many physiological functions during homeostasis, it is often termed as the key regulator during an inflammatory response and therefore mainly associated with pro-inflammatory functions (Bradley, 2008). Elevated TNFα-levels have been predominantly found in individuals suffering from inflammation or infections and it is often correlated with disease severity (Kwiatkowski et al., 1990; Robak et al., 1998; Waage et al., 1987). Apart from being crucial in acute and chronic inflammation, autoimmune diseases and cancer-related inflammation, TNFα is crucial in homeostatic processes during embryogenesis (Chu, 2013). Moreover, signaling via TNFR1induces cell death, whereas general TNF-signaling activates the NFκB-pathway stimulating cellular survival (Sedger and McDermott, 2014; Tartaglia et al., 1993). These versatile functions highlight the central role of TNFα during health and diseases.

Based on its central role in modulating host immunity, TNFα has been targeted in many inflammatory diseases. Some autoimmune disorders, such as rheumatoid arthritis and psoriasis, have been treated for more than a decade successfully with TNFα-inhibitors (Kivelevitch et al., 2014). Etanercept, approved in 1998, is a potent soluble TNFR, which reduces circulating TNFα after administration (Moreland, 1998).

1.1.3.6. The kidney harbors a dense macrophage network

The kidney, which is the target organ for this study, is seeded with numerous macrophages. The diverse ontogeny of macrophages described earlier in this thesis has demonstrated different macrophage populations to exist in tissues. The expression profile and function of macrophage are greatly modulated by the local tissue environment.

Renal macrophages are predominantly monocyte-derived in adults

The murine kidney develops at around E10.5 without the presence of renal macrophages (Rae et al., 2007). Although YS-derived macrophages populate the fetal kidney from E12.5, the percentage of these macrophages decrease exponentially from E13.5 until adulthood (Hoeffel et al., 2015), while the percentage of monocyte-derived macrophages substantially increases with age (Epelman et al., 2014; Hoeffel et al.,

2015). The origin of these monocyte-derived macrophages remains unclear (Epelman et al., 2014; Hoeffel et al., 2015; Sheng et al., 2015) and during adulthood the fetal-generated renal macrophage population (F4/80^{high}) maintains themselves by self-renewal during homeostasis. Nevertheless, it has been shown that transferred bone marrow cells contribute to the F4/80^{high} macrophage population in the kidney under homeostatic conditions (Schulz et al., 2012). In case of renal injury or inflammation, renal macrophages proliferate locally or are reconstituted by circulating BM-derived monocytes that differentiate into macrophages once the niche of kidney-resident macrophages becomes available (Isbel et al., 2001; Lever et al., 2019). Even though the YS-derived macrophage population is reported to be CSF1 dependent, postnatal administration of CSF1 in mice increased the renal macrophage population and kidney growth in general (Alikhan et al., 2011).

The population of renal macrophages can be classified into three subtypes

Regardless of their origins, the local micromilieu mainly shapes the phenotype and function of kidney macrophages. A recent study classified five distinct subpopulations of mononuclear phagocyte cells (MPCs) in the kidney. The mononuclear phagocyte cells (MPCs), including monocytes, macrophages and DCs, were recently identified by the surface expression of F4/80, CD103, CD14, CD16 and CD64 (Kawakami et al., 2013). Among these cells, five different subpopulations were identified by differential expression of CD11b and CD11c. The ability of phagocytosis, T cell activation via antigen presentation and the secreted cytokines upon LPS stimulation were different among these five subpopulations (Kawakami et al., 2013). Comparing kidney macrophages to macrophages from other organs, a previous study has identified an organ-specific expression signature with yet to be determined function (Mass et al., 2016). Besides, a more recent study differentiated the F4/80^{+} CD64^{+} renal macrophage population, similar to Kawakami *et al.,* according to their CD11b and CD11c expression into three transcriptionally independent subpopulations: a population of kidney resident macrophages (CD11b^{int} CD11c^{int}) and two monocyte-derived populations (CD11b^{high} CD11c$^{high\ or\ low}$) (Puranik et al., 2018).

1.1.3.7. Macrophages critically contribute to tissue homeostasis and health

Macrophages are the most abundant leukocytes in the healthy kidney and their role in embryogenesis has been investigated extensively (Munro and Hughes, 2017). Macrophages infiltrate the kidney early during embryogenesis and support kidney development by improving the formation of branch tips and nephrons (Rae et al., 2007). The frequent cellular apoptosis during organogenesis enriches the evolving organ with cellular debris, which is cleared by macrophages (Camp and Martin, 1996). This clearance is conducted via efferocytosis, a process by which dying cells are removed by phagocytic cells (deCathelineau and Henson, 2003). The efficient removal of cellular debris is crucial for appropriate organ development and efferocytosis dysfunction results in inflammation, which can culminate in organ dysfunction. Furthermore, macrophages are suggested to promote renal angiogenesis and lymphangiogenesis (Kerjaschki, 2005; Lee et al., 2011a). A recent study has demonstrated that renal macrophages not only regulate the albumin transport between the renal capillaries and the peritubular space (Bell et al., 1978), but also additionally control the trans-endothelial transport of small immune complexes in the kidney and thereby maintaining renal homeostasis (Stamatiades et al., 2016). In addition, macrophages function as tissue-resident sentinel cells inducing an immune response to filtered antigenic particles and thus protect the kidney from infection (Weisheit et al., 2015).

1.1.3.8. Macrophages crucially contribute to the regeneration potential of diseased kidneys

The kidney has a remarkable regeneration potential after injury generated by infections or inflammation (Kusaba and Humphreys, 2014). In addition to the epithelial self-duplication capacity, renal macrophages critically contribute to kidney regeneration. CSF1 and IL-34, mainly secreted by tubular epithelial cells, mediate the survival of macrophages within the kidney (Baek et al., 2015; Isbel et al., 2001). Both molecules signal via the CSF1-R, the key pathway for the regulation of macrophage proliferation, differentiation and survival (Baek et al., 2015). After injury, macrophages remove dead cells, resolve inflammation via cytokine secretion and orchestrate the remodeling of tissue matrix (Herbert et al., 2004; Humphreys and Bonventre, 2007; Sola et al., 2011). Depletion of macrophages during this repair phase resulted in continued inflammation and thereby impeded tissue restoration (Kim et al., 2010).

The micromilieu of the injured or inflamed kidney, can be pro-or anti-inflammatory. Given that macrophages influence the renal microenvironment, macrophage-derived molecules can be beneficial or detrimental for renal homeostasis (Lee et al., 2011b) (Ricardo et al., 2008). Correspondingly, macrophages have been implicated in numerous renal diseases, such as glomerulonephritis, lupus nephritis or acute kidney injury (AKI) (Nikolic-Paterson and Atkins, 2001) (Baek, 2019). Herein, the disease severity often correlates with macrophage accumulation (Eardley et al., 2008; Hill et al., 2001; Lan et al., 1991).

The infiltration of macrophages modulates the local immune response, as they remove cellular debris and thereby promote tissue healing. However, healing can revert to tissue fibrosis, a process of excessive tissue scarring. Depletion of macrophages correlated with reduced fibrosis severity and impeded kidney injury in a model of acute ischemia reperfusion injury and in a model of unilateral ureter ligation (Jo et al., 2006; Kitamoto et al., 2009; van Goor et al., 1992). Besides this, different macrophage targeting approaches, such as disruption of recruitment, functional modulations through genetic approaches or adoptive transfer, have identified macrophages to promote renal injury in numerous kidney diseases (Feng et al., 1999; Ikezumi et al., 2003; Tomita et al., 2000).

1.2. The kidney regulates blood pressure and sustains fluid and salt balance

The two bean-shaped kidneys located in the retroperitoneal space filter blood to sustain fluid and salt homeostasis, thereby regulating blood pressure. Moreover, metabolites and foreign substances, such as drugs and toxins, are removed from the circulation and excreted in the urine. In addition to filtration, the kidney produces hormones such as renin and erythropoietin to regulate hematopoiesis, electrolyte concentrations and blood pressure (Acharya and Olivero, 2018). Optimal filtration ensures excretion of metabolites like hydrogen, ammonium and uric acid, but retention of water, salts and nutrients.

The nephron (from greek, *nephros*, meaning “kidney”) is the filtration unit of the kidney and each human kidney contains approx. one million nephrons (Hinchliffe et al., 1991). In comparison, murine kidneys are composed of 12,500 nephrons each (Klingberg et al., 2017). The nephrons are embedded in a capillary network and are composed of a renal corpuscle and a tubule. The renal corpuscle, where primary filtration occurs, is composed of the glomerulus and the surrounding Bowman’s capsule (Figure 3).

The Bowman’s space, which is located between the glomerular tuft and the epithelial cells of the Bowman’s capsule, collects the primary urine produced in the glomerulus. The kidney of an adult human produces approximately 180 l of primary urine daily. The process conducted in the glomeruli is detailed in the following chapter. The renal tubule reabsorbs the majority of the previously excreted fluid and salts into the peritubular capillaries. The tubule can be subdivided into three sub-compartments: the proximal tubule, the loop of Henle and the distal tubule. The proximal tubule reabsorbs the majority of the produced primary urine (approx. 65 %). Macroscopically, the kidney can be subdivided into cortex and medulla. Along with the renal corpuscle, the upper proximal tubule is localized in the renal cortex, whereas the other nephron-components are found in the renal medulla. The U-shaped loop of Henle mainly concentrates urine by reabsorption of water (approx. 30 % of the primary urine). The reabsorption rate in the distal tubule is very low (approx. 1 % of the primary urine), but tightly hormonally regulated to optimize the balance of retention and secretion. Each nephron ends in the ureter connecting the kidney to the urinary bladder, where the final urine is stored prior to excretion (Taschenatlas Physiologie, Chapter 16, S. Silbernagl, A. Despopoulos, W.-R. Gay, 7. Auflage, 2007, Thieme)

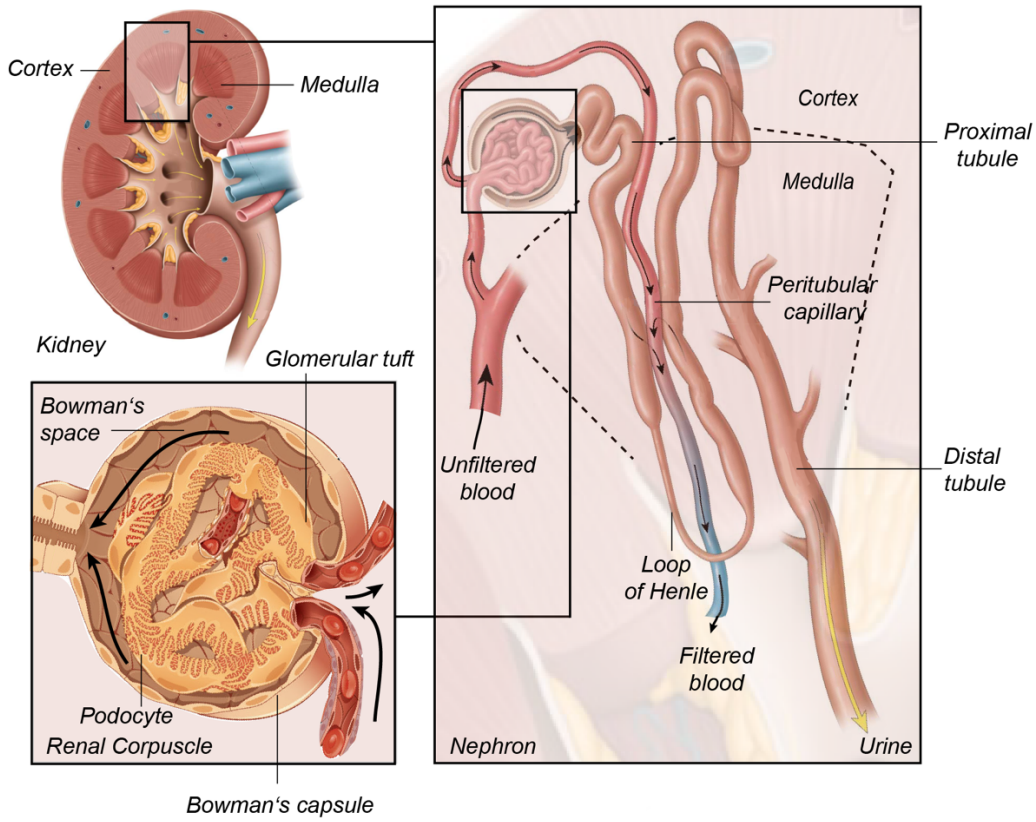

Figure 3: Anatomy of the kidney
Structural scheme of the kidney. The tubular system and the glomerulus are shown in more detail. Adapted from https://commons.wikimedia.org/wiki/File:Juxtaglomerular_Apparatus_and_Glomerulus.jpg and https://pkdcure.org/what-is-pkd/adpkd/kidney-101/.

1.2.1. The blood-urine barrier is composed of the glomerulus

The glomerulus constitutes the blood-urine barrier where the primary filtration occurs. The blood flowing into the glomerular microvasculature by an arteriole is filtered through the three-layered glomerular filtration barrier (GFB). This filtration barrier is composed of the endothelial cells, the underlying glomerular basement membrane (GBM) and the foot processes of podocytes covered with filtration slit diaphragms (Miner, 2011; Venkatachalam and Rennke, 1978). The partly fenestrated endothelial cells have a pore size of 70-100 nm, thus retaining the cellular blood compartments in the circulation (Pollak et al., 2014).

The GBM consists of a specialized layer of extracellular matrix, which is produced by endothelial cells as well as podocytes during glomerulogenesis (Abrahamson, 1985). Moreover, the GBM is a tightly packed negatively charged layer of extracellular matrix proteins without pores. Collagen IV is the major component of the GBM and macromolecules bigger than 50 kDa (approx. 10-25 nm) are retained. Moreover, the charge of circulation molecules determines their secretion. The negatively charged GBM leads to the retention of molecules with similar charge. The last component of

the glomerular filtration barrier, namely the slit diaphragm in-between the podocyte foot processes, is composed of nephrin and has a pore size of 5 nm. Besides the filtration function, the podocytes critically stabilize the free-standing capillary loops of the glomerulus (Pollak et al., 2014). The integrity of all three GFB compartments is crucial for efficient filtration, as the disruption of a single component results in proteinuric diseases (Haraldsson et al., 2008).

In addition to the endothelium with the mounting podocytes, mesangial cells compose the glomerular tuft. These smooth muscle cells structurally support the endothelium, contract the glomeruli to modulate the ultrafiltration rate and are reported to clear the GFB of remaining debris (Floege et al., 1993; Mene et al., 1989). The glomerulus is localized within the Bowman's space and is restricted by the Bowman's capsule. This capsule is composed of a basement membrane, lined with a monolayer of adherent parietal epithelial cells (Shankland et al., 2014).

The glomerular filtration rate (GFR) conceptually represents the overall volume filtered per minute through the glomerular filtration barrier in all glomeruli in both kidneys. In healthy adults approx. 100 ml/min are filtered with major circadian oscillations (Koopman et al., 1989). The GFR provides a stable metric to determine the renal function and thereby allows classification and monitoring of renal diseases. It is determined by the level of creatinine in blood serum, patients' age, gender and weight (Fenton et al., 2018). Recent studies have revealed certain limitations in this model, as the creatinine excretion varies not only with age, gender and body mass but also with the volume of muscle mass. Therefore, certain ethnologies with higher muscle to body mass ratio, like Africans, have higher creatinine levels in the blood serum while maintaining the same GFR (Eastwood et al., 2010). Furthermore, determining the GFR in children according to the creatinine levels is complicated (Mian and Schwartz, 2017). To overcome those limitations, the combined assessment of creatinine and cystatin C for the calculation of the GFR was established (Inker et al., 2012).

1.2.2. The role of the glomerulus in many kidney diseases

As explained in the previous chapter, the glomerulus is the central renal filtration unit. Moreover, the integrity of the cellular and molecular glomerular components is mandatory to ensure an appropriate blood filtration. Given the crucial role for host homeostasis, glomerular dysfunction is the leading cause of many chronic and end-stage renal diseases (Shankland et al., 2014). Glomerular diseases, also termed glomerulopathies, are characterized by destruction of the GFB, mostly leading to hematuria or proteinuria (Hebert et al., 2013). The GFB is damaged to such an extent in hematuria that erythrocytes can pass the filtration barrier and are excreted. Damage to the GFB, leading to proteinuria, is spatially smaller so that “only” large plasma proteins, such as albumin, are excreted.

Glomerular diseases are highly versatile and are characterized according to the disease cues as primary or secondary. Primary glomerular diseases are derived from local glomerular abnormalities, including genetic disorders and affect different components of the GFB. Different from the majority of diseases, in the glomerulus different cell types are often affected due to their close proximity in the glomerulus (Kitching and Hutton, 2016). A typical cause for glomerular endothelium dysfunction is thrombotic microangiopathies (TMAs). Having versatile molecular causes, TMAs are characterized by endothelial damage associated with fibrin and platelet deposition, which in turn leads to the rupture of the GBM and erythrocyte fragmentation, also termed schistocyte formation (Coppo and Veyradier, 2009). These schistocytes are formed due to vessel occlusions, resulting in elevated shear stress applied the circulating erythrocytes. Dysfunctions of the GBM are often associated with mutations in collagen VI or an altered composition of the GBM (Hudson et al., 1993; Suh and Miner, 2013). Mutations, leading to misfunction of proteins, such as nephrin and podocin, often cause glomerular diseases that originates from the podocytes.

Despite primary causes, glomerular diseases can arise from systemic inflammatory or metabolic diseases, then termed as a secondary glomerular disease (Hebert et al., 2013). The most common secondary glomerulopathies arise from diabetes or hypertension (Collins et al., 2005; Rowley et al., 2017). Both disease incidences increased in developed countries over the past decades, mainly due to malnutrition, obesity, reduced activity and drug abuse (Collins et al., 2005; de Boer et al., 2017).

Glomerulonephritis (GN) is a term used for a large variety of renal diseases, which originate from various primary or secondary cues ranging from the deposition of

antibodies or immune complexes, infections or drugs (Kitching et al., 2008). GN is often described as glomerular inflammation and can be differentiated into a proliferative and non-proliferative form (Mayadas et al., 2010). The gain of glomerular cells in the proliferative GN can be derived either from proliferation of glomerular cells, such as mesangial cells or from infiltrating leukocytes (Sethi et al., 2016). After diabetes and hypertension, GNs constitute the third leading cause of end-stage kidney diseases in the United States (McCullough et al., 2019).

1.2.3. Neutrophils aggravate glomerular diseases

Infiltration of neutrophils can be observed in many glomerular diseases (Camussi et al., 1980; Segerer et al., 2006). This is not surprising as neutrophils are the first responders to inflammation and are rapidly recruited to the site of action. Nevertheless, in glomerular diseases this recruitment is reported to promote inflammation and dysfunction of the glomerulus (Kitching and Hutton, 2016). Glomerular leukocyte recruitment occurs independent of the classical recruitment cascade, including rolling, adhesion and transmigration (Ley et al., 2007). Instead, leukocytes firmly adhere to the glomerular endothelium, which leads to an abrupt migration stop (Devi et al., 2013; Kuligowski et al., 2006). Moreover, platelets critically contribute to this firm adhesion of neutrophils in the microcapillaries of the glomerulus via P-selectin expressed on platelet surface (Kuligowski et al., 2006). Previous studies have shown that the neutrophil retention time within the glomerular tuft was elevated in response to inflammation (Devi et al., 2013). Moreover, adherent neutrophils secreted reactive oxygen species, proteases and cytokines as well as produced NETs, thereby damaging the GFB (Kessenbrock et al., 2009; Westhorpe et al., 2017).

1.3. Hemolytic uremic syndrome (HUS) severely damages the kidney

The hemolytic uremic syndrome (HUS) is characterized by a TMA (Rafat et al., 2017) and defined by the clinical triad of microangiopathic hemolytic anemia, thrombocytopenia and acute kidney injury. Initially, endothelial injury exposes the underlying collagen resulting in microthrombus formation. The intense appearance of such thrombi captures a vast majority of circulating platelets, thereby leading to thrombocytopenia. In addition, thrombi induce vessel occlusion, which increases the shear stress applied to circulating erythrocytes. Hence, fragmented erythrocytes generate schistocytes and establish a microangiopathic hemolytic anemia. Such a disease cascade is typical for the TMAs, but the outcome is dependent on the target organ (Ruggenenti and Remuzzi, 1991). In HUS, the vessel occlusion limits the renal perfusion and filtration, culminating in acute kidney injury. In contrast, thrombotic thrombocytopenic purpura affects the CNS, which leads to strong neurologic disorders (Ruggenenti et al., 2001). In 1955, the first HUS cases were reported in children (Gasser et al., 1955) and until today mainly children under five years are affected by this syndrome (Bell et al., 1997).

Two different diseases can lead to HUS. The atypical HUS (aHUS) is caused by a rare genetic disorder with an incidence of approx. 2 individuals per million (Loirat and Fremeaux-Bacchi, 2011). Herein, the overactivation of the C3 convertase and additional loss of regulatory mechanisms result in the overactivation of the alternative complement pathway (Sridharan et al., 2018).

The typical HUS, also termed diarrhea-associated HUS, can arise after infections with gram-negative, Shiga toxin-producing *E. coli* (STEC), often termed enterohaemorrhagic *E. coli* (EHEC). The pathogens ingested with food, colonize the gut and secrete virulence factors, such as Shiga toxin (Stx), via outer membrane vesicles released during bacterial growth (Kunsmann et al., 2015). The *E. coli*-derived toxins are structurally and functionally very similar to the toxin of *Shigella dysenteriae,* which has named the entire group of Shiga toxins (Levine et al., 1973). Nevertheless, it is important to differentiate between Shigella-infections and STEC-infections. The former leads to bacillary dysentery and is widely spread among young children in developing countries, whereas the latter causes hemorrhagic colitis or bloody diarrhea and is more common in developed nations (Kotloff et al., 2018; Lee and Tesh, 2019). Even though both infections can culminate in HUS, this study exclusively focuses on the typical HUS arising after STEC-infections (STEC-HUS) (Koster et al., 1978). For

the development of STEC-HUS, a systemic Stx toxemia is required (Karmali et al., 1983). Despite the affiliation of STEC-HUS to the TMAs, it has been shown that endothelial cells are not the exclusive target of Stx (Meyers and Kaplan, 2000). This might suggest that STEC-HUS is not only a simple consequence of endothelial injury leading to the previously described TMA-specific disease cascade.

1.3.1. EHEC infections can culminate in life-threatening STEC-HUS

STEC-HUS is a food-borne disease derived from undercooked beef products or unwashed vegetables, which have been frequently identified as pathogen-vectors (Frank et al., 2011b; Haack et al., 2003; Michino et al., 1999; Riley et al., 1983). Ruminants are the natural reservoir of STEC, thereby explaining the predominating role of beef products, such as milk and meat (Tzipori et al., 2004). Furthermore, in rural areas with high cattle density more STEC-infections and STEC-HUS cases are reported (Haack et al., 2003).

The first symptoms of a STEC-infection, namely diarrhea, abdominal pain and vomiting, occur approx. three days after ingestion (Bell et al., 1994). After an additional two to three days, patients often (90 %) report blood in their stool, mainly derived from damaged interstitial epithelium, and hence seek medical care. HUS develops in approx. 15 % of STEC- infected patients seven days after disease onset, whereas the vast majority spontaneously resolves the infection (Lopez et al., 2010). Approx. 40 % of STEC-HUS patients require at least temporary renal replacement therapy, such as hemodialysis (Trachtman et al., 2012). Residual renal impairment will remain in approx. 20 % of STEC-HUS patients (Andreoli et al., 2002). The clinical course of STEC-HUS is summarized in Figure 4. Though the kidney is the prime target of Stx, impairments of the central nervous system (CNS) are also observed in approx. 10-25 % of STEC-HUS patients (Trachtman et al., 2012). During the acute disease phase, these neurological effects account as the major cause of mortality. Antibiotics, normally given to patients with bacteria-induced diarrhea, were not determined as beneficial in STEC infections and were even found to increase HUS incidence following the infection (Bell et al., 1997; Wong et al., 2000). In addition to bacterial lysis followed by toxin release, certain antibiotics were reported to enhance the production of outer membrane vesicles containing the Stx and the production of the toxin itself (Bauwens et al., 2017).

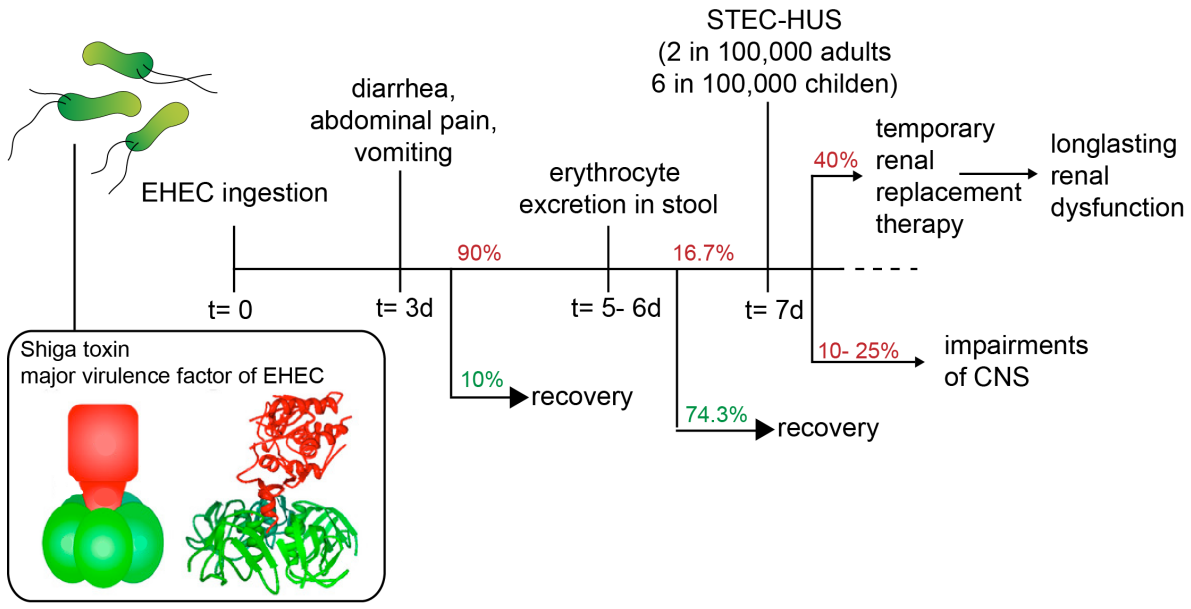

Figure 4: Clinical course of STEC-HUS development and schema of Stx
Detailed scheme showing the symptoms that can occur during STEC-HUS and the possible remaining impairments. Additionally the main virulence factor of EHEC is schematically displayed. Stx scheme was modified from (Kavaliauskiene et al., 2017). CNS: central nervous system, EHEC: enterohaemorrhagic E. coli, HUS: Hemolytic uremic syndrome, STEC: Shiga toxin-producing E. coli

More than 200 different STEC serotypes have been identified in samples of infected patients (WHO, Report June 1998, Germany, Berlin). However, only a few serotypes have the capability to induce STEC-HUS after hemorrhagic colitis or bloody diarrhea. The precise mechanism remains elusive, but there is growing evidence that certain horizontally acquired gene cassettes enhance the pathogen invasiveness, thereby facilitating STEC-HUS induction (Karmali, 2009). An identified gene cassette, for example, allows the bacteria to invade the interstitial epithelium (Moon et al., 1983).

Despite the availability of antibiotics to treat bacterial infections, epidemic STEC-outbreaks have occurred in the last decades (Bell et al., 1994; Frank et al., 2011a; Michino et al., 1999). The most frequent EHEC serotype in humans, O157:H7, is highly infectious requiring only 100-500 bacteria to induce severe infections (Karmali, 2009). Even though O157:H7 has the strongest association with STEC-HUS (Tarr et al., 2005), non-O157 serotypes caused some of the recent outbreaks. The serotype of the German outbreak in 2011, O104:H4, exceeded all previously reported HUS-incidence rates and has been identified as hybrid of EHEC and enteroaggregative *E. coli* (Bielaszewska et al., 2011; Frank et al., 2011b).

STEC-HUS has an incidence of 6 in 100,000 in children younger than five years, and of 2 in 100,000 in adults (Trachtman et al., 2012). Despite STEC-HUS being a considerable health threat, no effective therapy is available (Fakhouri et al., 2017). STEC-HUS patients only receive supportive care such as intravenous hydration or

hemodialysis and renal transplants in severe STEC-HUS cases. In some rare cases, the approved drug Eculizumab for the treatment of the aHUS was reported to benefit STEC-HUS patients, but no general benefit could be determined for STEC-HUS (Delmas et al., 2014; Lapeyraque et al., 2011). Furthermore, targeting of the CXCR4/SDF axis and employment of an anti-Stx antibody were suggested as potential therapy strategies (Donohue-Rolfe et al., 1999; Petruzziello-Pellegrini et al., 2012). Unfortunately, no clinical benefit has been reported from any of the previously mentioned strategies.

1.3.2. Shiga toxin is the central virulence factor of EHECs

In the 1980s, Shiga toxin (Stx) was discovered as the virulence factor leading to STEC-HUS (Koster et al., 1978). Different Stx subtypes were associated with different disease severities and frequencies; Stx1a and Stx2a were identified as the most virulent with Stx2 being the most pathogenic in mice (Melton-Celsa, 2014; Sasaki et al., 2002). Structurally, Stx is composed of a large, enzymatically active A subunit linked to a pentameric B subunit, which mediates receptor binding (Sandvig and van Deurs, 1996). Upon host infection, the invaded pathogens produce Stx in the intestine. After bacteriolysis, it traverses the gut epithelium and subsequently distributes systemically by the circulation. The detailed mechanism of how the toxin escapes the intestinal tract is not fully understood yet (Hurley et al., 1999). There is evidence that once in blood, Stx uses $CD11b^+$ cells as vehicle, delivering the toxin to the target organs, expressing the high-affinity receptor globotriaosylceramide (Gb_3) (Niu et al., 2018). In the kidney, the epithelium, endothelium and glomerular mesangial cells express the Gb_3 (Lingwood, 1994). Gb_3 is structurally variable and the microenvironment of the cellular surface influences the binding affinity to Stx (Distler et al., 2009). After receptor binding, Stx is internalized via receptor-mediated endocytosis (Sandvig and van Deurs, 1996). Intracellularly, the A subunit is activated and acts on the 28S ribosomal subunit, inhibiting protein synthesis (Tumer and Li, 2012).

1.3.3. Neutrophils are highly activated and recruited in STEC-HUS

STEC-HUS patients have elevated numbers of circulating leukocytes, such as neutrophils and monocytes, which has been associated with severe disease progression (Buteau et al., 2000; Coad et al., 1991; Exeni et al., 2018; Walters et al., 1989). Moreover, the cytokine TNFα was increased in blood of STEC-HUS patients (Karpman et al., 1995). In addition to the Stx released by the EHEC, gram-negative bacteria secrete LPS which induces inflammation and primes the immune system. LPS causes endotoxemia, which is frequently determined in patients and induces cytokine production that facilitate STEC-HUS development (Koster et al., 1978).

Locally in the kidney, histological analyses have revealed increased neutrophil levels within the glomeruli (Inward et al., 1997). In addition to the enhanced presence of circulating neutrophils, neutrophil elastase levels were elevated, which is an indicator of increased neutrophil activation (Milford et al., 1989). Studies have shown that isolated neutrophils of STEC-HUS patients, cocultured *in vitro* with human endothelial cells, exhibited higher adhering and injuring potential (Forsyth et al., 1989). Furthermore, neutrophils, isolated from STEC-HUS patients, produced more NETs, a mechanism that potentially promotes microvascular thrombosis (Ramos et al., 2016).

1.3.4. Monocytes and neutrophils critically contribute to STEC-HUS pathogenesis in preclinical models

To investigate the immune mechanisms of the host to STEC-HUS in more detail, preclinical mouse models of STEC-HUS were employed, in which the disease was either induced by inoculation with STEC or by systemic application of Stx combined with LPS to mimic the gram-negative bacterial STEC-infection. LPS itself induces inflammation, but it has been previously investigated that the disease characteristics, such as renal injury, are not LPS-derived (Keepers et al., 2006).

These preclinical models were found to reproduce human neutrophil count and activation levels (Fernandez et al., 2000). Neutrophils were activated in response to STEC-HUS, shown by the upregulation of CD11b (Fernandez et al., 2000). Beyond CD11b-upregulation, murine neutrophils exhibit a greater adhesion ability and enhanced cytotoxic capacity in STEC-HUS (Fernandez et al., 2000). The systemic depletion of neutrophils ameliorated mortality and renal injury in STEC-HUS (Fernandez et al., 2006). Furthermore, ROS production by neutrophils critically contributed to disease pathogenesis, and anti-oxidants were determined to ameliorate the STEC-HUS characteristics: mortality, platelet activation and renal damage (Gomez et al., 2013).

Further murine studies have shown that monocytes and neutrophils promote disease progression. Monocytes contributed to STEC-HUS by cytokine-production and experimental disruption of the CCR1 cytokine signaling pathways resulted in ameliorated renal damage (Ramos et al., 2012). In addition, *Ccr2*-deficient animals, lacking inflammatory monocytes, exhibit reduced renal injury and improved survival (Pohl et al., 2018).

Despite detailed studies on neutrophils and monocytes, the role of resident kidney macrophages in STEC-HUS has not been addressed appropriately. *In vitro* studies indicated the production of proinflammatory cytokines, such as IL-1β, IL-6 and TNFα, in monocytes and macrophages (Foster et al., 2000; Tesh et al., 1994). In a preclinical STEC-HUS model, depletion of hepatic and splenic macrophages ameliorated the STEC-HUS pathogenesis (Palermo et al., 1999). A drawback of this study was the usage of clodronate liposomes for macrophage depletion that in addition to macrophages also diminishes circulating monocytes, a cell population that contributes to STEC-HUS pathogenesis (Pohl et al., 2018).

Besides cellular components, secreted cytokines have been implicated in promoting STEC-HUS. The neutrophil attractants CXCL1 and CXCL2, both produced by parietal cells, enhanced STEC-HUS in mice (Roche et al., 2007). Furthermore, Stx alone was not sufficient for STEC-HUS induction and co-factors, namely TNFα, IL-1β and LPS, were required (Kaplan et al., 1990; van de Kar et al., 1992). Harel *et al.* demonstrated that Stx induced local TNFα-production in the kidneys, suggesting TNFα was needed to prime the renal tissue for Stx-mediated tissue damage (Harel et al., 1993). In addition, *in vitro* studies confirmed that TNFα enhances endothelial Stx-sensitivity by the upregulation of the Gb_3 receptor (van de Kar et al., 1992). Furthermore, the effect of Stx that promotes leukocyte adhesion to cultured endothelium *in vitro* was suggested to be mediated by TNFα (Morigi et al., 1995). Cultured macrophages were found to secrete TNFα after stimulation with Stx *in vitro* (Foster et al., 2000).

Despite common employment of murine models in research, they rarely reproduce the complete phenotype observed in humans. All murine STEC-HUS models mimic clinical features of renal histopathologic changes, but further hallmarks, namely platelet activation, schistocyte formation and leukocytosis, are only reproduced in some models, such as combined Stx/LPS application (Keepers et al., 2006; Mohawk and O'Brien, 2011). Moreover, the Stx/LPS application model eliminates experimental variation due to the amount of Stx delivered into the circulation after STEC-inoculation. Hence, a combined intravenous application of Stx/LPS is the most appropriate model for STEC-HUS.

2. Material and methods

2.1. Material

2.1.1. Mice

All mice were bred and housed under specific-pathogen free conditions in the central animal facility of the Medical Research Center of the University Hospital Essen. As the STEC-HUS phenotype was previously observed to be stable in male mice, these mice – aged 8-14 weeks– were used. For IVM, younger male mice, aged 3-4 weeks were employed. In addition to in-house breeding, male C57BL/6 mice were purchased from Charles River. As the used preclinical STEC-HUS model applies Stx and LPS in a weight-dependent manner, age-matched groups were compared within the experiments. *Cx3cr1*$^{eGFP/+}$ mice were on a C57BL/6 background, thus ensuring comparability to wildtype mice. The animal experiments were conducted in agreement with the guidelines for care and use of laboratory animals and were approved by the "Landesamt für Natur, Umwelt und Verbraucherschutz" (LANUV) Recklinghausen.

Table 1: Employed mice strains

Strain	**First described**	**Animal facility**	**Description**
C57BL/6	C.C.Little, 1921	ZTL MFZ, Charles River	Inbred wildtype strain
Cx3cr1$^{eGFP/+}$	Jung, 2000	ZTL MFZ	Reporter-strain, Heterologous expression of GFP under the control of the *CX$_3$CR1* promotor expressed among others by macrophages, not CX$_3$CR1-deficient

2.1.2. Chemicals and reagents

Table 2: Used chemicals and reagents

Chemical/ reagent	**Manufacturer**
2,4,6-Tris-aminomethyl-phenol	Serva
2-Dodecenylsuccinic-acid (DDSA)	Serva
Bovine serum albumin (BSA) Fraction V	GE Healthcare
Calibrite APC-labelled microbeads	BD Biosciences
Collagenase D	Sigma Aldrich
Complete Protease Inhibitor Mix	Roche
CXCR2 Antagonist (SB225002)	Sigma-Aldrich
Disodium phosphate (0.2 M; Na_2HPO_4)	Carl Roth GmbH
DNase I	Sigma Aldrich
D-Sucrose	Carl Roth GmbH
Enbrel (Etanercept)	Pfizer
Ethanol, 70 %	Carl Roth GmbH
Ethanol absolute	Merck
Ethylendiaminetetraacetic acid disodium salt (EDTA)	Merck Millipore
Fetal calf serum (FCS)	Biochrom
Forene 100 % (Isoflurane)	Abbott GmbH & CoKG
Glutaraldehyde	Sigma-Aldrich
Glycid Ether	Serva
GolgiStop	BD Biosciences
Heparine-Natrium, 25.000 U	Ratiopharm
Hydrofluoric acid	Fa. ACROS Organics
Hydrogen peroxide	Sigma-Aldrich
Immu Mount	Sakura Finetek
Ketamine 10 %	Medstar
L-Glutamine	Sigma-Aldrich
Lipopolysaccharide (LPS)	Sigma-Aldrich
L-Lysine monohydrochloride	Sigma-Aldrich
Methylnadic anhydride (MNA)	Serva
Monosodium phosphate (NaH_2PO_4)	Sigma Aldrich
N-Hexane	Carl Roth GmbH
Sodium hydroxid (NaOH)	Carl Roth GmbH
Osmium tetroxide, 4 %	Science Services
Paraformaldehyde, 95 % (PFA)	Sigma-Aldrich
PBS tablets	Life Technologies

Chemical/ reagent	Manufacturer
Penicillin/ Streptomycin	PAA Laboratories GmbH
PermWash Buffer	BD Biosciences
Privigen hIgG, 100 mg/ml, 10 %	CSL Behring
Propylenoxide	Serva
RMPI 1640 medium	Life Technologies
Shiga toxin	Toxin Technologies
Sodium azide (NaN_3)	Carl Roth GmbH
Sodium chloride (NaCl)	Sigma Aldrich
Sodium periodate ($NaIO_4$)	Carl Roth GmbH
Tissue Tek OCT Compound	Sakura Finetek
Triton X-100	Carl Roth GmbH
VenPure SF ($NaBH_4$)	Sigma Aldrich
Veterinary tissue glue	Sutures
Xylazine 2 %	WDT

2.1.3 Kits

Table 3: Used kits

Kit	Manufacturer
ABC Vectastain system	Vector Laboratories
Bio-Plex Pro Mouse IL-6 Assay, 1 x 96 well	Bio-Rad
Bio-Plex Pro Mouse KC Assay, 1 x 96 well	Bio-Rad
Bio-Plex Pro Mouse MIP-2 Assay, 1 x 96 well	Bio-Rad
Bio-Plex Pro Mouse TNF-Alpha Assay, 1 x 96 well	Bio-Rad
Bio-Plex Pro Reagent Kit with Flat-Bottom Plate, 1x96 well	Bio-Rad
DAB Peroxidase Substrate Kit	Vector Laboratories

2.1.4. Antibodies and dyes

Table 4: Used antibodies and dyes

Antibody/ dye	Clone	Conjugate	Conc.	Company	Usage
Anti-mouse CSF1R	AFS98	none	20 µg/g or10 µg/g	BioXCell	*In vivo* macrophage depletion
CD11b	M1/70	PerCP-Cy5.5, APC	1:200	BioLegend	Neutrophil identification and activation status in flow cytometry
CD31	MEC13.3	AF594	1:200	BioLegend	Endothelial identification and neutrophil activation in flow cytometry
CD45	30-F11	APC-Cy7, APC	1:200	BioLegend	Leukocyte identification in flow cytometry
CD64	X54-5/7.1	PE, PE-Cy7	1:200	BioLegend	Macrophage identification in flow cytometry
Chicken anti-GFP	n/a	none	1:5000	Aves	Labeling of CX_3CR1^+ cells for TEM
DAPI	n/a	none	1:5000	Life Technolog.	Nucleus staining in IHC
EpCAM	G8.8	AF647, BV605	1:200	BioLegend	Epithelial cell identification in flow cytometry
F4/80	BM8.1	BV510, APC, APC-Cy7	1:400 (FC) 1:100 (IHC)	BD Biosciences, Tonbo Bioscience	Macrophage identification in flow cytometry and IHC
Goat anti-chicken	n/a	Biotin	1:200	Jackson Immuno Research	Secondary labeling of CX_3CR1^+ cells for TEM
Gp1bβ	n/a	DyLight649	1:200 (FC)	Emfret Analytics	Platelet identification in flow cytometry

Gr1	RB6-8C5	PE	1:200 (IHC) 2mg/ mouse (IVM)	BioLegend	Labeling of monocytes and neutrophils in IHC and IVM
Ly6C	HK1.4	PerCP-Cy5.5	1:1000	eBioscience	Monocyte identification in flow cytometry
Ly6G	1A8	BV421, PE	1:200	BioLegend	Neutrophil identification in flow cytometry
Rat IgG2a	2A3	none	20µg/g or 10µg/g	BioXCell	Isotype control for *in vivo* macrophage depletion
TNFα	MP6-XT22	BV421	1:100	BioLegend	Intracellular labeling of TNFα in flow cytometry
Qdots	n/a	655	10µl (stock: 2µM)	Life technologies	Vascular label in IVM

2.1.5. Solutions, buffers and media

Table 5: Used solutions, buffers and media and their composition

Solutions, buffer or media	Composition and Preparation	Usage
0.1 %GA/ 4 % PFA	160 µl GA in 40 ml 4 % PFA	Organ fixation for TEM
30 % Sucrose	60 g D-Sucrose 0.2 l P-buffer	Organ dehydration for IHC
4 % Paraformaldehyde (PFA)	20 g PFA 480 ml PBS Heat to 70 °C Add NaOH until clear Adjust pH to 7.4	Fixative used for IHC, TEM and flow cytometry
Anesthesia	8 ml PBS 1 ml Ketamine (100 mg/ml) 1 ml Xylazine (20 mg/ml)	Anesthesia induction for IVM
Blocking Buffer (flow cytometry)	1:66 human IgG in flow cytometry buffer	Blocking of unspecific bindings in flow cytometry
Blocking Buffer (IHC)	50 ml PBT 500 µg BSA	Blocking of unspecific bindings in IHC
Blocking Buffer (TEM)	TBS 10 % FCS 3 % BSA	Blocking of unspecific bindings in TEM

Solutions, buffer or media	Composition and Preparation		Usage
Epon 812	Component A Component B	50.1 g DDSA 37.2 g Glycid Ether 200 ml ddH_20 54.25 g MNA 60 g Glycid Ether 200 ml ddH_20	Embedding resin for TEM
	64.6 g Component A 48.4 g Component B 1.5 ml DMP		
Erylysis buffer	15.58 g NH_4Cl 0.07 g EDTA disodium 2 g $NaHCO_3$ ad. 2 l ddH_2O Adjust pH to 7.3 and sterilize by filtration		Erylysis
Flow cytometry buffer	1x PBS 2 % FCS 0.1 % NaN_3		Used in flow cytometry
Digestion buffer for flow cytometry	Medium	RMPI 1640 10 % FCS 1 % Penicillin/ Streptomycin 0.1 % NaN_3	Digestion of kidney for flow cytometry
	10 ml medium 10 mg Collagenase 1 mg DNase-I		
PB-buffer	28.48 g Na_2HPO_4 5.52 g NaH_2PO_4 In 1 l ddH_2O		Used as primary storage buffer for TEM-sections
PBS (free of Ca and Mg ions)	0.5 l dH_2O 1 PBS tablet (5 g)		Versatile usage
PBT	0.05 % Triton-X 100 in PBS		IHC

Solutions, buffer or media	Composition and Preparation		Usage
PLP buffer	P-buffer	243 ml Na_2HPO_4 (0.2 M) in ddH_2O (autoclaved) 57 ml NaH_2PO_4 (0.2 M) in dH_2O (autoclaved) 300 ml dH_2O (autoclaved) Adjust pH to 7.4	Organ fixative for IHC
	L-Lysine (0.2 M)	6.59 g L-Lysine monohydrate In 200 ml P-buffer Adjust pH to 7.4	
	18.75 ml L-Lysine 18.75 ml P-buffer 12.5 ml 4 % PFA (pH= 7.4) 0.106 g $NaIO_4$		
Protease Inhibitor Mix	1 tablet complete protease inhibitor 10 ml PBS		Protease inhibition for LEGENDplex™
TBS	6.05 g Tris 8.76 g NaCl Adjust pH to 7.4 Ad. ddH_2O to 1 l		Buffer used for TEM-staining

2.1.6. Machines and equipment

Table 6: Used machines and equipment

Machine/ Equipment	Type	Manufacturer
Autoclave	VX-150	Systec-Linden
Automated Olympus analyzer	AU 400	Beckmann Coulter
Centrifuge	5424R 5819R	Eppendorf
Tissue Cauterizer	Change-A-Tip™ high-temp handle	Bovie
Cryostat	CM1950	Leica
Dissecting microscope	S8AP0	Leica
Flow cytometer	LSR Fortessa	BD Biosciences
Fridge/ Freezer	+4 °C/ -20 °C/ -80 °C	Liebherr
Heating block	Thermomixer R	Eppendorf
Ice machine	AF100	Scotman Ice-System
Inverted epifluorescence microscope	Axio Observer Z1	Zeiss
Isoflurane anesthetic device	n/a	UNO
IVC mouse cages	SealSafePLUS	Tecniplast
Microtome	Ultracut S	Reicher
Ventilation pump	MiniVent Type 845	Hugo Sachs Elektronik
Pipettes		Eppendorf
Shaker	MTS2/4	
Perfusion Pump	Single Syringe Pump, "Just Infusion™"	ProSense Laboratory& Process equipment
Tissue homogenizer	ULTRA-TURRAX®	IKA
Transmission electron microscope	Tecnai Spirit 120 kV	FEI
Vibratome	VT 1000S	Leica
Vortex	Vortex-Genie 2	Scientific Industries
Waterbath		Julabo

2.1.7. Consumables

Table 7: Used consumables

Consumable	Manufacturer
6-, 12-, 96- well plate	TPP Switzerland
BD Micro-Fine™+ Insulinspritzen U-100 Insulin 0.5 ml	BD Biosciences
BD Micro-Fine™+ Insulinspritzen U-100 Insulin 1 ml	BD Biosciences
Bottle Top Filter 500 ml 45 mm, 0.22 µm	Corning
Coverslip 40 x 24 mm	Oehmen Labortechnik
Coverslip 60 x 24 mm	Oehmen Labortechnik
Cryomolds	Weckert Labortechnik
Disposal bag	Oehmen Labortechnik
Eppendorf tube (1.5 ml; 2 ml)	Sarstedt
Falcon cell strainer (µm)	BD Biosciences
Falcon tubes (15 ml; 50 ml)	Labomedic
Flow cytometer tube	Sarstedt
Gloves	B Braun
Heparinized micro capillaries	Brand
High vacuum grease	Labchem
Hydrophobic pen	Dako
Hypodermic needle 23 G 0.6 x 25 mm	BD Biosciences
Hypodermic needle 26 G 0.45 x 23 mm	BD Biosciences
Hypodermic needle 27 G 0.4 x 13 mm	BD Biosciences
Hypodermic needle 30 G 0.3 x 13 mm	BD Biosciences
Leukosilk	BSN Medical
MatTek glass	Oehmen Labortechnik
Multichannel pipette basin	Brand
Nylon mesh, 100 µm	Oehmen Labortechnik
PCR-tubes	Biozym Biotech Trading
Pipette filter tips 100-1000 µl	Greiner Bio One
Pipette tips (10, 200, 1000, 5000 µl)	Greiner Bio One
Polyethylene tubing (inner diameter 0.28 mm, outer diameter 0.61 mm)	Smiths
Round Coverslips	ThermoScientific
Serological pipette (5; 10; 25 ml)	Greiner Bio One
Super frost glass slides	SuboLab GmbH

Consumable	Manufacturer
Syringe 10 ml	BD Biosciences
Syringe 1 ml	BD Biosciences
Syringe 20 ml	BD Biosciences
Washing glass basin	Oehmen Labortechnik

2.1.8 Software

Table 8: Employed software

Software	Company
Adobe Illustrator CS5	Adobe
Cytoscape	Open Source
Endnote X9	Thomson Reuters
FACS Diva 6.0	BD Biosciences
FlowJo 10	FlowJo LLC
Graph Pad Prism 6	GraphPad
ImageJ	NIH (Schindelin et al., 2012)
Imaris 7.6.5	Bitplane
LEGENDplex™ data analysis software 7.1.	BioLegend
Microsoft Office 2016	Microscoft Corporation
R-programming language	R Development Core Team
Zen blue	Zeiss

2.2. Methods

2.2.1. Stx-toxicity test

The Shiga toxin 2 (Stx), employed for the induction of the STEC-HUS in mice, loses activity over time. To ensure a stable disease induction among the experiments, the Stx-toxicity was tested on Vero cells prior to each experiment. These cells are cultured renal epithelial cells of *Chlorocebus sabaeus* and have previously been employed in Stx-activity assays (Noda et al., 1987). The initial Vero cell stock was a generous gift by Prof. K. Lang from the Institute of Immunology. The Stx was applied to Vero cells seeded into a 96-well plate (2,000 cell/well, grown for 24 hours prior to toxin application). Three days after incubation, the cell viability was measured using an MTT-assay. The ideal Stx-dose killed 50 % of the Vero cells within three days (IC_{50}).

2.2.2. Preclinical STEC-HUS mouse model

The Stx-dose was experimentally determined prior to each experiment as described in 2.2.1. and injected intravenously with LPS in PBS (0.05625 mg/g). Organs were harvested one and three days post-induction. Kidneys were used to perform immunofluorescence microscopy (IHC), transmission electron microscopy (TEM), flow cytometry and cytokine assays. The blood was analyzed pharmacologically and by flow cytometry.

2.2.3. Macrophage depletion, TNFα-inhibition and CXCR2-inhibtion

An antibody against the colony-stimulating factor 1 receptor (CSF1R) was employed for the depletion of tissue-resident macrophages (Figure 5, shown in green). Mice received two intraperitoneal injections of αCSF1R or the corresponding isotype control (IgG2a). 20 µg/g was injected 6 days prior to STEC-HUS induction and 50 % of this dose on the following day.

Etanercept (10 µg/g) was administered intraperitoneally 6 hours prior to Stx/LPS injection to block TNFα signaling (Figure 5, shown in red). PBS, used as solvent for Etanercept, was administered as control.

The CXCR2-antagonist (SB225002, 150 µl in 1 % DMSO) was injected once intravenously 1 hour prior to Stx/LPS treatment and additionally intraperitoneally 10 min prior to IVM imaging (Figure 5, shown in blue). The used solvent, namely 1 % DMSO, was injected as corresponding control.

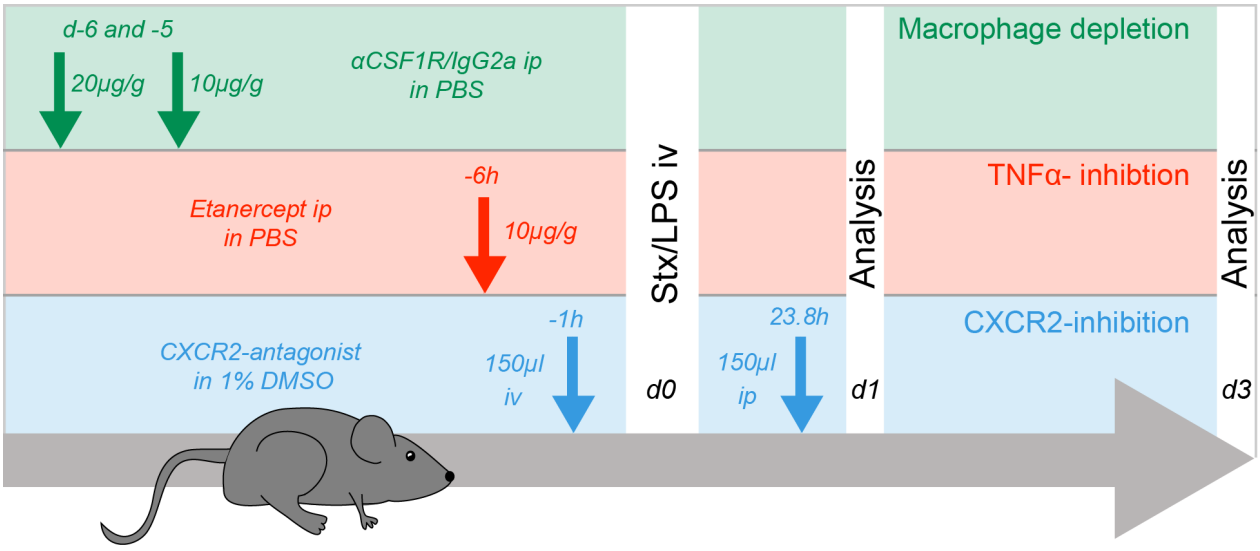

Figure 5: Scheme of experimental procedure

Macrophage depletion, TNFα inhibition and CXCR2-inhibition are summarized. In addition, the Stx/LPS injection and the different timepoints of analysis are indicated.

d: day, DMSO: dimethyl sulfoxide, ip: intraperitoneal, iv: intravenous, LPS: lipopolysaccharide, PBS: phosphate buffered saline, Stx: Shiga toxin

2.2.4. Terminal and non-lethal blood isolation

For terminal blood isolation, the animals were anesthetized via Isoflurane inhalation. Venous blood was collected from the right heart ventricle with a heparinized syringe (2 µl Heparin + 28 µl PBS). For non-lethal blood isolation, peripheral venous blood was collected from the tail vein with a heparinized micro-hematocrit capillary.

2.2.5. Pharmacological blood analysis

For pharmacological analysis, the plasma of the terminally collected blood was used (2.2.4). Therefore, the supernatant of centrifuged blood (10 min, 13,000 rpm, 4 °C) was collected. Blood urea nitrogen (BUN) and creatinine levels were determined by Prof. Faikah Gueler at the Medical School Hannover. An automated Olympus analyzer was used according to the standard protocol provided by the manufacturer.

2.2.6. Renal cytokine analysis

The kidney was homogenized in Protease Inhibitor Mix (800 µl, 4°C) using a tissue homogenizer. After centrifugation (10 min, 13,000 rpm, 4 °C), the supernatant was collected. Cytokines, namely CXCL1, CXCL2, IL-1β, IL-6 and TNFα, were measured using a flow-cytometry based bead assay (LEGENDplex™) following the manufacturer's protocol. The obtained data was analyzed with the corresponding Analysis Software Version 7.1.

2.2.7. Sample preparation for flow cytometry

Flow cytometry analyzes cells according to their size (forward scatter, FSC) and their granularity (sideward scatter, SSC). Moreover, fluorescently labelled antibodies were used to stain surface molecules to distinguish different cell types. Flow cytometry was employed to analyze changes in cell populations, differential expression of surface or intracellular markers, e.g. TNFα. Tissues were harvested one or three days post STEC-HUS induction and stored on ice.

2.2.7.1. Preparation of single cell suspension from the blood

40 µl of whole blood were erylysed (1 ml erylysis buffer, 5 min, RT) and the blood cells collected by centrifugation (5 min, 300 g, 4 °C, supernatant removed). The single cell suspension was subsequently stained with antibodies for flow cytometric analysis.

2.2.7.2. Preparation of single cell suspension from the kidney

Harvested kidneys were collected in chilled flow cytometry digestion buffer, ruptured manually with scissors and incubated (20 min, 37 °C, shaking). Prior to a second incubation, kidneys were meshed with a syringe plunger. Subsequently, samples were homogenized by vigorous pipetting and filtered (mesh size: 100 µm). In the obtained single cell suspension, erythrocytes were eliminated via erylysis (described in 2.2.7.1.). Due to high cell numbers, staining of 1/10 of each murine kidney was sufficient for flow cytometric analysis.

2.2.7.3. Staining for flow cytometry

For the surface marker staining, single cell suspensions were incubated with antibodies diluted in the flow cytometry blocking buffer (20 min, 4 °C, dark). The different concentrations of the antibodies are listed in Table 4. After removal of the antibodies (5 min, 300 g, 4 °C, supernatant removed), the samples were measured or fixed for intracellular staining.

For fixation, 100µl 4 % PFA was added (10 min, 4 °C, dark). If an additional intracellular staining was required, cells were permeabilizated with PermWash buffer and subsequently stained intracellularly. In order to quantify the intracellular TNFα production, blocking of the protein transport was required prior to surface staining, resulting in protein accumulation (GolgiStop 1 µg/ml RPMI medium, 4 h, 37 °C, 5 % CO_2).

Prior to measurement at the BD LSR Fortessa, 10,000 Calibrite APC beads were added to each sample for subsequent calculation of total cell counts.

2.2.7.4. Analysis of flow cytometry data

The obtained flow cytometry data was analyzed using the FlowJo 10 software. First, data sets were compensated to correct the measured spillovers from individual fluorochromes into other detection channels. Compensation allows for a clear differentiation of the positive and negative population. For compensation, “fluorescent minus one” (FMO) controls were used. These are fully stained pooled samples missing one fluorescent marker. Figure 6 compares the obtained raw data to a compensated sample (left to right) and the Ly6C FMO (= completely stained just not Ly6C) with a completely stained sample (top to bottom). The compensation matrix was adjusted until no false-positive signal was found in the FMO control. Moreover, the FMO is required to differentiate the negative population and positive population accordingly.

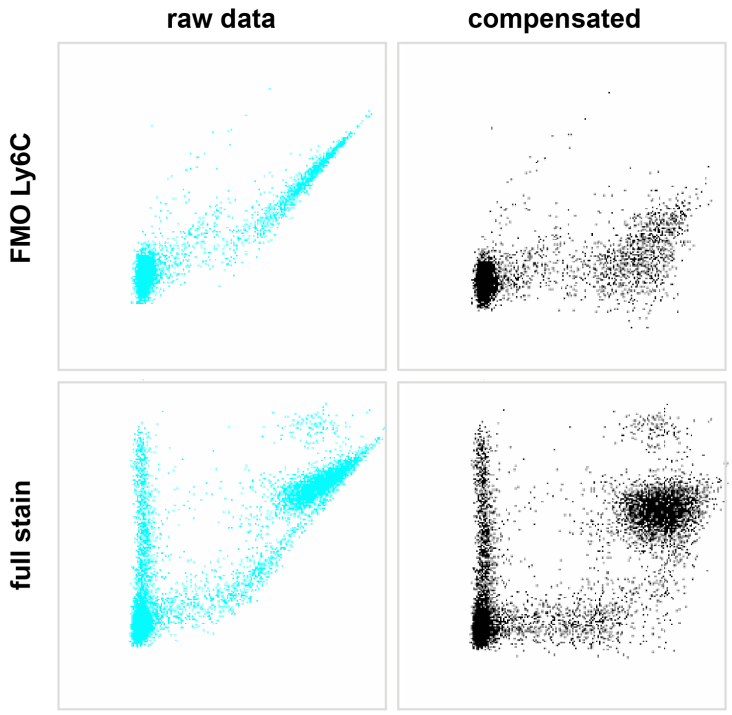

Figure 6: Flow cytometric compensation
Representative flow cytometry dot plots, comparing a Ly6C FMO (top row) to a completely stained blood sample (bottom row) and raw data (left column) to compensated data (right column). It shows that compensation allows for a better differentiation of positive signal from negative. Moreover, the necessity of FMOs is illustrated, as they are required to determine the negative population.
FMO: fluorescence minus one

After manual data compensation, data was analyzed by employing the respective gating strategies for blood (Figure 7) and kidney (Figure 8). To initially exclude the doublets from analysis, the measured width and height of FSC and SSC were opposed. Doublets are defined as two or more particles that are misleadingly considered as one event. This happens when two or more particles pass through the laser beam in such close proximity that the detected signal does not drop back to baseline in between, thereby creating one large event. The recorded voltage pulse of a doublet has the same height, but a different width than a singlet, thereby facilitating their differentiation.

The depicted gates for each fluorescent antibody were determined according to the corresponding FMO control. For blood samples, Gp1b, Ly6G and Ly6C were stained to determine platelets, monocytes and neutrophils. Endothelial cells, macrophages, neutrophils and monocytes were differentiated in the renal tissue by staining of CD45, CD31, CD64, F4/80, Ly6G and Ly6C. The flow cytometer enabled detection of up to eight fluorochromes, thus some of the empty channels were used to determine further molecules. Altering among the conducted experiments, we additionally stained for CD62P, CXCR2, CD31 and intracellular for TNFα. The corresponding gates differed according to the cell population assessed but were all chosen to exclude the negative population visible in the corresponding FMO. After gating, the total number of cells was calculated using the Calibrite APC beads in the sample according to the following formula:

Total number of cells/ ml

$$= \frac{Number\ of\ measured\ cells * 10{,}000\ beads}{Number\ of\ measured\ beads}$$

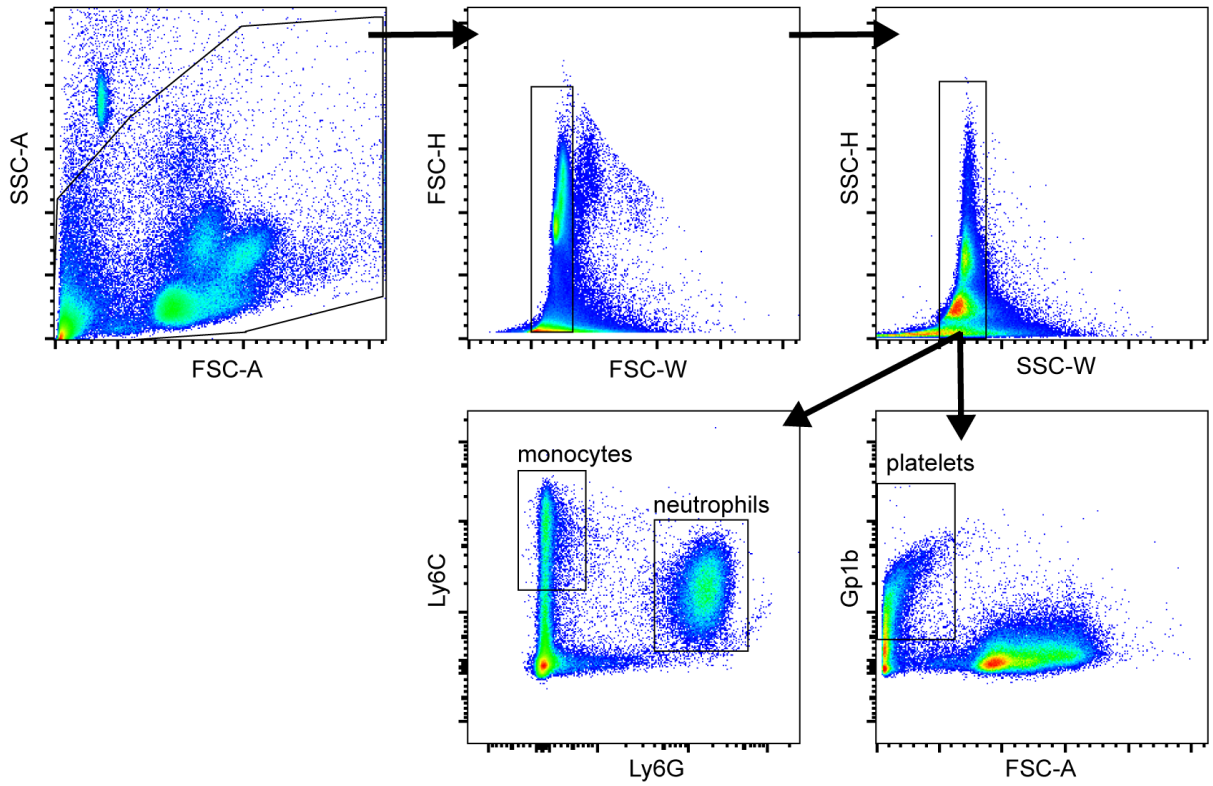

Figure 7: Blood gating strategy in flow cytometry
Employed to determine platelets, neutrophils and monocytes from the circulation by staining Gp1b, Ly6G and Ly6C. A: area, FSC: forward scatter, H: height, SSC: sideward scatter, W: width

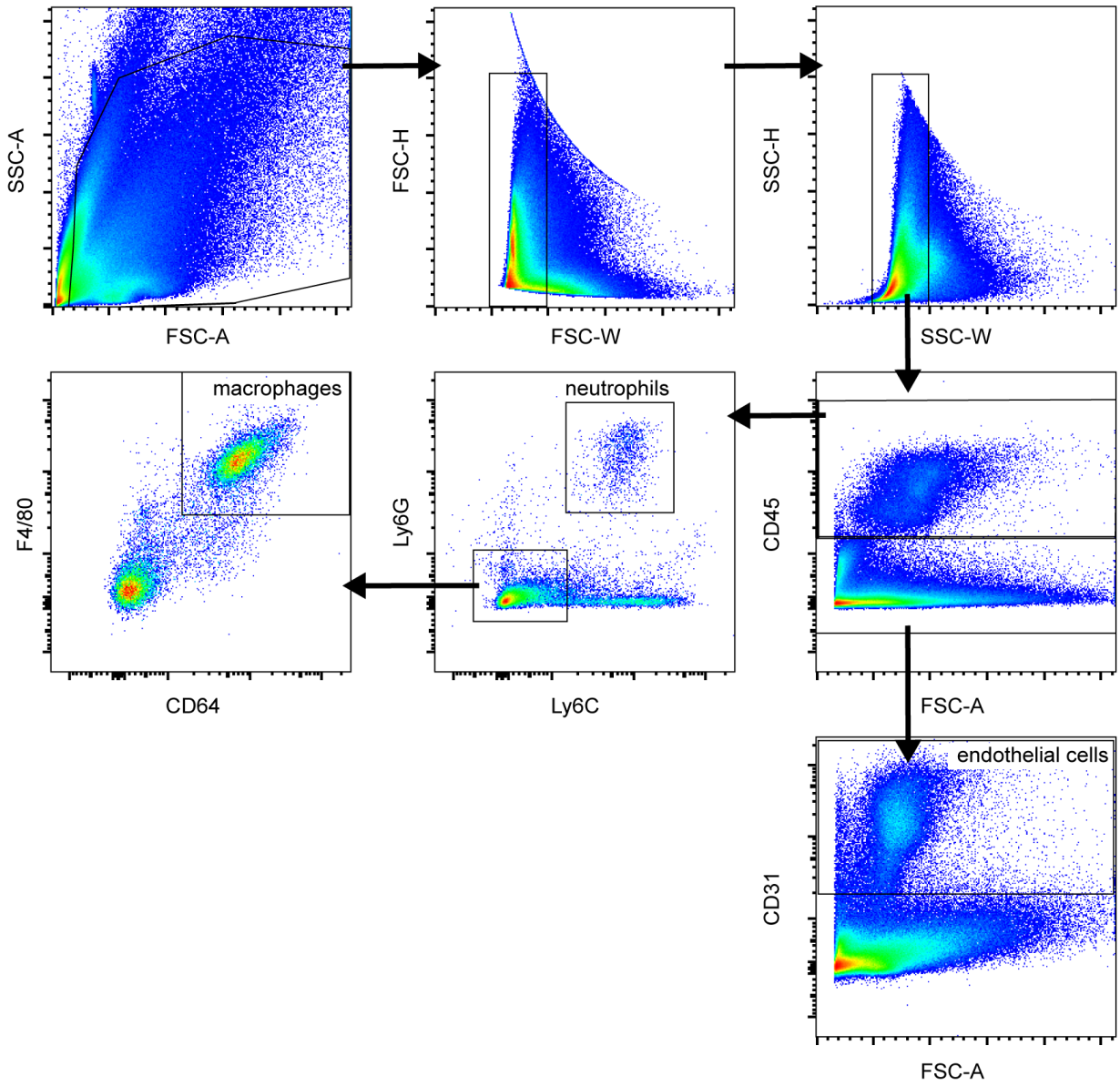

Figure 8: Kidney gating strategy in flow cytometry
Employed to determine endothelial cells, macrophages, neutrophils and monocytes in the renal tissue by staining CD45, CD31, CD64, F4/80, Ly6G and Ly6C.
A: area, CD: cluster of differentiation, FSC: forward scatter, H: height, SSC: sideward scatter, W: width

In addition to the number of cells, the geometric mean of fluorescence (GMOF) of each expression marker was determined. This parameter describes how strong a certain marker is expressed in the chosen population.

2.2.8. Immunofluorescent microscopy (IHC)

In immune fluorescent microscopy, the location, quantity and morphology of renal macrophages and neutrophils were analyzed one day post STEC-HUS induction. Sample preparation was conducted as previously described (Pohl et al., 2018). In brief, kidneys were halved and collected in PLP-buffer (> 12 h, 4 °C, Shaking). After subsequent dehydration in 30 % sucrose (> 12 h, 4 °C, Shaking), organs were embedded in Tissue Tek OCT and frozen in a container filled with dry ice and n-hexane. The sucrose-dehydration and the employed freezing strategy ensured a stable tissue protection. Consecutive sections (10 µm) were cut at the cryostat, collected on super frost glass slides and stored at –20 °C until staining. For staining, the sections were heat-fixed (10 min, 70 °C) and afterwards rehydrated with PBT (500 µl/slide, 1 h, RT). To avoid any unspecific staining, reduce background signal and thus increase the signal-to-noise ratio, sections were incubated with IHC-blocking buffer (500 µl/slide, 1 h, RT). After restricting the staining region with a hydrophobic pen, slides were treated with the antibody cocktail diluted in blocking buffer (200 µl/slide, 1 h, RT). The antibodies used in this study and their corresponding concentrations are listed in Table 4. Using Gr1, which detects both Ly6C and the neutrophil-specific Ly6G, was beneficial, because combination to F4/80 facilitates identification of three different leukocyte subsets, namely macrophages, monocytes and neutrophils. Hence, Gr1 was preferred over Ly6C and Ly6G since IHC can only differentiate few fluorochromes.

Henceforth, the sections were processed in a light-protected manner to minimize fluorochrome bleaching. Nuclei were stained with DAPI (200 µl/slide, 5 min, RT). Subsequently, the sections were washed, embedded with ImmuMount and sealed with a cover slip. After drying, the tissue sections were imaged at a magnification factor of 20 at the inverted epifluorescence microscope in the Imaging Center Essen (IMCES). The images were stitched by the ZEN Software tool and analyzed with ImageJ.

2.2.9. Transmission electron microscopy (TEM)

TEM was employed to visualize the periglomerular macrophages and the parietal cells of the Bowman's capsule. *Cx3cr1*$^{eGFP/+}$ mice were transcardially perfused with cold PBS + 2 mM EDTA to remove blood from the circulation (2 ml, flowrate: 2 ml/min). Afterwards cold PBS + 4 % PFA + 0.1 % GA was applied transcardially, directly fixing the tissue to preserve the ultrastructure (7 ml, flowrate 1 ml/min). Low flowrates were applied to prevent tissue microruptures visible in TEM. After perfusion, the kidneys

were excised, halved and additionally fixed in PBS + 4 % PFA + 0.1 % GA (16 h, 4 °C, shaking). The tissue was then protected from light to preserve the GFP-label and sections were incubated slightly shaking. The fixative was washed off with PBS, sections were cut (70 µm) using a vibratome and processed free-floating in PB-buffer.

Immunostaining was performed free-floating as previously described (Bisht et al., 2016a; Bisht et al., 2016b; Stamatiades et al., 2016). In brief, sections were quenched in 0.1 % $NaBH_4$ in PBS and in 0.3 % H_2O_2 in PBS (5 min each, RT). After incubation with the TEM blocking buffer (1 h, RT) the primary antibody was applied to facilitate binding to the GFP (host: chicken, ON, 4°C). Details on the antibodies and concentrations are provided in Table 4. The next day, the antibody was removed by dual washing with TBS (> 30 min, RT) followed by incubation with the secondary species-specific antibody in TBS + 0.01 % Triton-X 100 (anti-chicken, host: goat, Biotin-labelled, 1.5 h, RT). Reagent A and B from the ABC Vectastain Kit were diluted 1:100 in TBS and applied on the sections (1 h, RT). The DAB reaction was conducted with the DAB Peroxidase Substrate Kit using the manufacturer's protocol. The reaction was neutralized after 3 min with repetitive washing of sections in ddH_2O. Next, 1 % Osmium tetraoxide was used as a post-fixative, washed off with ddH_2O after incubation (30 min, on ice). The free-floating sections were subsequently dehydrated in an ascending Ethanol-gradient (30, 50, 70, 95, 2x 100 %; 10 min each), incubated with 100 % propylene oxide (10min) and finally immersed in Epon 812 / propylene oxide (1:1; ON). Small regions were excised and fixed with Epon 812 to a sample holder prior to Epon 812 incubation (4 h, RT). For cutting, the sample was embedded on a MatTek glass with an Epon 812 filled PCR-tube. After Epon 812 hardening, the MatTek glass was removed with hydrofluoric acid, semi-thin sections (50 nm) were cut on a microtome and collected on a cooper grid for imaging (grid mesh size: 50, coated with ButvarTM resin). Micrographs were collected on a Transmission electron microscope. Imaging and final sample preparation were performed at the Max-Planck Institute of Molecular Physiology, Department of Structural Biochemistry by Sabine Dongard and Dr. Oliver Hofnagel.

2.2.10. Intravital microscopy (IVM)

In this study we used IVM to investigate neutrophil adhesion to the glomerular microvasculature. Given that the renal tissue gains density with increasing age of mice, 3-4 weeks old *Cx3cr1*$^{eGFP/+}$ mice were used for IVM to ensure optical resolution of the glomeruli. One day after STEC-HUS induction, anesthesia was injected ip into mice. The employed IVM technique has been described previously (Devi et al., 2013). In brief, the jugular vein was catheterized with a polyethylene tubing for antibody administration prior to imaging (Gr1 and QTracker, details see Table 4). The solid kidney was excised, fixed on a customized, heated stage, immersed in PBS and coverslipped for imaging. Three randomly chosen fields of view, each including at least three glomeruli, were imaged for 30 min, generating a z-stack-recording every 30 s (z-step size: 6 µm). The obtained videos were processed and analyzed using Imaris 7.6.5.

2.2.11. Statistics

For the representation of the results graphs displaying a scatter plot with bar were created using GraphPad Prism 6. Results are presented as means ± SEM and p-values are depicted in the figures. Normal distribution was tested with the D'Agostino-Pearson omnibus normality test. Two groups were statistically compared by an unpaired t-test if data were normally distributed. Otherwise, unpaired Mann-Whitney (two-tailed) or Kruskal-Wallis tests were performed to compare two or more groups. Where applicable, Dunn's multiple comparison post-hoc corrections were applied. Two-way ANOVA with a Sidak multiple comparison was applied for comparison of multiple parameters (i.e. time and treatment). Significance and normal distribution were calculated using GraphPad Prism 6.

3. Results

Despite the availability of antibiotics, STEC-infections frequently cause epidemics challenging the health system (Bell et al., 1994; Frank et al., 2011b; Michino et al., 1999). Once STEC-infection proceeds to STEC-HUS, patients are treated with supportive care such as plasmaphoresis and transfer, temporal and permanent renal replacement. Even though many different therapy targets have been identified to directly treat STEC-HUS, none have resulted in an effective therapy. Previous studies have identified versatile players of the host immune system that contribute to STEC-HUS severity (Fernandez et al., 2006; Gomez et al., 2013; Pohl et al., 2018). Among others, accumulation and activation of neutrophils were identified as pivotal factors in disease pathogenesis (Buteau et al., 2000; Fernandez et al., 2007). Even though ROS and NETs have previously been identified as damaging factors to the renal endothelium (Gomez et al., 2013), the detailed process inducing such neutrophil recruitment and activation, remains elusive.

Although resident macrophages populate versatile tissues, such as the kidney, their role in STEC-HUS has not been determined yet. A study from 1999 depleted hepatic and splenic macrophages which did have a beneficial effect on the survival of mice (Palermo et al., 1999). Moreover, the study determined that such hepatic and splenic macrophages are responsible for systemic TNFα levels (Palermo et al., 1999). This confirmed previous work that demonstrated the crucial role TNFα plays in STEC-HUS development (van de Kar et al., 1992). Nevertheless, the function of renal macrophages has not been investigated in STEC-HUS.

Besides understanding the mechanistic role of macrophages in STEC-HUS and the upstream events leading to neutrophil activation and recruitment, our study seeks to identify potential therapy targets for STEC-HUS.

3.1. Renal injury occurs after three days in the employed preclinical STEC-HUS model

In order to investigate the role of resident macrophages in STEC-HUS we used a preclinical mouse model in which Shiga toxin (Stx) is injected intravenously in combination with lipopolysaccharide (LPS). LPS is used to mimic the gram-negative bacterial infection of a STEC-HUS and prime the immune system. With kidney dysfunction being a pivotal hallmark of STEC-HUS, the pharmacological analysis of the murine blood serum provided a straightforward measure to access animal wellbeing and disease progression. Creatinine and blood urea nitrogen (BUN) were assessed, as they are routinely used clinically for the determination of kidney function and their elevation indicates an acute renal dysfunction. Three days after Stx/LPS administration a significant increase of these both kidney injury markers were detectable (Figure 9). Furthermore, neither Stx/LPS nor LPS alone elevated the creatinine or the BUN levels one day post injection. Notably, only the combined administration of Stx/LPS induces the increase of the kidney injury markers. Hence these findings validate that Stx is the central mediator for the renal injury observed in STEC-HUS.

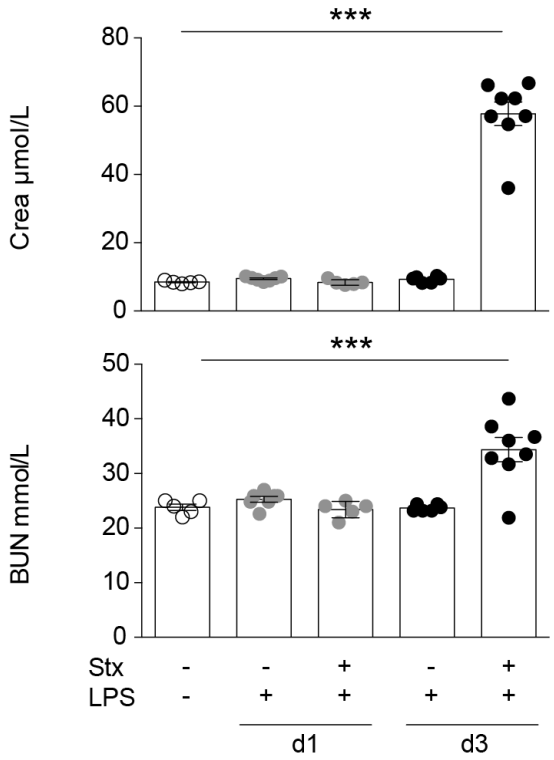

Figure 9: Preclinical STEC-HUS model induced by the intravenous application of Stx/LPS
*To assess the renal injury the levels of creatinine (top) and blood urea nitrogen (bottom) in the murine blood serum were monitored, n= 5-8. White circles depict healthy mice, grey circle mice one day post- Stx/LPS administration and black circles mice 3 days post STEC-HUS induction. Results are presented as means ± SEM, *** p< 0.001. BUN: blood urea nitrogen, Crea: creatinine, d: day, L: liter, LPS: lipopolysaccharide, mmol: millimole, µmol: micromole, Stx: Shiga toxin*

3.2. The dense renal macrophage network is not reduced by STEC-HUS

Next, macrophages were characterized in both, healthy and diseased kidney environments, to investigate their role in STEC-HUS. Using immunofluorescence microscopy, we confirmed a dense renal macrophage network (F4/80$^+$ Gr1$^-$ DAPI$^+$) throughout the entire kidney, which remained unaltered in numbers and location on day one after STEC-HUS induction (Figure 10).

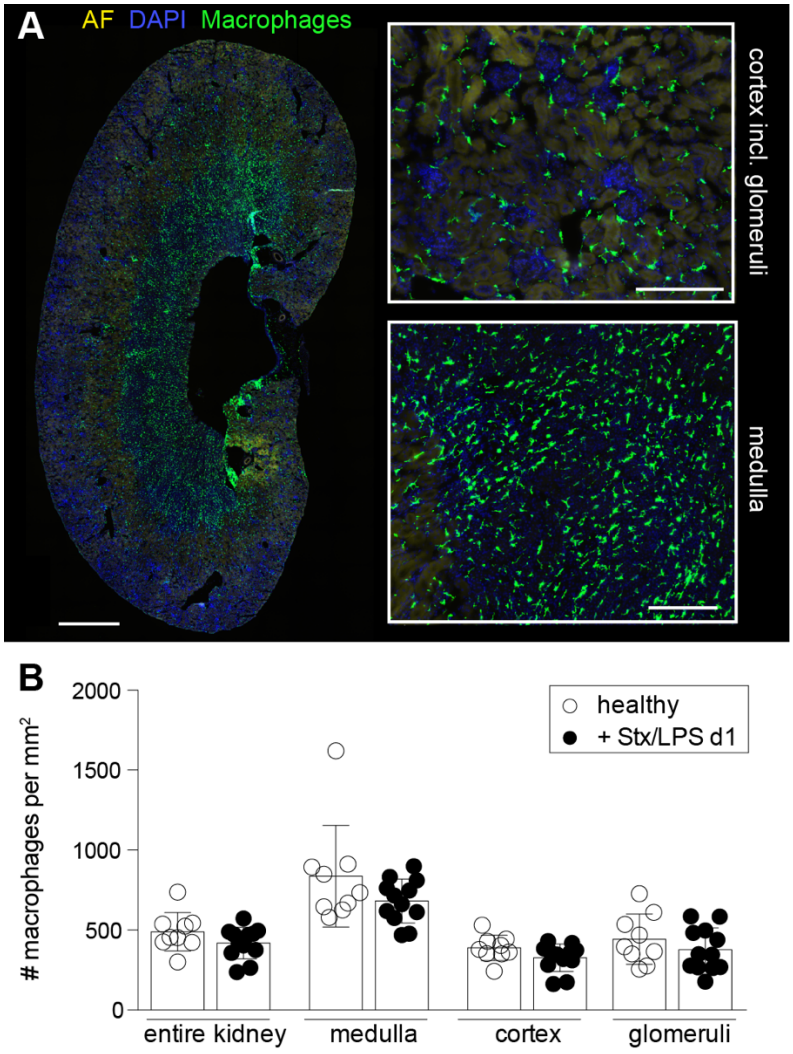

Figure 10: Renal macrophage locate in the tubular space and form a dense network
(**A**) *Entire kidney section of immunofluorescence microscopy is shown on the left with two exemplary zooms of the renal cortex (top) and the medulla (bottom). The dense renal macrophage (green) network is visible. AF (yellow), F4/80 (green) and DAPI (blue) were used to identify renal macrophages (F4/80$^+$ Gr1$^-$ DAPI$^+$). Scale bar overview: 1000 µm, Zooms: 200 µm.* (**B**) *Quantification of microscopy images results in no changes in neither macrophage number nor localization on d1 after Stx/LPS injection, n= 9-12.*
Results are presented as means ± SEM. AF: autofluorescence, d: day(s), DAPI: 4',6-diamidino-2-phenylindole, LPS: lipopolysaccharide, mm: millimeter, Stx: Shiga toxin

To further determine the exact location of the renal macrophages, transmission electron microscopy (TEM) was employed. As shown in Figure 11 the GFP$^+$ macrophages of *Cx$_3$cr1*$^{eGFP/+}$ mice were immunostained and visualized for TEM (Stamatiades et al., 2016). The macrophages (pseudo-colored: green) were located in the tubular space in close proximity to parietal epithelial cells (pseudo-colored: purple) (Figure 11).

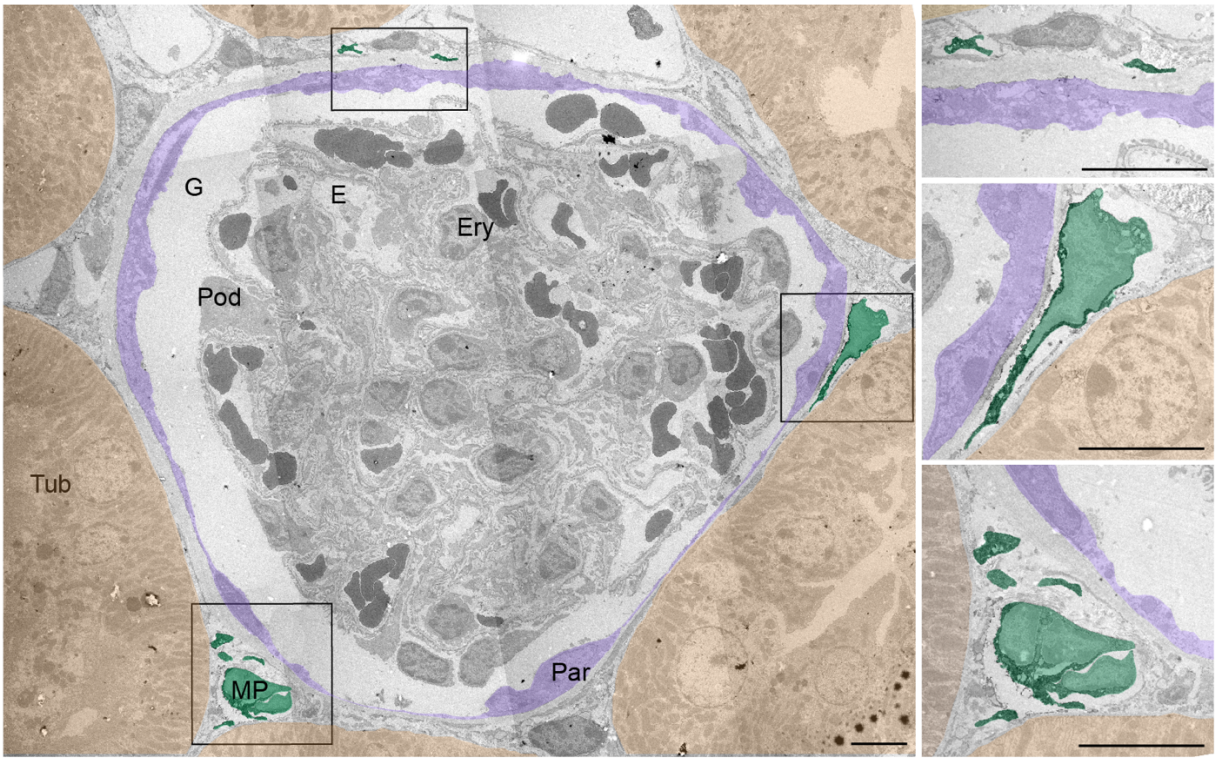

Figure 11: Renal macrophages localize in the tubular space in close proximity to parietal epithelial cells
TEM of Cx3cr1$^{eGFP/+}$ kidney section identified numerous macrophages (green) underneath the parietal cells (purple) of the bowman's capsule and in between the renal tubules (orange). Representative for 3 individual mice. Scale bar: 5µm.
E: endothelium, Ery: Erythrocyte, G: Glomerulus, MP: macrophage, Par: Parietal epithelial cell, Pod: Podocyte, TEM: Transmission electron microscopy, Tub: Tubulus

In addition to spatial distribution, we characterized renal macrophages in regards to their behavior and activation. Intravital microscopy on *Cx$_3$cr1*$^{eGFP/+}$ mice was performed to observe the migratory capacity of macrophages (CX$_3$CR1$^+$ Gr1$^-$) in steady state and one day post STEC-HUS induction. Within 30 min macrophages did not majorly migrate but exhibited marginal dendritic activity (Figure 12). These observations did not change one day after Stx/LPS application (not shown). The minimal movement of renal macrophages confirmed the previously made hypothesis of a tissue-resident macrophage population in the kidney. Of note, inflammatory monocytes were excluded from these analyses by their Gr1-positivity in addition to expression of CX$_3$CR1.

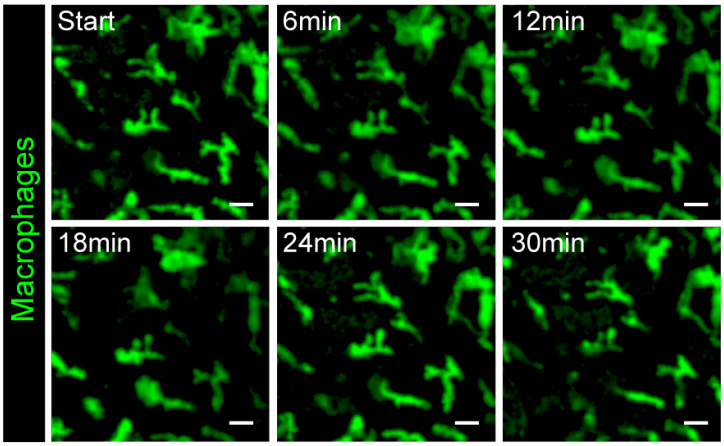

Figure 12: Immotile renal macrophages

Observation of renal macrophages (CX3CR1^{+} Gr1^{-}, green) by IVM for 30min. The macrophages were immotile and only exhibited marginal dendrite activity. Scale bar: 10 µm. Representative for 5 healthy mice. In Stx/LPS the same observations were made by IVM one day after disease induction (not shown).

3.3. Tissue-resident renal macrophages get activated among STEC-HUS

For a more detailed characterization of kidney macrophages ($CD45^+$ $F4/80^+$ $CD64^+$ $Ly6C^-$), we assessed their activation status by flow cytometry. Upon STEC-HUS induction we determined a significant increase in the macrophage activation marker CD64 on their surface, which was strongest three days after STEC-HUS induction (Figure 13).

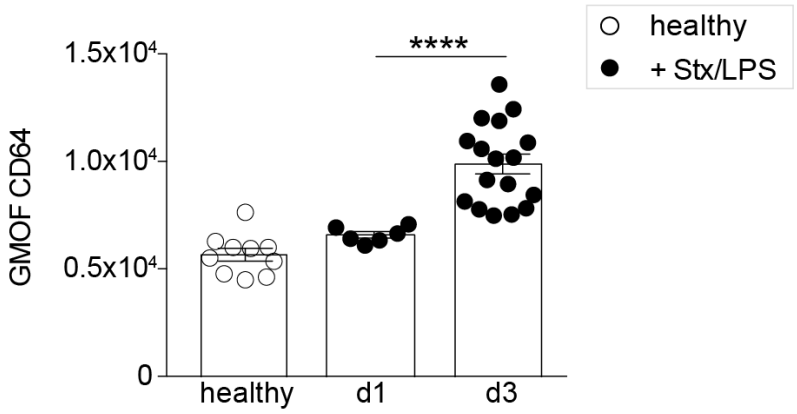

Figure 13:Macrophages get activated during STEC-HUS
Upon STEC-HUS (d1 and d3), flow cytometry of the homogenized murine kidney revealed an upregulation of the activation marker CD64 on the surface of renal macrophages ($CD45^+$ $F4/80^+$ $Ly6C^-$). The employed gating is provided in Figure 8*, n= 6-17.*
*Results are presented as means ± SEM. ****p< 0.0001. CD: cluster of differentiation, d: day(s), GMOF: geometric mean of fluorescence, LPS: lipopolysaccharide, Stx: Shiga toxin*

In addition to the direct analysis of macrophages, we investigated renal macrophages in the context of their microenvironment. To correlate the presence of macrophages to the proteomic tissue microenvironment, we employed spatial mass spectrometry (MS) imaging. Herein, we focused on the renal cortex, which has been identified as region with major changes due to STEC-HUS (Pohl et al., 2018). The spatial MS identified 6829 proteins, which were determined by at least two unique peptides. Among these proteins, the macrophage marker F4/80 was identified and correlated to the other proteins. This strategy was utilized to investigate the proteins that are directly correlated to F4/80 thus depending on the presence of macrophages. 234 proteins, differentially expressed among healthy and STEC-HUS induced mice (Table 9), were determined to strongly correlate (p-value < 0.01) with the abundance of macrophages. Next, these proteins were also analyzed using the pathway enrichment tool Cytoscape with the ClueGO plugin (Bindea et al., 2009). This tool comprehensively groups and visualizes proteins to biological contexts thereby providing a valuable overview of the altered proteomic micromilieu in certain

conditions. The results showed enriched pathways induced by STEC-HUS as nodes and corresponding clusters, which are defined by the annotated proteins (234 in this study, Figure 14). The three clusters of metabolism, morphogenesis and biogenesis were dominantly identified in the enrichment analysis. Interestingly, proteins involved in TNFαR-signaling were abundant in all three major clusters (Figure 14).

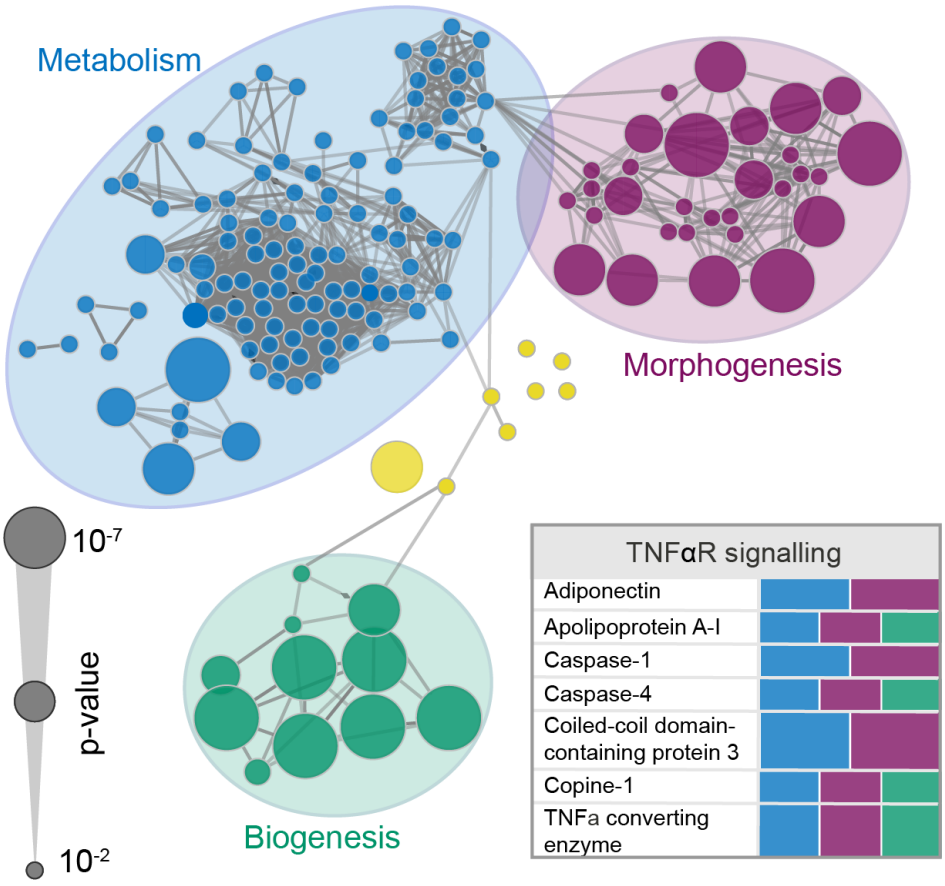

Figure 14: Phenotypical switch of macrophages in response to STEC-HUS
Correlation of F4/80 to the other proteins identified by spatial MS revealed 234 proteins to be regulated in correlation to macrophages and were differentially expressed (p< 0.01) after STEC-HUS induction compared to healthy control mice. A pathway enrichment analysis of these correlated proteins demonstrate enhances metabolic processes and an upregulation of TNFα signaling, n= 6-8..
TNFα: tumor necrosis factor α, R: receptor

These findings provide first hints that macrophages might regulate STEC-HUS response via TNFα-signaling. To further investigate this hypothesis, we stained TNFα intracellular in renal tissue macrophages for flow cytometry. The majority of renal macrophages was TNFα-positive and intracellular TNFα accumulated in macrophages after Stx/LPS treatment (Figure 15). Conclusively, these findings demonstrate that renal macrophages directly produce TNFα in response to STEC-HUS.

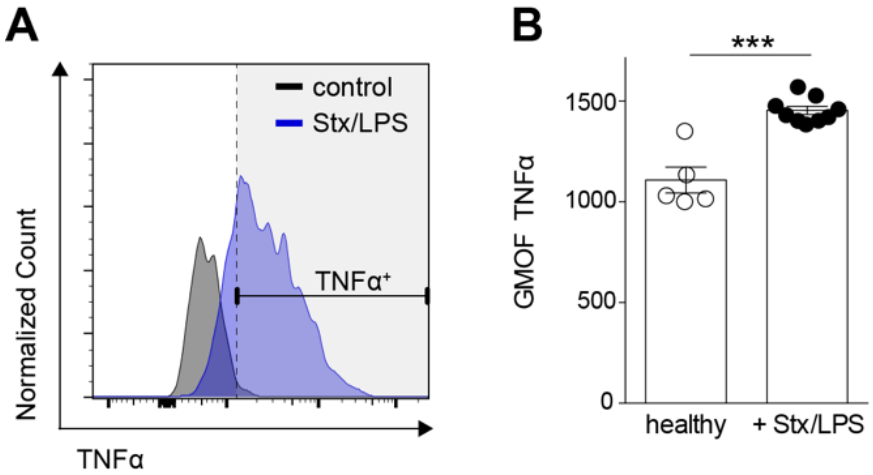

Figure 15: Macrophages respond on day 3 after STEC-HUS induction by TNFα-upregulation
(**A**) *Representative histogram of intracellular TNFα (green) in macrophages (CD45$^+$ F4/80$^+$ CD64$^+$ Ly6C$^-$) in comparison to the staining control (black, FMO) revealed production of TNFα by macrophages three days after Stx/LPS treatment, n= 8.* (**B**) *Flow cytometry of the homogenized murine kidney showed that TNFα expression was increased in renal macrophages (CD45+ F4/80+ CD64+ Ly6C–) of Stx/LPS injected animals in comparison to healthy controls. The employed gating strategy is provided in* Figure 8*, n=5-9.*
*Results are presented as means ± SEM. ***p< 0.001. GMOF: geometric mean of fluorescence, LPS: lipopolysaccharide, Stx: Shiga toxin, TNFα: tumor necrosis factor α*

3.4. Renal macrophages express CSF1R and are efficiently depleted by αCSF1R

Generally, macrophages are described as sentinel cells and local regulators of immune responses and their survival, proliferation and differentiation is controlled by CSF1-signaling (Pollard, 2009). Hence, CSF1R-antibodies (αCSF1R) resemble a well-established approach for macrophage depletion in numerous tissues (MacDonald et al., 2010). In this study, we aimed at depleting tissue-resident macrophages, including renal macrophages, to assess their role in STEC-HUS. By flow cytometry, tissue-resident macrophage within the kidney were determined as CSF1R-positive and showed that intraperitoneal injection of αCSF1R efficiently depleted them (Figure 16). IgG2a was administered as corresponding isotype control.

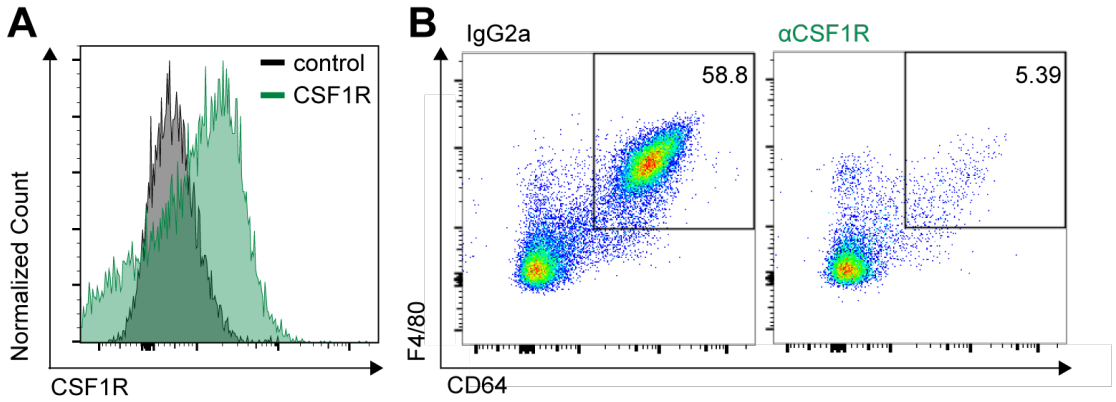

Figure 16: Renal CSF1R-positive macrophages are depleted by αCSF1R
Flow cytometry of the homogenized murine kidney revealed that tissue macrophages ($CD45^+F4/80^+CD64^+Ly6C^-$) express CSF1R and can be depleted via intraperitoneal αCSF1R administration. (**A**) *Depicted is the representative GMOF of CSF1R on renal macrophages compared to an FMO-staining control.* (**B**) *Pseudo-color dot plot showing the macrophage population in the indicated gate comparing isotype control (IgG2a) to αCSF1R-treated mice. The employed gating strategy is provided in* Figure 8*, n=5.*
α: antibody, CD: cluster of differentiation, CSF1R: colony-stimulating factor 1 receptor, FMO: fluorescence-minus-one, IgG2a: corresponding isotype, GMOF: geometric mean of fluorescence

Additionally, immunofluorescence microscopy was employed to illustrate depletion efficiency of resident macrophage (F4/80$^+$ Gr1$^-$ DAPI$^+$) within the kidney (Figure 17 A). Furthermore, such analysis revealed that the macrophage network, more pronounced in the renal medulla than in the cortex and implemented glomeruli, was depleted evenly among the three distinct kidney compartments (Figure 17 B).

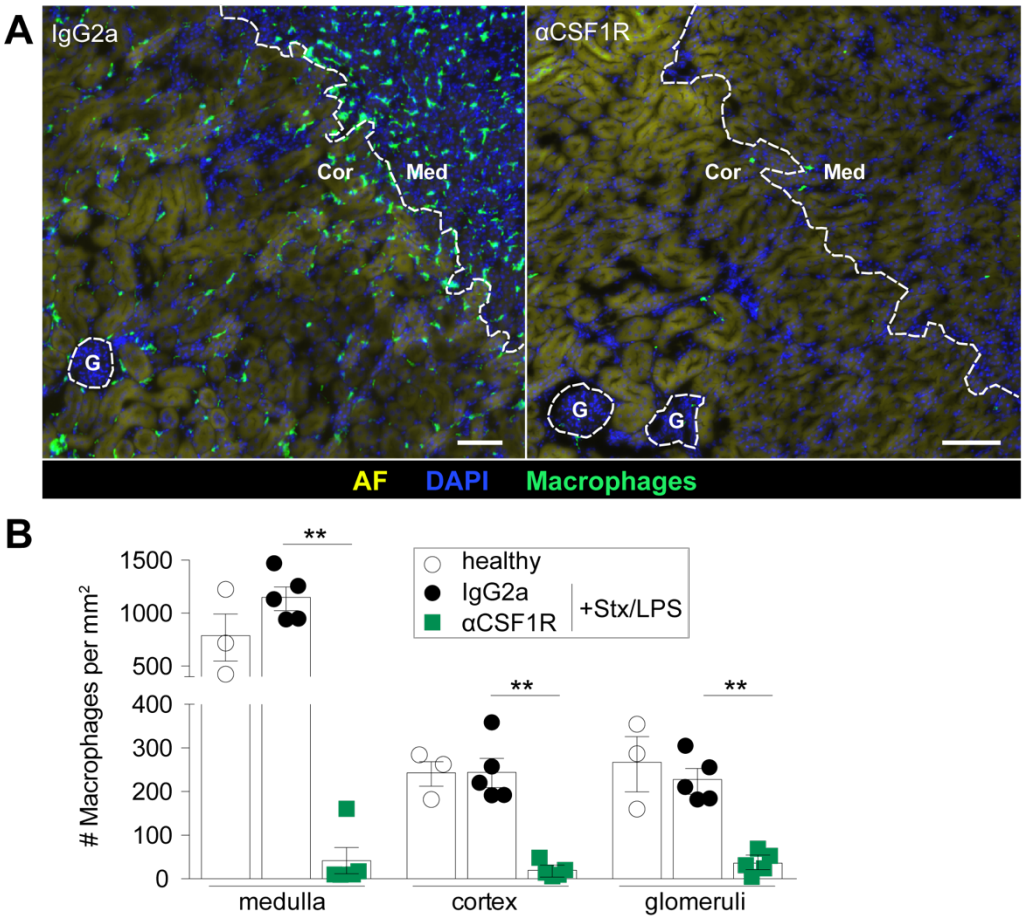

Figure 17: Macrophages are depleted uniformly in the renal medulla, cortex and glomeruli by αCSF1R
(**A**) *Immunofluorescence microscopy showed that the dense macrophage network (F4/80$^+$ Gr1$^-$ DAPI$^+$) present in the IgG2a control is depleted by αCSF1R. Scale bar: 100 µm. Image is representative for 5 animals.* (**B**) *Quantification of immunofluorescence microscopy images revealed a uniform renal macrophage (F4/80$^+$ Gr1$^-$ and DAPI$^+$) depletion in the medulla, cortex and glomeruli, n= 3-5.*
*Results are presented as means ± SEM. **p< 0.01. αCSF1R: antibody against the colony-stimulating factor 1 receptor, AF: autofluorescence, Cor: kidney cortex, DAPI: 4',6-diamidino-2-phenylindole, G: glomerulus, IgG2a: control isotype, Med: kidney medulla*

In a previous study, the αCSF1R-depleted macrophage population has shown to both, reverse and recover, within four weeks (Kitic et al., 2019; Mora-Bau et al., 2015). To determine whether the depletion remained persistent for the time course of STEC-HUS (till d3), we monitored the resident macrophage population. Flow cytometry revealed that tissue macrophages were continuously diminished during the investigated disease course (Figure 18 A). In addition to differentiated tissue macrophages, their circulating precursors, namely monocytes, are CSF1R-positive

(Byrne et al., 1981). As their role has already been elucidated in STEC-HUS (Pohl et al., 2018), we aimed at establishing a depletion approach uniquely targeting tissue-resident macrophages. Flow cytometry of blood confirmed that the monocyte population (CD45$^+$ F4/80$^+$ Ly6C$^+$ Ly6G$^-$) was not affected by αCSF1R-treatment at disease induction (d0) (Figure 18 B).

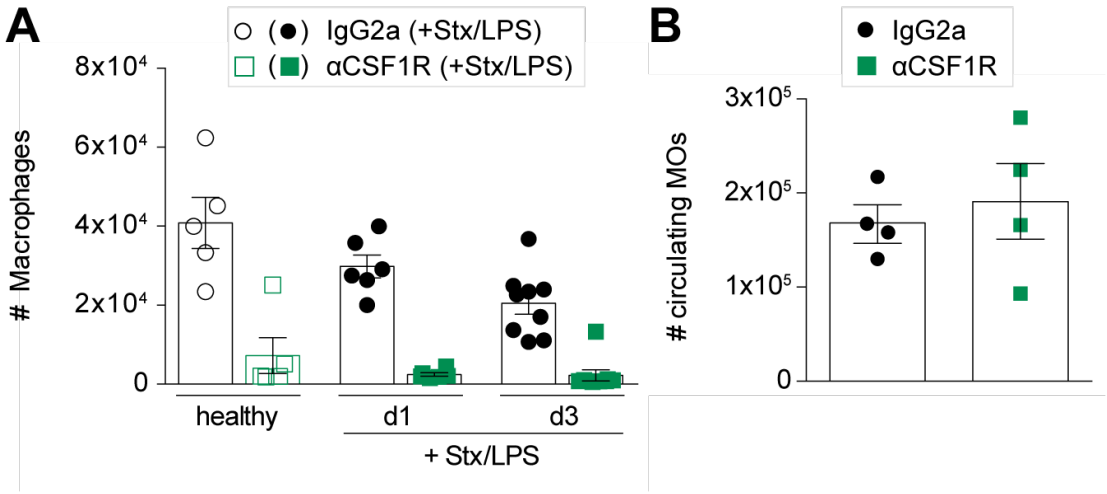

Figure 18: αCSF1R persistently depletes renal macrophages but not circulating monocytes
(**A**) *Flow cytometry of the homogenized murine kidney revealed that tissue macrophages (CD45$^+$ F4/80$^+$ CD64$^+$ Ly6C$^-$) remain depleted during STEC-HUS course of three days. n= 5-9.* (**B**) *In blood, flow cytometry demonstrated that administration of αCSF1R did not reduce circulating inflammatory monocytes (CD45$^+$ F4/80$^+$ Ly6C$^+$ Ly6G$^-$), n= 4. The employed gating strategies are provided in* Figure 8 *(kidney) and Figure 7 (blood).*
Results are presented as means ± SEM. αCSF1R: antibody against colony-stimulating factor 1 receptor, d: day(s), IgG2a: control isotype, LPS: lipopolysaccharide, MOs: monocytes, Stx: Shiga toxin

Previously, the renal macrophage population (F4/80$^+$ CD64$^+$) has been classified according to their CD11b and CD11c expression into two types of monocyte-derived macrophages (CD11b^{high} CD11c^{high} and CD11b^{high} CD11c^{low}) and long-lived kidney-resident macrophages (CD11b^{int} CD11c^{int}) (Puranik et al., 2018). By flow cytometry the kidney-resident macrophage population was determined as the most abundant cell population, followed by the CD11c^{high} monocyte-derived macrophages (Figure 19). αCSF1R-mediated depletion employed in this study mostly affected the kidney-resident macrophages and had only minor effects on the monocyte-derived populations (Figure 19).

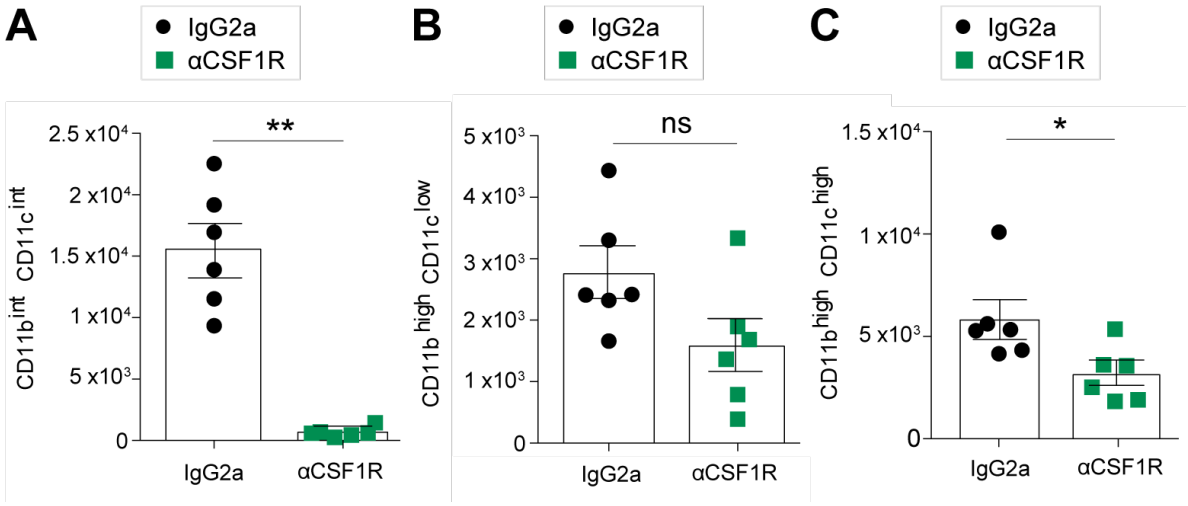

Figure 19: The population of kidney-resident macrophages is predominantly targeted by αCSF1R
*Renal macrophages (F4/80⁺ CD64⁺) were classified according to Puranik et al.,2018 into kidney-resident macrophages (CD11b^int CD11c^int, **A**) and two subtypes of monocyte-derived macrophages (CD11b^high CD11^low and CD11b^high CD11c^high, **B** and **C**). αCSF1R administration strongly depleted kidney resident macrophages and had less pronounced effects on the monocyte-derived macrophages. The depicted cell populations were delineated via subgating from the macrophage population* Figure 8*, n=6.*
*Results are presented as means ± SEM. * p< 0.05, ** p< 0.01. αCSF1R: antibody against colony-stimulating factor 1 receptor, IgG2a: control isotype*

3.5. Macrophage depletion reduces TNFα and kidney injury

Hepatic and splenic macrophages have been shown to promote STEC-HUS development (Palermo et al., 1999). As the underlying mechanism remains elusive, we sought to investigate both: (i) how renal macrophages contribute to STEC-HUS and (ii) the mechanism that contributes to disease progression. To this end, we employed the previously established macrophage depletion in our preclinical mouse model. To further investigate the role of macrophages for local TNFα levels, we performed a flow-cytometry based bead assay (LEGENDplex™) on kidney homogenates. In accordance with macrophages identified as TNFα-source, depletion of this cell population reduced local TNFα levels in the kidney. In absence of tissue macrophages, TNFα was reduced to baseline levels of healthy mice (Figure 20 A), thus suggesting macrophages are a major source of TNFα.

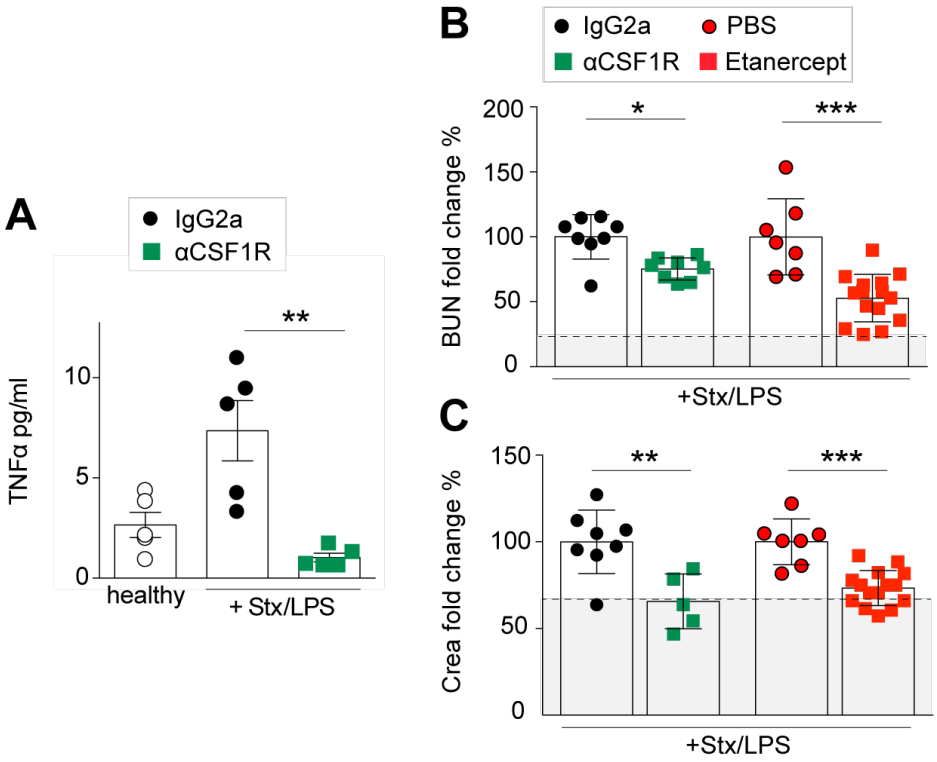

Figure 20: Macrophage depletion reduces TNFα and kidney injury

(**A**) *αCSF1R-mediated macrophage depletion diminished local TNFα in the kidney to baseline levels one day after Stx/LPS administration. Cytokine levels were analyzed in kidney homogenates by LEGENDplexTM. n= 5.* (**B, C**) *BUN and Crea levels were determined in the blood serum to monitor the renal injury induced in STEC-HUS. The two employed intervention strategies: intraperitoneal αCSF1R-antibody injection for macrophage depletion and intravenous Etanercept application for TNFα-neutralization, both reduced kidney injury in STEC-HUS. IgG2a and PBS were administered as corresponding controls. The dashed line and grey sector indicate levels of healthy individuals, n= 7-15.*

*Results are presented as means ± SEM. * p< 0.05, ** p< 0.01, *** p<0.001. αCSF1R: antibody against colony-stimulating factor 1 receptor, BUN: blood urea nitrogen, Crea: Creatinine, IgG2a: control isotype, LPS: lipopolysaccharide, ml: milliliter, PBS: phosphate buffered saline, pg: picograms, Stx: Shiga toxin*

To investigate the direct contribution of macrophages and TNFα to STEC-HUS pathogenesis, we assessed BUN and creatinine levels in murine blood serum from macrophage-depleted (αCSF1R treatment) and TNFα-inhibited (Etanercept treatment) mice. Etanercept contains a TNFR that binds TNFα and thereby neutralizes the cytokine. It was administered in PBS, thus this vehicle was used for treatment of corresponding control animals. Both kidney injury markers were significantly decreased by both intervention strategies (Figure 20 B, C), thereby highlighting a central role of macrophages and their product TNFα in STEC-HUS. Etanercept restored the renal function comparably efficient than macrophage depletion. Nevertheless, comparison of both renal injury markers revealed that none of these interventions fully recovered the renal function measured in healthy animals.

To exclude that macrophages themselves were affected by TNFα-inhibition, these cells were quantified by flow cytometry at day three when renal dysfunction was measured. This analysis revealed that the tissue-resident macrophages were only significantly reduced by αCSF1R-treatment, but not by Etanercept injection (Figure 21). Hence, we excluded that beneficial effects induced by Etanercept originated from side-effects resulting in a diminished macrophage population and thus ameliorated kidney function was purely based on TNFα-inhibition.

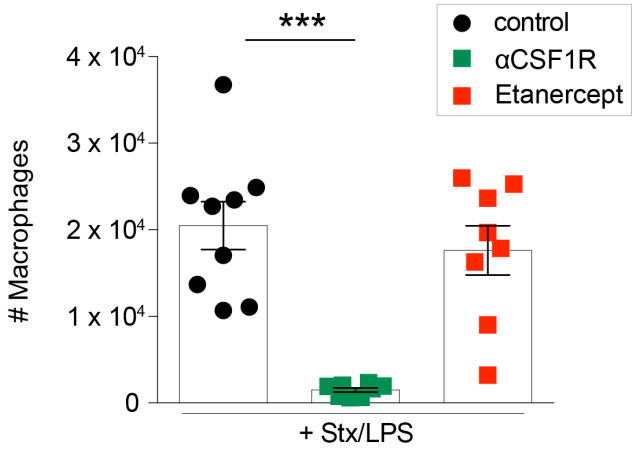

Figure 21: Etanercept does not diminish renal tissue-resident macrophages
Flow cytometry of kidney homogenates three days after Stx/LPS injection revealed that macrophages (CD45⁺ F4/80⁺ CD64⁺ Ly6C⁻) were only reduced by αCSF1R. The corresponding flow cytometry gating strategy is provided in Figure 8*, n=8-9.*
*Results are presented as means ± SEM. *** p<0.001. αCSF1R: antibody against colony-stimulating factor 1 receptor, LPS: lipopolysaccharide, Stx: Shiga toxin*

3.6. STEC-HUS hallmarks are promoted by macrophages

After we identified macrophages and their product TNFα as critical contributors to renal dysfunction in STEC-HUS we sought to identify the underlying mechanisms. For this, we analyzed central hallmarks of STEC-HUS, namely endothelial injury, platelet activation and subsequent thrombocytopenia (Robson et al., 1988; Tarr et al., 2005) in control and macrophage-depleted mice by flow cytometry. The corresponding gating strategies to delineate endothelial cells in the kidney and platelets in peripheral blood are detailed in Figure 8. The detrimental effects of Stx on endothelial cells were described more than three decades ago (Kavi et al., 1987). Gb_3, the Stx-receptor, is expressed -among others- by endothelial cells and toxin binding can inhibit protein biosynthesis, resulting in apoptosis (Tumer and Li, 2012). Endothelial dysfunction is a major hallmark of all TMAs and has been extensively described in STEC-HUS (Petruzziello-Pellegrini et al., 2013). Therefore, we initially assessed endothelial injury in the kidney by Annexin V staining, which binds to phosphatidylserine expressed on apoptotic cells. With elevation of kidney injury markers (Figure 14), we detected increasing numbers of apoptotic (Annexin V^+) endothelial cells ($CD45^-$ $CD31^+$) three days after STEC-HUS induction (Figure 22 A). Compared to healthy or d1 mice, the number of apoptotic endothelial cells doubled on day three in isotype-treated mice. This increase was dampened by the depletion of tissue macrophages. Moreover, one day after Stx/LPS-injection, the circulating platelets ($Gp1b^+$, small cells) were activated unlike in healthy mice. The platelet activation was determined by increased CD62P levels. In mice lacking macrophages, such platelet activation was fully abolished (Figure 22 B). CD62P is found on the surface of activated platelets and is stored intracellularly in α-granules prior to representation on the surface. Once transported to the platelet's surface, CD62P levels correlated with the size and stability of thrombi (Merten and Thiagarajan, 2000). Hence, the enhanced activation of platelets in STEC-HUS can be associated with a greater ability of thrombus formation.

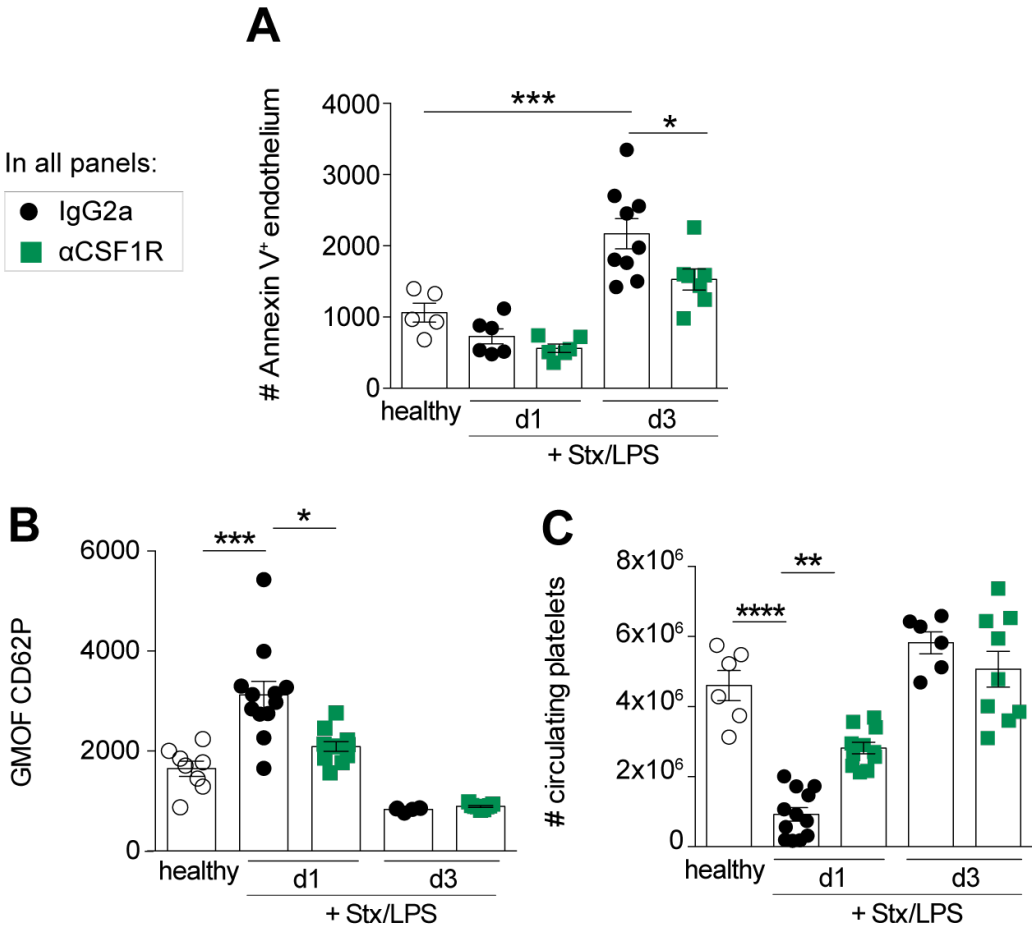

Figure 22: Macrophages promote STEC-HUS hallmarks

The typical hallmarks of STEC-HUS, namely endothelial injury (**A**), *platelet activation* (**B**) *and thrombocytopenia* (**C**) *were analyzed by flow cytometry. Platelet activation was measured by the GMOF of CD62P. The corresponding gating strategies are shown in Figure 8 (kidney, A) and Figure 7 (blood, B and C), n= 5-12.*

*Results are presented as means ± SEM. *p< 0.05, **p< 0.01, ***p< 0.001, ****p<0.0001. αCSF1R: antibody against colony-stimulating factor 1 receptor, CD: cluster of differentiation, d: day(s), GMOF: geometric mean of fluorescence, IgG2a: control isotype, LPS: lipopolysaccharide, Stx: Shiga toxin*

Next, assessing the number of circulating platelets by flow cytometry confirmed the frequently observed thrombocytopenia of human patients in our murine disease model one day after STEC-HUS induction (Figure 22 C). Moreover, we found macrophage depletion to partially restore thrombocytopenia. Conclusively, these results indicate that macrophages are upstream of endothelial injury, thrombocytopenia and platelet activation, which are closely related symptoms in STEC-HUS.

3.7. Tissue-resident macrophages enhance the neutrophil response

Neutrophils have previously been reported to promote STEC-HUS and increased abundance of neutrophils is associated with a poor prognosis (Buteau et al., 2000). Moreover, tissue macrophages are known to mediate neutrophil recruitment in multiple situations (Kolaczkowska and Kubes, 2013). To investigate the role of macrophages in the neutrophil response in STEC-HUS, we employed our established αCSF1R-depletion model. First, we addressed effects that the tissue-resident macrophage population might have on circulating neutrophils followed by effects seen in the local kidney tissue. Hence, we contribute to the understanding how neutrophils are primed to aggravate STEC-HUS (Fernandez et al., 2006; Gomez et al., 2013).

3.7.1. Activation of circulating neutrophils is orchestrated by tissue-resident macrophages

Replicating clinical situations, we determined increased levels of neutrophils within the circulation upon STEC-HUS by flow cytometry (Figure 23). After pre-gating for leukocytes ($CD45^+$) neutrophils were characterized as $Ly6G^+$ $Ly6C^{dim}$ (Figure 23 A) and we observed that more neutrophil patrol the circulation one day after STEC-HUS induction (Figure 23 B).

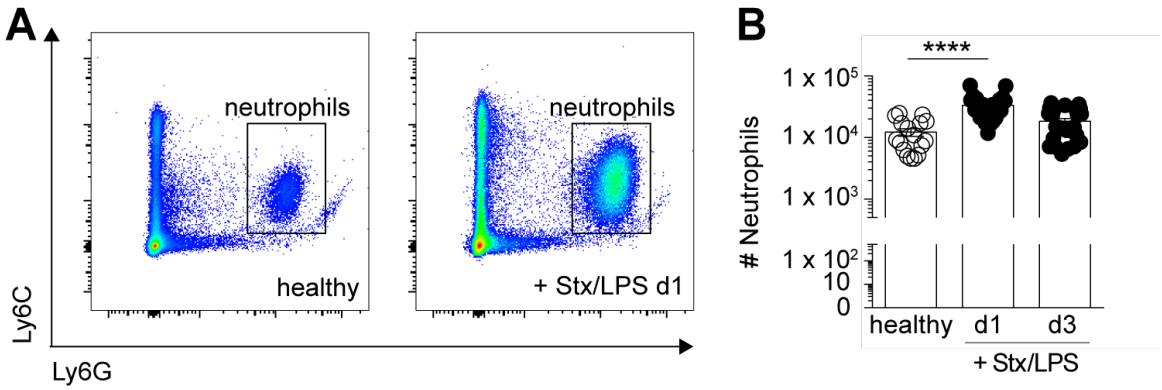

Figure 23: Circulating neutrophils accumulate one day after STEC-HUS induction
(**A**) *Circulating neutrophils were identified in flow cytometry as $CD45^+$ $Ly6G^+$ $Ly6C^{dim}$. Pseudo-color dot plots compare healthy mice to Stx/LPS-induced mice (d1) and are representative for 12-16 mice.* (**B**) *Quantification of circulating neutrophils during experimental STEC-HUS course by flow cytometry. Detailed gating strategy is provided in Figure 7, n= 12-16*
*Results are presented as means ± SEM. ****p< 0.0001. d: day(s), corresponding isotype, LPS: lipopolysaccharide, Stx: Shiga toxin*

To understand the role of tissue-resident macrophages on circulating neutrophils we monitored their activation status by flow cytometry. Herein, neutrophils were highly activated, especially one day after disease induction, thus correlating temporally with enrichment of neutrophil in circulation. In our study, we demonstrate neutrophil activation by upregulation of platelet endothelial cell adhesion molecule-1 (PECAM-1), also known as CD31, and CD11b on the cellular surface (Figure 24).

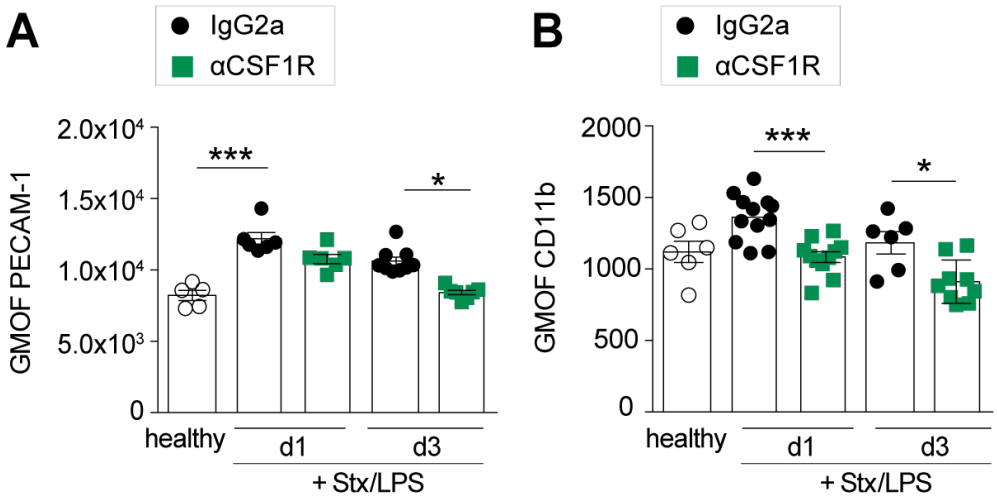

Figure 24 Tissue-resident macrophages activate circulating neutrophils
(**A**) *The disease-mediated increase of PECAM-1 on circulating neutrophils was dampened by macrophage depletion. n= 5-8.* (**B**) *CD11b-expression on circulating neutrophils (CD45⁺ Ly6G⁺ Ly6C^{dim}) increased in STEC-HUS mice. Such upregulation was completely abolished in αCSF1R-treated mice. n= 6-12. The detailed gating strategy is provided in Figure 7.*
*Results are presented as means ± SEM. *p< 0.05, ***p< 0.001. αCSF1R: antibody against colony-stimulating factor 1 receptor, CD: cluster of differentiation, d: day(s), GMOF: geometric mean of fluorescence, IgG2a: control isotype, LPS: lipopolysaccharide, PECAM-1: platelet endothelial cell adhesion molecule 1, Stx: Shiga toxin*

Such neutrophil activation might be derived from systemically applied Stx/LPS acting on the circulating cells directly. Another activation cue, priming neutrophils for tissue invasion, might be the increased systemic cytokines that have previously been reported to increase in STEC-HUS (Kaplan et al., 1990; Palermo et al., 1999). Furthermore, we determined PECAM-1 and CD11b, both known to regulate neutrophil extravasation and migration, to be regulated by tissue-resident macrophages. Lack of macrophages, induced by αCSF1R administration, reduced PECAM-1 upregulation on day one and completely ablated it on day three. Disease-mediated CD11b-increase on circulating neutrophils was completely abolished in αCSF1R-treated mice (Figure 24). Activation of circulating neutrophils by upregulation of CD11b has previously been reported (Fernandez et al., 2000), but our study indicate that macrophages are central regulators for this activation.

3.7.2. Renal neutrophil infiltration is promoted by tissue-resident macrophages

After having investigated the systemic effects tissue-resident macrophages mediated in STEC-HUS, we next investigated the role of these cells in the local kidney environment. Macrophages are described as resident cells, regulating their environment via secretion of signaling molecules like cytokines. Hence, we performed further cytokine assays to determine the renal inflammatory milieu. In addition to local TNFα-levels, IL-1β and IL-6 were elevated one day after STEC-HUS induction (Figure 25). Replicating the trends observed for TNFα, IL-1β and IL-6 were also regulated by tissue-resident macrophages as their depletion by αCSF1R decreased these cytokine levels. These findings showed that in STEC-HUS the kidney becomes inflamed and a pro-inflammatory milieu is established my renal macrophages, which in turn potentially recruits leukocytes, such as neutrophils.

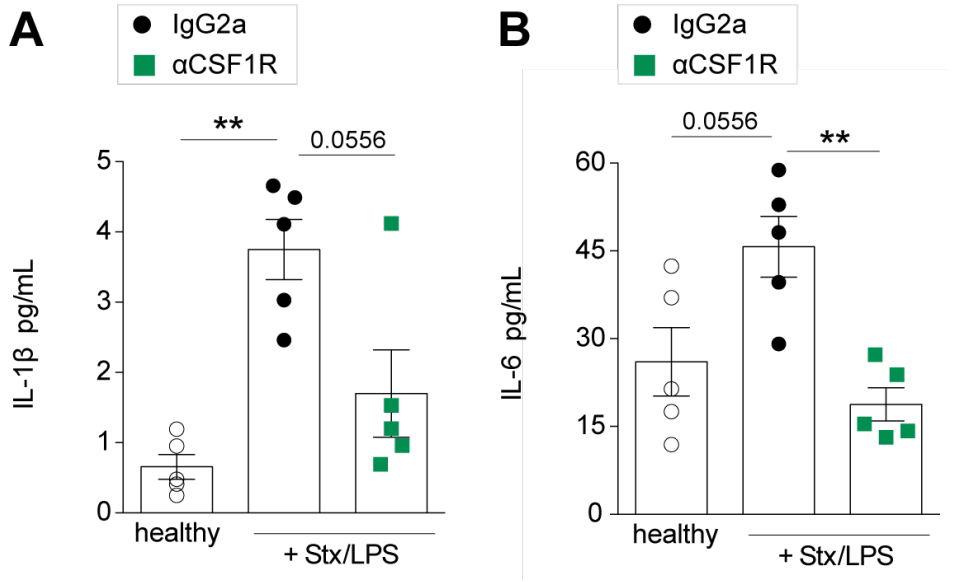

Figure 25: The pro-inflammatory cytokine milieu in STEC-HUS is regulated my tissue-resident macrophages
αCSF1R-mediated macrophage depletion diminished local IL-1β (**A**) *and IL-6 levels* (**B**) *in the kidney one day after STEC-HUS induction. Cytokine levels were analyzed in kidney homogenates by LEGENDplex™, n= 5.*
*Results are presented as means ± SEM. **p< 0.01. αCSF1R: antibody against colony-stimulating factor 1 receptor, IgG2a: control isotype, IL: Interleukin, LPS: lipopolysaccharide, ml: milliliter, Stx: Shiga toxin, pg: picogram(s)*

After determining the pro-inflammatory environment in the kidney and the activation of circulating neutrophils, both prerequisites for tissue infiltration of neutrophils, we next investigated this infiltration in the kidney. Flow cytometry demonstrated significant neutrophil infiltrates ($CD45^+$ $Ly6G^+$ $Ly6C^{dim}$) upon STEC-HUS induction in kidney homogenates. Such infiltrates were especially pronounced one day after disease onset, but still significantly elevated three days later (Figure 26).

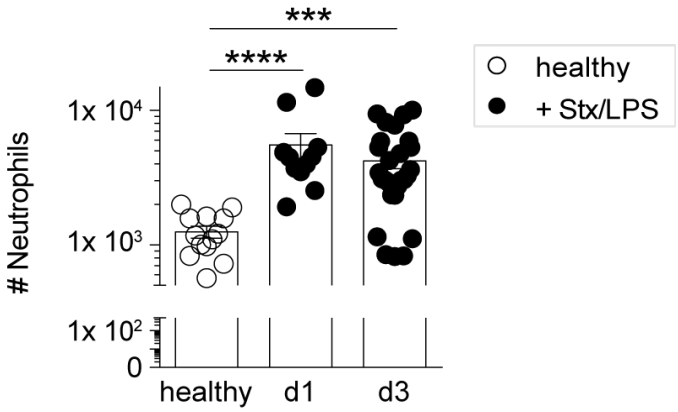

Figure 26: Neutrophils infiltrate the kidney upon STEC-HUS
Flow cytometry of the homogenized kidney revealed that neutrophils (CD45$^+$ Ly6G$^+$ Ly6C^{dim}) infiltrate the kidney during the experimental time course of STEC-HUS with biggest infiltrates seen one day after disease onset. Corresponding gating strategy is provided in Figure 8, n= 12-19.
*Results are presented as means ± SEM. ***p< 0.001, ****p< 0.0001. d: day(s), LPS: lipopolysaccharide, Stx: Shiga toxin*

As flow cytometry only identifies an organ-wide neutrophil influx, we performed immunofluorescence microscopy on renal tissue sections one day after STEC-HUS induction to investigate how neutrophils localize within the diseased kidney. One day after disease induction was the timepoint of choice, as here the strongest neutrophil infiltration was determined by flow cytometry. In the employed microscopic approach, the antigens Gr1 and F4/80 were fluorescently labeled to distinguish inflammatory monocytes (Gr1$^+$ F4/80$^+$ DAPI$^+$) and tissue macrophages (Gr1$^-$ F4/80$^+$ DAPI$^+$) from neutrophils (Gr1$^+$ F4/80$^-$ DAPI$^+$). Figure 27 A compares representative images of a healthy control to a diseased kidney one day after STEC-HUS induction. Analysis of these tissue sections by ImageJ demonstrated that in diseased tissue numerous neutrophils accumulate within the cortex and the glomeruli. In contrast, neutrophil density within the medulla was not affected. Even though the glomeruli exhibit the highest neutrophil density, the strongest neutrophil influx was observed in the renal cortex (Figure 27 B).

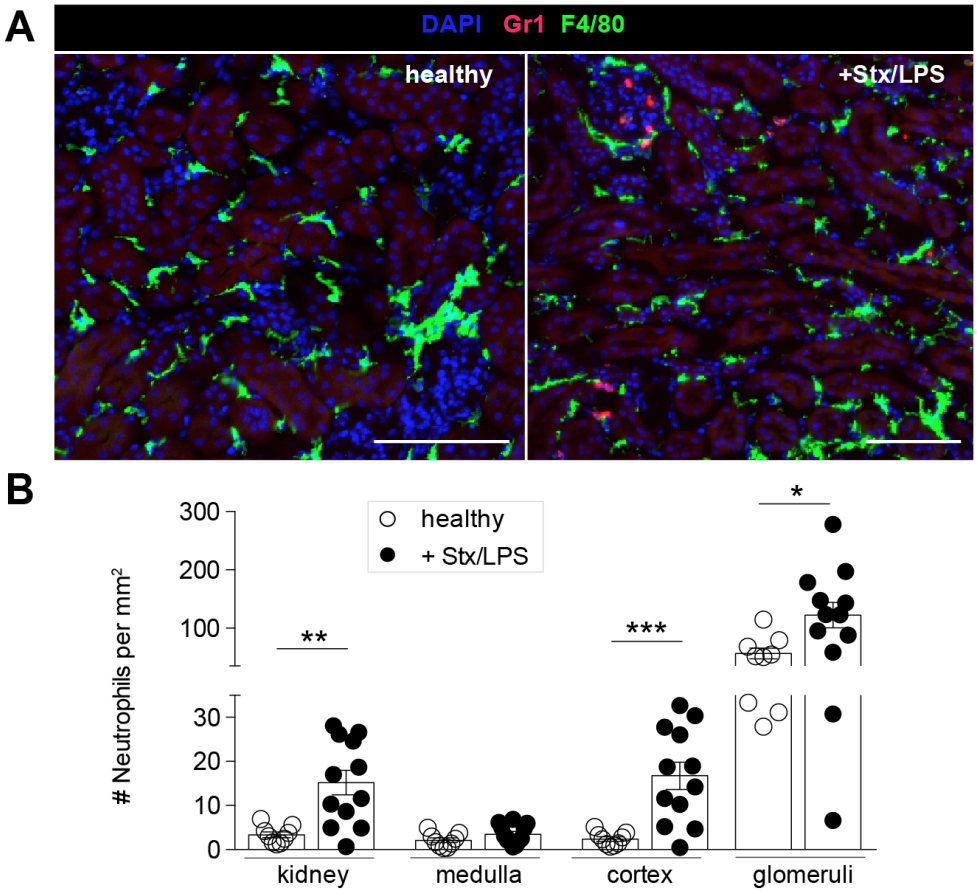

Figure 27: Neutrophils infiltrate the kidney cortex

*Immunofluorescent microscopy was employed to localize neutrophils in the kidney. Gr1 (red), F4/80 (green) and DAPI (blue) were stained to differentiate inflammatory monocytes (Gr1$^+$ F4/80$^+$ DAPI$^+$, tissue macrophages (Gr1$^-$ F4/80$^+$ DAPI$^+$) and neutrophils (Gr1$^+$ F4/80$^-$ DAPI$^+$). (**A**) A representative cortical region with implemented glomeruli of a healthy mouse (left) and a Stx/LPS injected mouse one day after disease onset (right). Scale bar= 50 µm. (**B**) Quantification from the immunofluorescent microscopy images showing the density of neutrophils in the overall kidney, further subdivided into medulla, cortex and glomeruli. Of note, the data presented in this figure was previously generated in my master thesis supported by Judith-Mira Pohl, n= 9-12.*

*Results are presented as means ± SEM. *p< 0.05, **p< 0.01, ***p< 0.001. DAPI: 4',6-diamidino-2-phenylindole, LPS: lipopolysaccharide, mm: millimeter(s), Stx: Shiga toxin*

For determination of the contribution of tissue-resident macrophages to neutrophil recruitment, we integrated αCSF1R-mediated macrophage depletion into the experimental setup. Flow cytometry revealed that macrophage depletion weakened neutrophil infiltration into the kidney three days post STEC-HUS induction, thereby demonstrating the central role of macrophages for disease-mediated neutrophil recruitment (Figure 28). Similar trends were observable on day one after disease onset but did not exhibit significance (data not shown).

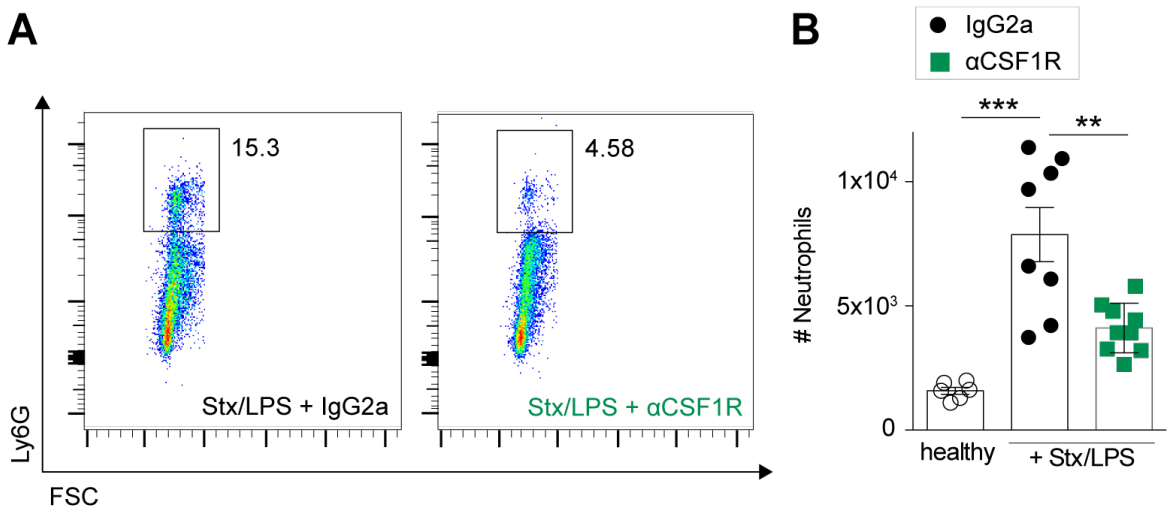

Figure 28: Macrophage depletion reduces neutrophil infiltration into the kidney
Flow cytometry of the homogenized kidney revealed that the neutrophil influx (CD45⁺ Ly6G⁺ Ly6C^{dim}) in response to STEC-HUS is dampened on day three when macrophages are depleted. (**A**) *Representative Pseudo-color dot plots from flow cytometry depict the reduced neutrophil population upon αCSF1R-treatment.* (**B**) *Quantification of flow cytometry revealed the significant reduction of neutrophil infiltrates into the kidney. Corresponding gating strategy is provided in Figure 8, n= 6-9.*
*Results are presented as means ± SEM. **p< 0.01, ***p< 0.001. αCSF1R: antibody against colony-stimulating factor 1 receptor, FSC: forward scatter, IgG2a: control isotype, LPS: lipopolysaccharide, Stx: Shiga toxin*

In summary, reduced recruitment of neutrophils to the kidney in response to STEC-HUS upon macrophage depletion might be a consequence of less activated circulating neutrophils, which we also describe herein.

3.7.3. Etanercept reduces activation of circulating neutrophils and their accumulation in the kidney

We determined tissue macrophages to control the activation of circulating neutrophils followed by their infiltration into the target organ, namely the kidney. Next, we aimed to unravel the underlying mechanism. As previous studies have shown that TNFα induces CD11b upregulation on circulating neutrophils, we investigated this parameter in TNFα-inhibited mice (Montecucco et al., 2008). Moreover, we have demonstrated that TNFα-inhibition by Etanercept ameliorated STEC-HUS-induced renal dysfunction (Figure 20, B and C). Etanercept was administered in PBS, thus this vehicle was used for treatment of the corresponding controls. To investigate the effects of Etanercept on neutrophils in our preclinical STEC-HUS model, we determined expression levels of CD11b on the surface of circulating neutrophils (Figure 29 A). The significant upregulation of CD11b after STEC-HUS induction was completely abolished by Etanercept treatment. Hence activation of neutrophils in response to STEC-HUS might be TNFα-mediated, which is released and produced by tissue-resident

macrophages. Moreover, it was previously shown that elevated TNFα levels in tissues prolong neutrophil survival (Takano et al., 2009). To investigate whether TNFα contributes to neutrophil accumulation in the kidney we employed flow cytometry on renal homogenates. Etanercept significantly reduced renal neutrophils on d3 ($CD45^+$ $Ly6G^+$ $Ly6C^{dim}$) that accumulated in response to STEC-HUS (Figure 29 B).

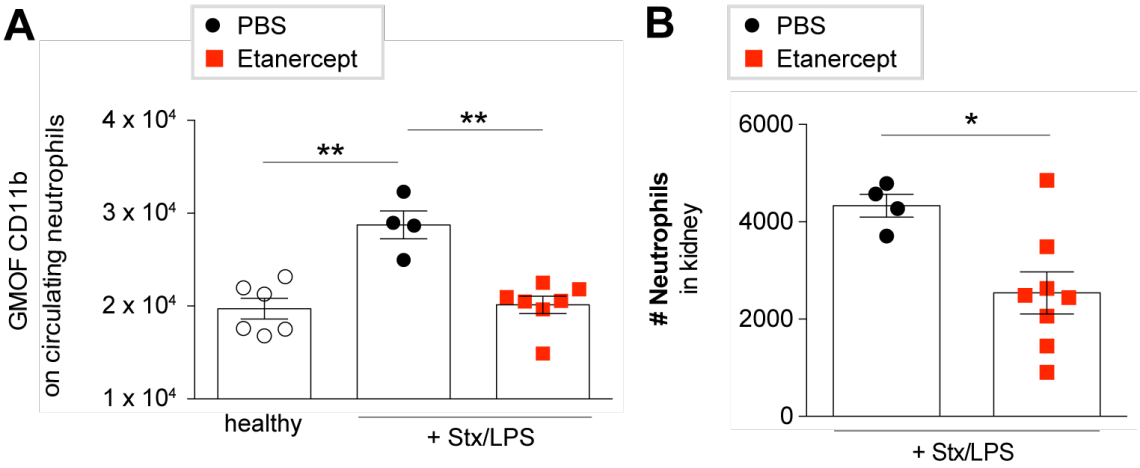

Figure 29: Etanercept decreased neutrophil activation and recruitment
(**A**) *CD11b-expression on circulating neutrophils ($CD45^+$ $Ly6G^+$ $Ly6C^{dim}$) increased in STEC-HUS mice. Such upregulation was completely abolished in mice treated with Etanercept, n= 4-7. The detailed gating strategy is provided in Figure 7.* (**B**) *Quantification of flow cytometry revealed the significant reduction of neutrophil infiltrates into the kidney. Corresponding gating strategy is provided in Figure 8, . n= 4-8*
*Results are presented as means ± SEM. *p< 0.05, **p< 0.01. CD: cluster of differentiation, d: day(s), GMOF: geometric mean of fluorescence, LPS: lipopolysaccharide, PBS: phosphate buffer saline, Stx: Shiga toxin*

Depicted in Figure 21, we demonstrate that Etanercept did not reduce tissue-resident macrophages. Therefore, neutrophil activation and accumulation within the kidney were not induced by reduced tissue-resident macrophages, but by TNFα directly.

3.7.4. Tissue macrophages regulate CXCL1 and CXCL2 expression, which recruit neutrophils via CXCR2

We determined tissue macrophages and TNFα to control the activation of circulating neutrophils, followed by their accumulation in the kidney. Next, we aimed to determine the detailed mechanism attracting neutrophils to the kidney upon STEC-HUS. In addition to TNFα, IL-1β and IL-6, the CXCR2-binding chemokines CXCL1 and CXCL2 might regulate neutrophil infiltration, regulated by tissue-resident macrophages. One day after STEC-HUS induction, CXCL1 and CXCL2 were significantly increased within the kidney in IgG2a control animals (Figure 30). Consistently, we observed the strongest neutrophil recruitment to the kidney at this timepoint (Figure 26). Upregulation of CXCL1 and CXCL2 in response to STEC-HUS was nearly completely absent (Figure 30), suggesting that macrophages regulate the secretion of these chemokines.

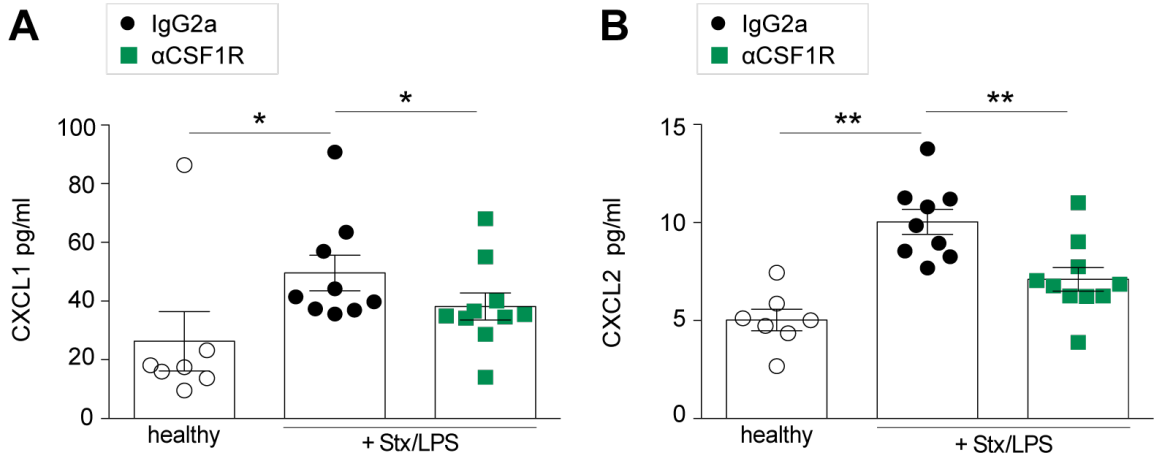

Figure 30: Renal CXCL1 and CXCL2 levels macrophage-regulated
αCSF1R-mediated macrophage depletion prevented local CXCL1 (**A**) *and CXCL2* (**B**) *upregulation in response to STEC-HUS analyzed in kidney homogenates by LEGENDplex™. n= 7-10.*
*Results are presented as means ± SEM. *p< 0.05, **p< 0.01. αCSF1R: antibody against colony-stimulating factor 1 receptor, CXCL: C-X-C motif ligand, IgG2a: control isotype, LPS: lipopolysaccharide, Stx: Shiga toxin*

In line with reduced levels of neutrophil-attractants, we previously observed dampened neutrophil recruitment when macrophages were depleted by αCSF1R (Figure 28 B). CXCR2 is the membrane bound receptor of the neutrophil attracting cytokines CXCL1 and CXCL2. To validate that circulating neutrophils are recruited by these two chemokines in our preclinical STEC-HUS model, we verified CXCR2-expression on circulating neutrophils (Figure 31 A). In addition to CXCR2-expression in healthy conditions, we even observed a significant receptor upregulation three days after STEC-HUS induction (Figure 31 B). Such upregulation sensitized neutrophils for detection of circulating CXCL1 and CXCL2.

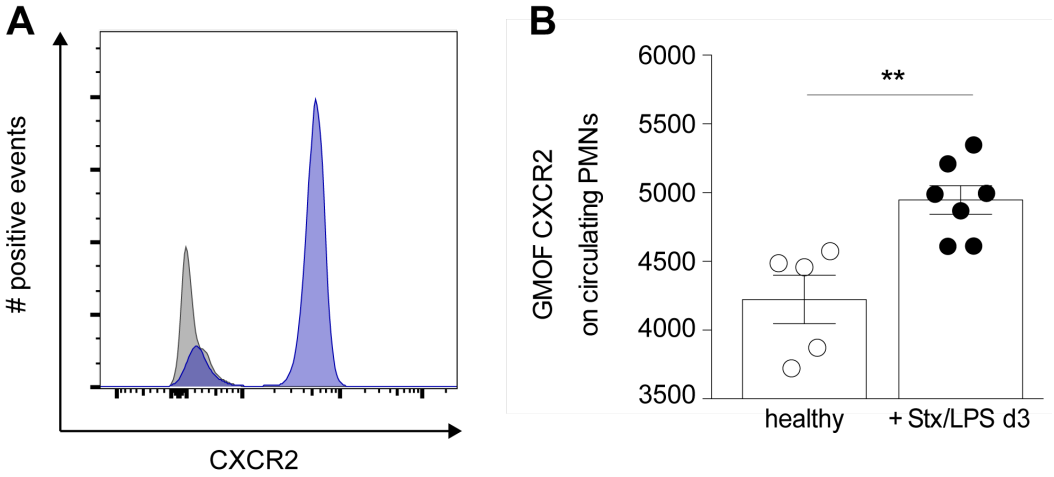

Figure 31: CXCR2 is upregulated on neutrophils in STEC-HUS
(**A**) *Histogram compares a FMO-control staining (grey) to a stained sample (blue) to validate a positive staining on circulating neutrophils (CD45$^+$ Ly6G$^+$ Ly6C^{dim}).* (**B**) *CXCR2 was upregulated on the surface of circulating neutrophils three days post-Stx/LPS injection. Corresponding gating is provided in Figure 7, n= 5-7.*
*Results are presented as means ± SEM. **p< 0.01, CXCR2: C- X- C chemokine receptor type 2, d: days, FMO: fluorescence- minus one, GMOF: geometric mean of fluorescence, LPS: lipopolysaccharide, Stx: Shiga toxin*

To further investigate the role of CXCL1/2-CXCR2-signaling for detrimental neutrophil recruitment, we targeted CXCR2-signaling by a corresponding antagonist (SB225002). Intravital imaging was employed as read-out technique and allowed the observation of neutrophils *in vivo* and thereby exceeded the previously made observations. Namely, additional to quantification and localization of recruited neutrophils within the renal tissue, we were now able to monitor and compare their migratory behavior among healthy and STEC-HUS induced mice. To this end, a fluorescently-labelled Gr1 antibody was administered into the circulation of *Cx$_3$cr1*$^{eGFP/+}$ mice to differentiate inflammatory monocytes (Gr1$^+$ CX$_3$CR1$^+$) and tissue macrophages (Gr1$^-$ CX$_3$CR1$^+$) from neutrophils (Gr1$^+$ CX$_3$CR1$^-$). In addition, fluorescent Qdots were intravenously administered to label the renal microvasculature. Time of analysis was one day after STEC-HUS induction, because most neutrophils were recruited until this timepoint. The speed, quantity and behavior of adherent neutrophils, classified as cells present in at least two consecutive frames, was analyzed. The behavior, classified as static or crawling, as well as the speed of adherent neutrophils was similar in healthy and Stx/LPS induced mice (data not shown). Nevertheless, significantly more neutrophils adhered within the renal microvasculature upon STEC-HUS induction (Figure 32 A, B), replicating the finding of immunofluorescence microscopy.

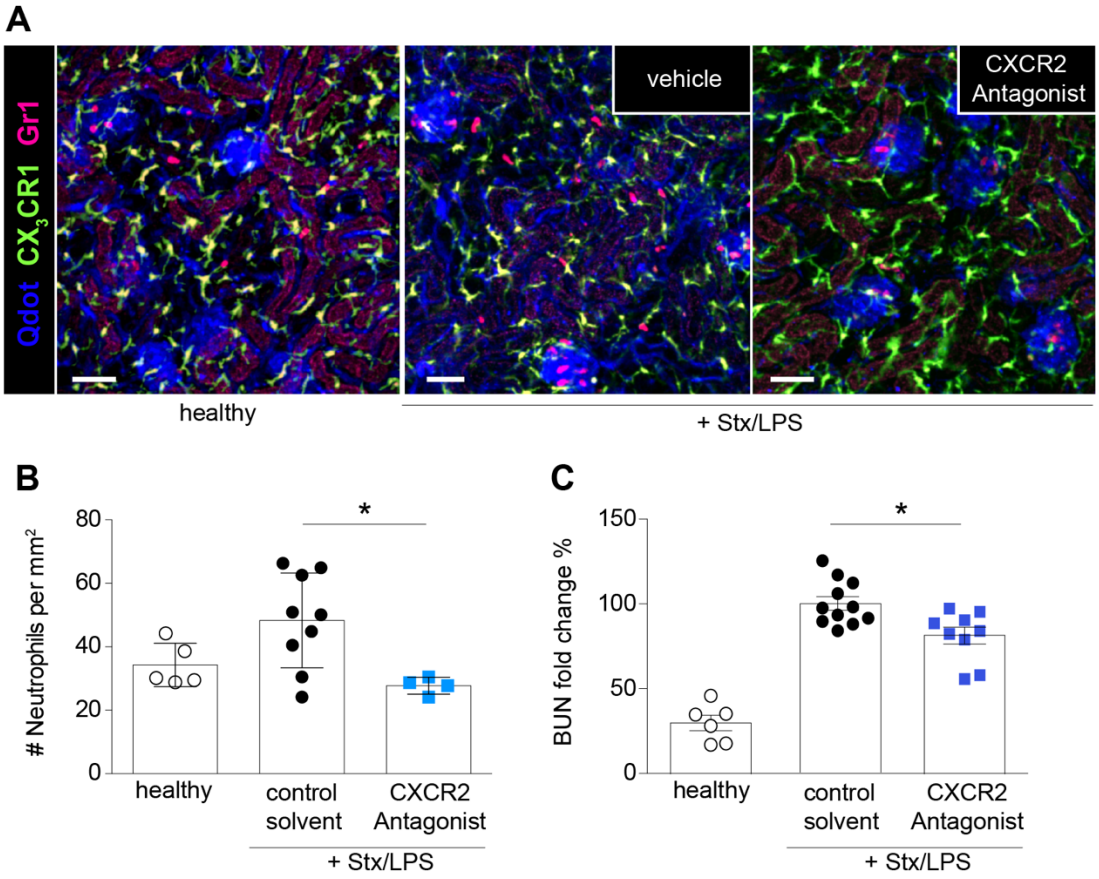

Figure 32: CXCR2-mediated neutrophil adhesion contributes to renal injury
(**A**) *Representative images of intravital microscopy showing glomeruli of a healthy (left), and two Stx/LPS-treated mice, one received a vehicle (DMSO, middle) and the other a CXCR2-antagonist (SB225002, right). Depicted are the vasculature (blue, Qdot⁺), neutrophils (pink, Gr1⁺) and renal macrophages (green, CX_3CR1^+). Scale bar: 20 µm.* (**B**) *IVM-quantification revealed enhanced adhesion of neutrophils to the glomerular vasculature one day after Stx/LPS application. CXCR2-antagonist administration ablated enhanced neutrophil adhesion. Of note, the data presented in this figure was previously generated in my master thesis supported by Judith-Mira Pohl. n= 5-6.* (**C**) *Administration of CXCR2-antagonist reduced renal injury assessed via BUN, n= 6-11.*
*Results are presented as means ± SEM. *p< 0.05, BUN: blood urea nitrogen, CXCR2: C- X- C chemokine receptor type 2, LPS: lipopolysaccharide, Stx: Shiga toxin*

These data indicate that CXCR2 mediates neutrophil adherence to the inflamed renal endothelium. Blocking of CXCR2 did not only reduce adherent neutrophils, but also decreased renal dysfunction, analyzed herein by BUN-levels in the blood serum (Figure 32 C). Conclusively, these findings verified the pivotal role of neutrophil adhesion to the renal endothelium and suggest that subsequent extravasation of neutrophils contributes to STEC-HUS pathogenesis.

4. Discussion

Several STEC-outbreaks, implicated with HUS described in the last decades, have not only caused economic burden for health systems, but were also associated with increased mortality (Bell et al., 1994; Frank et al., 2011a; Michino et al., 1999). In clinics, STEC-HUS patients receive supportive, nonspecific care addressing disease symptoms such as kidney impairments and strong diarrhea instead of targeting underlying cues. Severe cases also progress to chronic or even end-stage renal diseases and are thus a long-lasting burden on the health system by chronic requirement for dialysis. This current situation demands for further studies that elucidate the disease mechanisms during pathophysiological processes culminating in STEC-HUS. Furthermore, host immunity plays a central role in disease aggravation, but the complete processes herein are not fully understood and hence both therapeutic and preventative measures for STEC-HUS remain elusive.

In this study, we investigated the role of renal macrophages in STEC-HUS pathogenesis and thereby aimed to identify a novel therapeutic target. The employed macrophage depletion, prior to STEC-HUS induction, ameliorated the disease significantly. In addition to reduce the characteristic hallmarks of a TMA, namely endothelial injury, thrombocytopenia and kidney injury, we demonstrate macrophages to undergo a phenotypical and functional switch in response to STEC-HUS. We demonstrated that elevated cytokine levels, namely TNFα, IL-1β, IL-6, CXCL1 and CXCL2, in STEC-HUS were regulated by tissue-resident macrophages. The reduced neutrophil recruitment in the absence of renal macrophages suggested these cells contribute to the onset of STEC-HUS. Besides, we demonstrated CXCL1 and CXCL2 to facilitate neutrophil recruitment via CXCR2 into the diseased kidney. Finally, we showed that targeting tissue-resident macrophages, TNFα-signaling and the CXCR2-axis ameliorated kidney injury, thereby attributing crucial roles in STEC-HUS pathogenesis. Conclusively, our findings provide novel indications that macrophages and the produced TNFα, CXCL1 and CXCL2 are upstream of neutrophil recruitment and promote STEC-HUS.

4.1. There is an unmet need for STEC-HUS therapy

The previously suggested therapy targets did not result in effective therapies, thus novel targets are required to develop a STEC-HUS therapy. Specifically, CXCR4-signaling was shown to contribute in disease pathogenesis as Plerixafor, a CXCR4-antagonist approved in autologous stem cell transplantation (De Clercq, 2019), restored renal function, thrombocytopenia and murine survival in a preclinical STEC-HUS approach (Petruzziello-Pellegrini et al., 2012). Nevertheless, neither effective therapy nor clinical trials inhibiting CXCR4 in STEC-HUS have evolved since then.

A promising approach of systemic application of Stx-binding substances suggested neutralizing of the circulating toxin after release from the intestines, thus preventing toxin-receptor binding and inhibiting any detrimental cell-intrinsic signaling. Tested in a murine STEC-HUS model, the application of an anti-Stx2 antibody drastically improved murine well-being (Sauter et al., 2008; Yamagami et al., 2001). Challenging to the specificity of these antibodies might be the vast heterogeneity of Stx. Currently, Stx1 has three subtypes and Stx2 seven subtypes impairing the efficiency of individual Stx-binding antibodies (Baranzoni et al., 2016). Testing a Gb3 polymer, known to bind efficiently to both Stx1 and Stx2, in a preclinical STEC-HUS model showed protection of mice against a lethal EHEC dose (Watanabe et al., 2004). In a randomized human study, a synthetic toxin binder that utilizes Gb_3, was administered with no positive effects on STEC-HUS onset, renal impairment or survival (Trachtman et al., 2003). Failing effectivity in these studied might be reasoned to the late administration of these neutralizing agents. In a preclinical STEC-HUS study conducted in mice, it was shown that Stx circulates already 24 hours post-infection (Yamagami et al., 2001). Notably, comparisons to the results of this study have to consider that the employed model directly applies Stx into circulation, thus the 24 hours been described in the study by Yamagami *et al.* are not comparable to the 24 hours in our study. Even though such kinetics are most likely not comparable among species, STEC-HUS patients are only treated with Stx-specific agents after a definitive diagnosis of STEC-infection after culture (Serna and Boedeker, 2008), which might be too late to prevent binding of Stx to Gb_3. To bypass the unmet need of a human STEC-HUS therapy, a detour was considered targeting the natural reservoir of STEC to reduce human exposure to the pathogen and conclusively limit infection. To target the natural reservoir, cattle vaccinations have been tested that resulted in reduced STEC prevalence, but was not

implemented into agricultural routine, most likely due to the economic burden on the farmers (Potter et al., 2004).

4.2. Macrophages in diseases and the resulting therapeutic opportunities – applicable to STEC-HUS?

To identify a novel target for STEC-HUS therapy that has a potentially enlarged temporal window of effective therapy application, we investigated mechanisms downstream of Stx-Gb_3 binding. We focused on tissue-resident macrophages because, additional to the previously shown positive effects of targeting macrophages and their precursors in STEC-HUS, macrophages are known resident sentinel cells that contribute critically to organ homeostasis (Herbert et al., 2004; Kim et al., 2010; Palermo et al., 1999; Pohl et al., 2018; Sola et al., 2011). Moreover, we hypothesized macrophages to orchestrate the neutrophil response, known to critically promote STEC-HUS (Fernandez et al., 2007; Fernandez et al., 2006).

In the employed STEC-HUS model we confirmed a previously described dense renal macrophage network (Hume and Gordon, 1983; Soos et al., 2006). Depleting macrophages in this study statistically reduced characteristic hallmarks of a TMA, namely endothelial injury, thrombocytopenia and kidney injury. In contrast to the study conducted by Palermo *et al.* (i) the tissue-resident macrophage population was studied and (ii) the circulating monocytes were not affected. Palermo *et al.* have described hepatic and splenic macrophages to contribute to renal injury in the murine STEC-HUS model (Palermo et al., 1999). Depletion of these macrophages and additionally of circulating monocytes via clodronate liposomes (Van Rooijen and Sanders, 1994) reduced mortality and systemic TNFα levels. However, Palermo *et al.* did not investigate the contribution of renal macrophages or any other tissue-resident macrophage population. Moreover, monocytes promoting STEC-HUS and their additional depletion might contribute to beneficial effects observed by Palermo *et al.* (Pohl et al., 2018; Ramos et al., 2012).

Despite determining the phenotypical and functional switch in macrophages, they were notably not affected by Stx/LPS in their number, localization, mortality or dendritic activity. Moreover, we revealed a central role for macrophages in promoting STEC-HUS as we determined the hallmarks of a TMA, namely endothelial injury, platelet activation, thrombocytopenia and renal injury to be enhanced by tissue-resident macrophages. In other renal diseases, such as chronic kidney disease or renal fibrosis,

macrophage accumulation correlates to disease severity (Eardley et al., 2008; Nikolic-Paterson et al., 2014). In STEC-HUS only local infiltration of inflammatory monocytes has been reported (Pohl et al., 2018).

Macrophages are frequently described to activate inflammatory responses that exceed host-protective requirements and induce chronic inflammation. Among others, atherosclerosis and renal fibrosis are macrophage-promoted inflammatory diseases (Moore and Tabas, 2011; Nikolic-Paterson et al., 2014). In atherosclerosis, a leading cause of death among industrial nations (Lloyd-Jones et al., 2010), monocytes are recruited to the subendothelial matrix where they differentiate into macrophages (Gerrity, 1981; Mestas and Ley, 2008). Upon ingestion of lipoproteins, macrophages are called foam cells and reprogrammed to stimulate chronic inflammation (Gerrity, 1981; Moore and Tabas, 2011). Comparably, in our study we described macrophages to undergo a functional and phenotypically switch. By flow cytometry, we determined CD64 to be upregulated on renal macrophages, which is associated with a proinflammatory macrophage phenotype. Moreover, the TNFR-signaling was enhanced in correlation to macrophages in the renal cortex of STEC-HUS mice thereby further hinting towards a proinflammatory role of macrophages. In other kidney diseases interstitial and glomerular macrophage infiltration is frequently described and macrophages promote fibrosis by the recruitment of fibroblasts or by direct differentiation into myofibroblasts (Eardley et al., 2008). Moreover, macrophages were determined to promote renal inflammation by secretion of cytokines and a central role was attributed to IL-1β and TNFα (Ma et al., 2010). In our study, we determined the same cytokines are upregulated by macrophages, thus supporting the concept of macrophages promoting STEC-HUS pathogenesis. In lupus nephritis, an autoimmune disorder that drastically impairs renal function, metabolic reprogramming of tissue-macrophages represents a currently employed therapeutic target (Jing et al., 2020). In an experimental disease approach, the kinase inhibitor GW2580, inhibiting CSF1R-signaling, was beneficial in murine lupus nephritis (Chalmers et al., 2017). For STEC-HUS, we do not only describe that macrophages exhibit a proinflammatory phenotype and contribute to the production of inflammatory cytokines, but we furthermore provide first evidence that targeting macrophages via CSF1R ameliorates the disease.

Beyond inflammatory diseases, macrophages are known to promote cancer. In solid tumors, macrophages are the most abundant host-derived cells (Yang and Zhang, 2017). These TAMs adopt a pro-tumoral phenotype and are described as

immunosuppressive (Biswas et al., 2006). They favor tumor growth by local suppression of host immunity, predominantly T-cell response, and ensure tumor-nutrition by stimulating angiogenesis (Dwyer et al., 2017; Murdoch et al., 2008). TAMs promote tumors to such extent that their numbers often correlate to disease progression (Komohara et al., 2014).

Given the common disease-promoting role of macrophages, their targeting by reprogramming or ablation has long been subject of scientific discussions and seems to also be applicable to STEC-HUS (Ponzoni et al., 2018; Schultze, 2016). Macrophage-targeting has been very challenging due to the difficult differentiation of host-harming and host-protecting macrophages. Furthermore, macrophages develop heterogeneously among different tissues as the microenvironment critically shapes their differentiation, phenotype and function. It is often difficult to distinguish macrophages, dendritic cells (DCs) or mutual monocyte precursor. Based on this, characterizing kidney resident cells as macrophages is not necessarily appropriate as they are hardly distinguishable from DCs (Weisheit et al., 2015).

Unfortunately, no exclusive markers for tissue macrophages and DCs are known and hence for histological visualization, we stained for CX_3CR1 or F4/80 with the latter a conventional macrophage marker, but also been expressed by DCs (Soos et al., 2006). F4/80^{bright} cells in the kidney exhibit DC and macrophage features (Puranik et al., 2018). The depletion method via αCSF1R-administration, employed in this study, was previously described to target resident macrophages (MacDonald et al., 2010). This approach was visually revealed in *Csf1r*-GFP mice, which are mainly defined to have GFP^{+} macrophages (Sasmono et al., 2003). However, the CSF1R promoter, which controls GFP-expression in these mice, is additionally expressed in DCs (MacDonald et al., 2005). Such nomenclature-based issues were extensively debated by scientists and are not novel (Gottschalk and Kurts, 2015). Therefore, it would be most appropriate to term the studied cells “renal mononuclear phagocytes”, as suggested elsewhere (Kawakami et al., 2013). However, we decided to term the targeted cells macrophages based on accumulating literature evidence (Cao et al., 2015; Puranik et al., 2018). We estimate such concerns to be purely nomenclatural and not affecting the scientific results presented in this study.

Despite the diverse ontogeny of macrophages, a macrophage-targeting drug was approved in the context of solid tumors very recently (Lamb, 2019). Macrophages were reported to promote tumor resistance, their ablation was shown to overcome frequent

therapy limitations and was shown to reduce solid tumors (Arlauckas et al., 2017; Escamilla et al., 2015; Paulus et al., 2006; Ries et al., 2014). Especially targeting macrophage recruitment via the CSF1/CSF1R axis was extensively studied, resulting in the approval of Pexidartinib (Cannarile et al., 2017; Lamb, 2019). In combination with other cancer therapies, including radiation, immune checkpoint blockades or chemotherapy, or as monotherapy, the CSF1R-inhibition was revealed in various cancers (Mitchem et al., 2013; Pyonteck et al., 2013; Xu et al., 2013; Zhu et al., 2014).

We propose that STEC-HUS could be an additional disease cured by targeting CSF1R-signaling and testing of the therapeutic effect of Pexidartinib in the herein employed preclinical STEC-HUS model is a promising experiment that has to be addressed in the future. The recent approval for solid cancers and satisfying tolerability in patients highlights the attractiveness of CSF1R antagonists for STEC-HUS treatment. Systemic macrophage ablation has to be carefully suggested as only a small subset of host macrophages promotes disease progression. The other macrophages located in other tissues execute their normal host-beneficial functions. Therefore, systemic macrophage ablation should exclusively be considered in devastating diseases without any cure, such as STEC-HUS. Even though tissue-resident macrophages were systemically depleted in this study, we did not observe any negative side effects of this intervention. Nevertheless, skepticism towards macrophage depletion can be raised for STEC-HUS, as it is an infection-driven disease and macrophages critically contribute to pathogen clearance by phagocytosis and cytokine secretion leading to neutrophil recruitment (Davies et al., 2013). Bacterial STEC-infections are limited to the intestine and exclusively Stx escapes into systemic circulation (Brigotti et al., 2011). Patients seeking medical attention and receive therapy have systemically distributed toxin as the major threat and not the STEC-infection of the intestine. We consider systemic macrophage targeting required for therapy, because tissue- or organ-specific drug delivery is challenging, if not impossible, in clinic so far. Moreover, macrophage populations have been reported to recover after CSF1R-mediated depletion, thus excluding any long-lasting damage induced by therapy (Mora-Bau et al., 2015). To further investigate the therapeutic relevance of CSF1R-targeting in STEC-HUS, experiments administering αCSF1R or Pexidartinib after STEC-HUS induction are required. Therefore, kinetic experiments administering the tested therapeutic agent at different timepoints after disease

induction have to be executed. A therapeutic effect can be acknowledged herein if previously observed beneficial effects can be replicated.

4.3. Neutrophil response in STEC-HUS is orchestrated by tissue-resident macrophages

In this study we showed that neutrophil activation in the circulation and subsequent accumulation within the target organ is reduced in absence of macrophages. Hence, beyond understanding the central role of macrophages in STEC-HUS, we hypothesized they enhance the neutrophil response (Wynn and Vannella, 2016). Numerous studies have addressed the role of the innate immunity in STEC-HUS pathogenesis (reviewed in (Exeni et al., 2018)). Especially neutrophils have been determined to favor STEC-HUS development (Fernandez et al., 2006; Milford et al., 1989; Ramos et al., 2016) and we confirmed their recruitment and activation in our preclinical STEC-HUS model. After attributing a detrimental role of neutrophils for STEC-HUS, it is required to elucidate the underlying cues facilitating their activation and recruitment.

Our study demonstrated that macrophage depletion resulted in reduced activation of circulating neutrophils shown by upregulation of PECAM-1 and CD11b. Such effect on cells in the circulation upscaled the role of tissue macrophages from a renal to a systemic effect. This might be explained by macrophage-derived cytokines entering the circulation. PECAM-1 can facilitate neutrophil transmigration and chemotaxis (O'Brien et al., 2003), but also enhance the binding capacity of neutrophils via CD11b (Berman and Muller, 1995). CD11b, which was upregulated on circulating neutrophils in a macrophage-dependent manner in response to STEC-HUS, is a central integrin mediating neutrophil adhesion, transmigration and tissue recruitment (Zhang et al., 2006). Conclusively, we can hypothesize that the diminished neutrophil activation, by less CD11b and PECAM-1 expression on their surface, is one prerequisite resulting in reduced neutrophil accumulation in the tissue of macrophage-depleted mice. Moreover, circulating $CD11b^+$ cells were reported to serve as carrier for Stx, but increased CD11b levels and its correlation to enhanced Stx binding was not investigated (Niu et al., 2018). Mac-1, composed of CD11b and CD18, was determined to promote detrimental neutrophil adhesion contributing to GN and renal fibrosis (Dehnadi et al., 2017; Devi et al., 2013). Moreover, Mac-1 activation by adhesion was previously determined as prerequisite for ROS release by neutrophils (Nathan et al.,

1989). ROS production is a central defense mechanism of neutrophils, but in context of STEC-HUS it was shown to harm the host by promoting renal injury (Gomez et al., 2013). Hence, decreased expression of CD11b on neutrophils in response to macrophage depletion might not only reduce neutrophil binding and subsequent transmigration, but also direct aggressors, e.g. ROS, that contribute to renal dysfunction by endothelial injury. To validate whether macrophages control ROS-production, further experiments are required that compare ROS production of neutrophils in control and macrophage-depleted mice upon disease induction. Nevertheless, our study already provides first evidence that macrophages contribute to endothelial injury in the kidney and lower secretion of ROS by neutrophils in the absence of macrophages might comprise a potential mechanism.

Beyond activation of circulating neutrophils, the employed macrophage depletion significantly decreased accumulating neutrophils within the target organ of STEC-HUS, namely the kidney. Moreover, we showed that macrophage depletion also restored the TMA hallmarks including thrombocytopenia and diminished platelets activation. For the kidney it has specifically been shown that CD62P on platelet surfaces facilitates neutrophil adhesion in renal microcapillaries (Kuligowski et al., 2006). This highlights how macrophages may additionally contribute indirectly to renal neutrophil accumulation in STEC-HUS.

4.4. TNFα is a central mediator in disease development- does it resemble a promising therapy target?

In addition to promoting neutrophil activation and recruitment, the CSF1R-mediated macrophage depletion employed in this study, showed that not only the systemic (Palermo et al., 1999), but also the local TNFα levels were controlled by tissue-resident macrophages. Local TNFα production in the kidney was reported in response to Stx (Harel et al., 1993) and this inflammatory cytokine was identified as mandatory for development of STEC-HUS (van de Kar et al., 1992). Depletion of macrophages via αCSF1R in our preclinical model reduced the renal TNFα levels to baseline and macrophages were identified, among others, as direct cellular TNFα source, which we validated in our study by flow cytometry. In agreement, the employed proteomic approach revealed numerous molecules associated to TNF-signaling as upregulated in the microenvironment of macrophages. Thus, we proposed TNFα as central molecule by which macrophages promote STEC-HUS.

The role of TNFα in the development of STEC-HUS was first postulated in 1992 and it is significantly upregulated in the circulation of STEC-HUS patients (Louise and Obrig, 1992; Murata et al., 1998). Its role and the impact of TNFα blockade was investigated in different EHEC-infection diseases, e.g. in a murine model of flaccid paralysis (Isogai et al., 1998). Flaccid paralysis is a neurological condition described by reduced muscle tone without obvious cause and targeting TNFα by Nafamostat mesylate administration reduced lethality and histological abnormalities in the brain (Isogai et al., 1998). Noteworthy, Nafamostat mesylate is an anticoagulant drug that was reported to also suppress LPS-induced nitric oxide synthesis *in vitro* (Nakatsuka et al., 2000). Based on this knowledge, it is questionable whether the beneficial effects, induced by Nafamostat mesylate in the EHEC-infection model were purely TNFα-mediated. In another murine study, TNF-deficient mice exhibited reduced lethality in a model of STEC-HUS (Sasaki et al., 2002). Even though validating a central role of TNFα in STEC-HUS lethality, this study has not investigated the underlying mechanisms that resulted in reduced disease progression. To elucidate the detailed mechanism of TNFα in disease pathogenesis we administered Etanercept, which contains soluble TNFR-binding TNFα and thereby neutralizes the cytokine. The approved drug Etanercept is mainly administered to patients with rheumatoid arthritis (Garrison and McDonnell, 1999). TNFα-inhibition prior to Stx/LPS injection significantly reduced kidney injury to a comparable extend than αCSF1R-administration. Replicating the αCSF1R-induced phenotype supported the hypothesis of TNFα as major signaling molecule of macrophages to promote STEC-HUS. It was shown that TNFα upregulated the expression of Gb_3 on endothelial cells *in vitro*, thus rendering endothelial cells more susceptible to Stx damage and promoting Stx-mediated pathogenesis (Eisenhauer et al., 2001; van de Kar et al., 1992).

To understand how Etanercept contributes to restoration of the renal function, we accessed the role of TNFα on the neutrophil response, thus determined neutrophil activation and recruitment in Etanercept-treated animals. Similar to αCSF1R, Etanercept reduced CD11b expression on circulating neutrophils and their accumulation in the kidney. In literature, TNFα was reported to upregulate CD11b on neutrophils and thereby facilitates neutrophil binding and transmigration (Montecucco et al., 2008). Furthermore, TNFα upregulates the adhesion molecules E-selectin and P-selectin on endothelial cells and prolongs neutrophil survival in tissues (Griffin et al.,

2012; Pober and Sessa, 2007; Takano et al., 2009). P-selectin was reported to promote neutrophil binding and thereby facilitate their extravasation (Borges et al., 1997; Kuligowski et al., 2006). Conclusively, we suggest TNFα by renal tissue-resident macrophages to (i) upregulate CD11b on circulating neutrophils and (ii) extend neutrophil survival in peripheral tissues resulting in their accumulation in the kidney. Additionally, based on literature evidence but not addressed in our study, it can be hypothesized that TNFα enhances neutrophil binding to endothelial cells by upregulation of adhesion molecules. Not only affecting the leukocyte-endothelial interaction, upregulated E-selectin and P-selectin also activate and bind platelets resulting in thrombus formation and thus induce thrombocytopenia (Chen and Geng, 2006; Merten and Thiagarajan, 2004).

Beyond providing mechanistic insights, these findings suggest TNFα as potential target for STEC-HUS therapy. Similar to CSF1R-inhibition via Pexidartinib, TNFα-blockage via Etanercept has already been approved in different diseases. Hence, side effects of Etanercept are well studied, thus paving the way for Etanercept usage in STEC-HUS. Etanercept was initially approved in 1998 to treat rheumatoid arthritis, but until 2008, 43 post-approval trials were conducted aiming at dedicating new diseases for Etanercept treatment (van Luijn et al., 2011). Such studies led to further approvals for juvenile idiopathic arthritis, psoriatic arthritis, ankylosing spondylitis and plaque psoriasis (Gisondi et al., 2019). Other TNFα-inhibitors were beneficial for kidney diseases, such as diabetic nephropathy, nephroangiosclerosis, acute kidney transplant rejection, renal cell carcinoma, GN, sepsis and obstructive renal injury (Speeckaert et al., 2012; Vielhauer and Mayadas, 2007). In addition to Etanercept, other TNFα-inhibitors, such as Infliximab, Adalimumab and Certolizumab Pegol, are approved (Harris and Keane, 2010). Generally, these drugs are frequently reported to promote infections as well as reactivation of present diseases such as tuberculosis with no increased infection risk specifically for Etanercept (Downey, 2016; Winthrop, 2006). In randomized control studies, complementation of ongoing rheumatoid arthritis therapies with Etanercept did not increase infection rates (Bathon et al., 2000; Klareskog et al., 2004; Weinblatt et al., 1999). Thus, criticism that can be raised for the Etanercept treatment in STEC-HUS regarding the promotion of the EHEC-infection do not seem to apply. Beyond promoting infections, TNFα-inhibitors were reported as nephrotoxic, which would be detrimental in STEC-HUS as the kidney is already heavily affected by the disease. Similar to increased infection risk, harming effects on the

kidney could not be verified for Etanercept and individual case reports acknowledge successful Etanercept-treatment in rheumatism patients with renal insufficiency (Don et al., 2005; Sugioka et al., 2008). Moreover, suggesting Etanercept for STEC-HUS therapy does not implicate a continuous drug application comparable to rheumatoid arthritis. However, to determine the therapeutic benefit of TNFα-blockage in STEC-HUS, similar to αCSF1R, experiments injecting Etanercept after STEC-HUS induction are required.

Even though our study validated macrophages by flow cytometry as cellular TNFα source, Etanercept inhibits the inflammatory cytokine systemically and not uniquely TNFα produced by tissue-resident macrophages. To investigate whether macrophage-derived TNFα improves STEC-HUS, macrophage-specific TNFα-deficient mice are required. *Lyz2*-cre (Lysozyme C-2) or *Cx₃cr1*-cre are efficient promoters to target macrophages and can be crossed to mice in which the *tnf* gene is flanked by loxP sites (TNF-flox). The promoter *Lyz2* is expressed by macrophages, DCs and granulocytes, but the expression on $CD11c^+$ cells is reported to be relatively low (Hume, 2011). *Cx₃cr1* is one of the most specific macrophage markers existing, even though it additionally targets DCs (Jung et al., 2000). Promotors unique to macrophages are not existent yet, due to shared precursors with DCs. Conclusively, we suggest further experiments with *Cx₃cr1*-cre x *TNF*-flox mice to precisely determine the role of TNFα produced by tissue-resident macrophages and whether TNFα is the signaling molecule by which macrophages mediate STEC-HUS pathogenesis.

4.5. Production of CXCL1 and CXCL2 is macrophage regulated – crosstalk with epithelial cells by TNFα

After having attributed direct effects to TNFα for renal injury and on neutrophil activation, recruitment and survival in peripheral tissues, TNFα was further implicated with upregulation of CXCL1, CXCL2 and CXCL5 (Griffin et al., 2012; Vieira et al., 2009). In an experimental approach, TNFα-induced upregulation of CXCL1 and CXCL2 resulted in enhanced CXCR2-mediated neutrophil recruitment (Griffin et al., 2012). In the study by Griffin *et al.* IL-17 was attributed to a similar function, thereby suggesting a synergistic effect of IL-17 and TNFα. Vieira *et al.* have additionally demonstrated that targeting CXCL1, CXCL2 or TNFα via corresponding antibodies reduced neutrophil infiltration. In our study, were targeted TNFα by Etanercept, which

diminished neutrophils in diseased kidneys in STEC-HUS. Based on this, it can be further hypothesized that TNFα does not only directly orchestrate the neutrophil response, but might also indirectly regulate their migration via CXCL1 and CXCL2.

Studies on CXCL1 and CXCL2 identified their role in glomerular neutrophil recruitment and our study confirmed upregulation of the corresponding receptor of CXCL1 and CXCL2, namely CXCR2 on circulating neutrophils in response to STEC-HUS. Moreover, we employed intravital microscopy to investigate the role of CXCR2-signaling in the kidney. Comparing the neutrophil behavior in the kidney of healthy and diseased mice, revealed elevated levels of adherent neutrophils upon STEC-HUS. As previously suggested, pharmacological inhibition of CXCR2 dampened cortical and glomerular neutrophil numbers (Roche et al., 2007), but we additionally demonstrate renal dysfunction to be improved upon CXCR2-blocking. In addition to the upregulation of the corresponding receptor, we determined CXCL1 and CXCL2 levels to be decreased when macrophages were depleted by αCSF1R. This suggested that tissue-resident macrophages orchestrated the upregulation of CXCL1 and CXCL2 in response to STEC-HUS. Glomerular parietal epithelial cells were previously determined as cellular source of these neutrophil-attractants by histology (Roche et al., 2007). Such parietal epithelial cells replenish podocytes in the glomerular tuft and thus critically contribute to maintenance of glomerular filtration (Appel et al., 2009). Our data proposed that macrophages regulate such cytokine production and thereby suggests a novel crosstalk for macrophages and epithelial cells in the kidney.

Previous descriptions of macrophage-epithelial cells crosstalk in other conditions supports the likelihood of such interaction among renal tissue macrophages and parietal epithelial cells. In a previous study, macrophages infected with *Legionella pneumophilia* were found to render alveolar epithelial cells not only towards a proinflammatory phenotype, but also hypo-sensitive for the pathogen, thereby preventing an overshooting immune response to preserve the delicate lung tissue (Schulz et al., 2017). In the intestine, the immune function of macrophages, responsible for efficient host defense, was mediated by cytokines secreted by epithelial cells (Wells et al., 2011). In the kidney, tubular epithelial cells were determined to orchestrated macrophage polarization, which in turn regulated renal inflammation (Bolisetty et al., 2015). Such previous studies demonstrated that macrophage-epithelial crosstalk occurs frequently and can be bidirectional. In our model, we propose macrophages to stimulate CXCL1 and CXCL2 secretion in parietal epithelial

cells. Combining the results generated within the presented study with knowledge provided in literature, we hypothesize TNFα secreted by macrophages control CXCL1 and CXCL2 levels (Griffin et al., 2012; Vieira et al., 2009). Moreover, we microscopically observed numerous tissue-resident macrophages in close proximity to glomeruli and conclusively the parietal epithelial cells, thus providing the basic conditions required for such crosstalk. Additionally, glomerular macrophages were determined to produce TNFα in rabbits suffering from GN (Tipping et al., 1991).

Comparing the different intervention strategies employed in this study, namely macrophage depletion, TNFα-inhibition and CXCR2-blockade, the latter was determined to reduce kidney dysfunction shown by BUN and creatinine, least efficient in our preclinical model. Even though CXCR2 was systemically blocked and neutrophil adhesion to renal tissue was diminished to baseline, only a small improvement of the renal function was described. This suggests that the previously mentioned CXCR2/CXL1/2-mechanism is not the key mechanism of macrophages in STEC-HUS. Such hypothesis can be further supported by the rather down-stream function of CXCL1 and CXCL2 compared to the central and rather up-stream roles of tissue-resident macrophages and TNFα in STEC-HUS. Conclusively, this study provides compelling evidence for the central role of tissue-resident macrophages and the secreted TNFα in promoting STEC-HUS

5. Conclusion

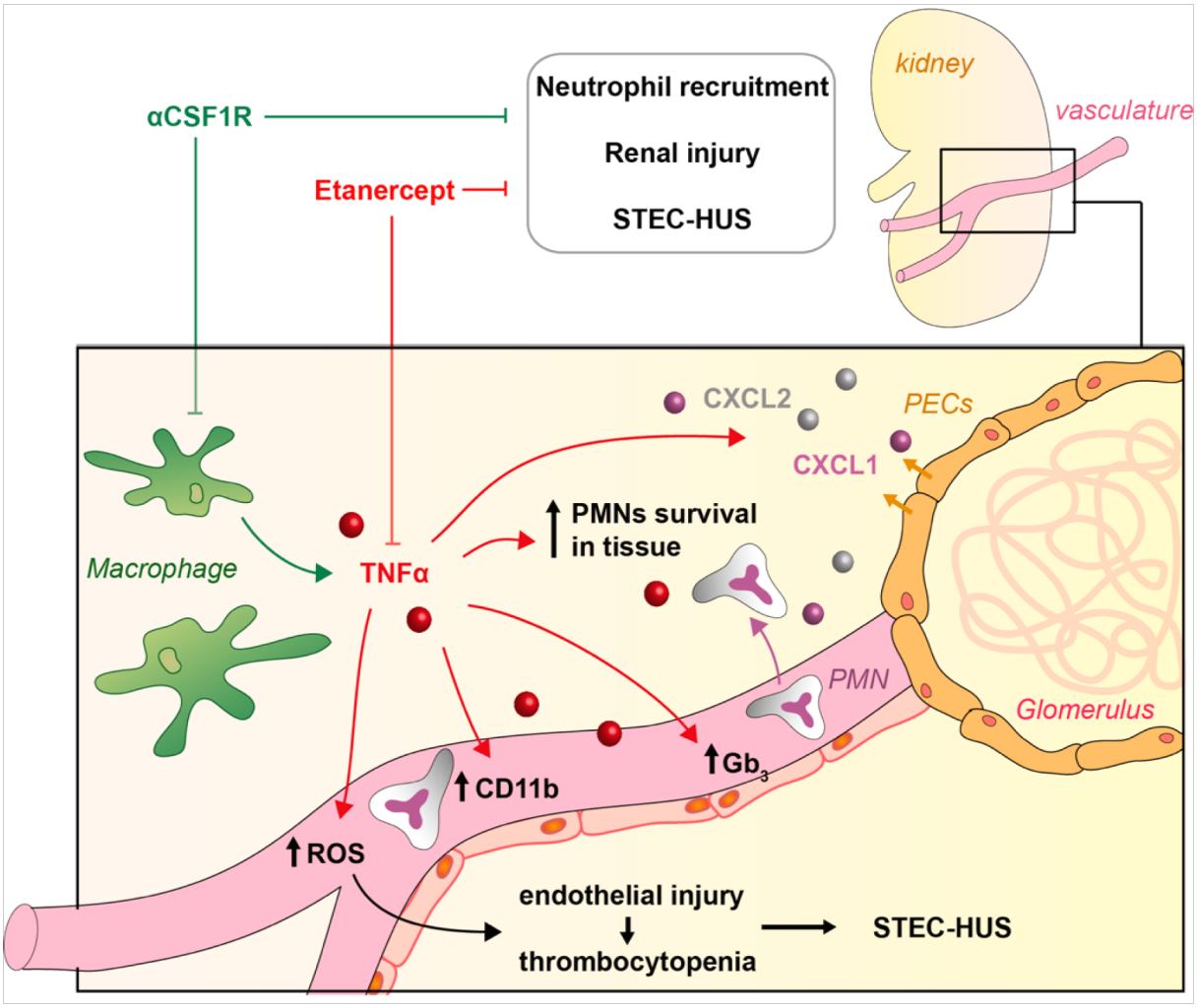

Figure 33. Macrophages critically contribute to STEC-HUS by TNFα secretion
The depicted scheme embeds the new findings obtained in this study into the previously knowledge from literature to suggest a complete mechanism for the role of macrophages and their product TNFα in STEC-HUS. Macrophages are a central source of TNFα, which in turn modifies multiple parameters leading to STEC-HUS progression. The secreted TNFα (i) increases CD11b on circulating neutrophils, (ii) enhances the ROS secretion of neutrophils, (iii) upregulates the expression of Gb_3 on endothelial cells thereby rendering them more sensitive to Stx, (iv) prolongs neutrophil survival in peripheral tissues and was last suggested to mediate the crosstalk of macrophages with glomerular parietal cells leading to CXCL1 and CXLC2 secretion. Moreover, both suggested intervention strategies, namely αCSF1R and Etanercept, are integrated into the scheme thereby highlighting the central role of such therapeutic strategies.
αCSF1R: antibody against colony-stimulating factor 1 receptor, CXCL: C-X-C motif ligand, Gb_3: globotriaosylcermide, HUS: hemolytic uremic syndrome, PECs: parietal epithelial cells, PMN: polymorphonuclear phagocyte (=neutrophil), ROS: reactive oxygen species, STEC: Shiga-toxin producing Escherichia coli, Stx: shiga toxin TNFα: tumor necrosis factor α

Our study determined macrophages as central regulators in STEC-HUS. Their depletion reduced STEC-HUS in mice by impeding renal injury, diminishing thrombocytopenia and endothelial injury, reducing renal inflammation, subsequent systemic neutrophil activation and recruitment to the kidney as depicted in the graphical abstract (Figure 33). Moreover, we propose macrophages as the main source of TNFα, and that these cells play a central mediator function in STEC-HUS

pathogenesis. We conclude that blockade of TNFα by Etanercept improves kidney function in STEC-HUS by decreasing the survival of neutrophils in tissues and reducing activation of circulating neutrophils. The activation-dependent CD11b-increase might promote renal injury by enhanced ROS-production, leading to endothelial injury. Additionally, TNFα promoted CXCL1 and CXCL2 secretion, chemokines that are produced by renal parietal epithelial cells in this model. Hence, TNFα does not only regulate neutrophil activation and survival, but also their migration to the diseased kidney. Systemic blockage of the corresponding receptor, CXCR2, ablated neutrophil adhesion and improved renal function in STEC-HUS.

Conclusively, this study suggests macrophage-derived TNFα to regulate a multitude of downstream signaling events in endothelial cells, parietal epithelial cells and neutrophils leading to the initiation and progression of STEC-HUS. Thus, targeting macrophages and their proinflammatory function might be a promising therapeutic approach for the treatment of STEC-HUS.

5.1. And what is next…?

This study has critically contributed to understanding the role of tissue-resident macrophages in STEC-HUS and has determined TNFα as central mediator for disease progression. Nevertheless, further experiments are required to address whether the provided conclusion and the proposed mechanism of this study can be completely validated. Moreover, continuative studies will elucidate whether macrophages utilize other signaling pathways, in addition to TNFα, to promote STEC-HUS. Therefore, the complete disease phenotype, including the TMA-hallmarks, the inflammatory environment by cytokine levels and the neutrophil behavior, have to be assessed after Etanercept administration and then compared to αCSF1R-treated mice. Overall, three possible results can be expected from such studies: TNFα-blockade can either replicate, impair or ameliorate the disease phenotype induced by αCSF1R. Complete replication of the previously described phenotype would support the proposed mechanism (Figure 33). In case Etanercept leads to an impairment in comparison to αCSF1R treatment, macrophages might promote STEC-HUS by additional signaling pathways than TNFα. In case Etanercept ameliorates STEC-HUS even better than αCSF1R administration, macrophages are not the unique TNFα source. In the latter scenario, microscopy will investigate which other cells produce TNFα in STEC-HUS mice. Moreover, employment of macrophage-specific TNF-deficient mice will contribute to specifically understand the role of macrophage-derived TNFα.

In this study, we propose macrophage targeting, via CSF1R and TNFα inhibition, as potential STEC-HUS therapies. Nevertheless, experiments administering the intervention strategies after disease onset are required to reveal the therapeutic benefit of the suggested targets in preclinical studies. Therefore, kinetic experiments with therapy instillation at different timepoints after disease induction have to be executed.

This study shows that macrophages promote STEC-HUS via TNFα. To exploit the complete benefit of this mechanistical understanding in disease therapy, more precise targeting techniques are required. To embed the herein achieved knowledge into therapy, the TNFα signaling of tissue-resident macrophages has to be specifically targeted. Hence, the molecular mechanism triggering tissue-resident macrophages to produce TNFα have to be elucidated. Moreover, we have to understand what renders specific macrophage populations different in the different tissue microenvironments. To this end, proteomic analysis comparing the protein expression profiles of distinct

macrophage populations in multiple microenvironments can be employed and help to determine specific proteins mediating the distinct macrophage phenotypes. These investigations can contribute to identify more specific targets than CSF1R and TNFα and thus facilitate a very targeted therapy with very limited side effects. Such knowledge would not only be beneficial for STEC-HUS, but also for all other macrophage-driven diseases.

Nevertheless, with more specific tools not being available yet, we suggest αCSF1R and TNFα as potential therapy targets to overcome the unmet need for STEC-HUS treatment.

V. Acknowledgments

First of all: I know that these written words cannot express the deep gratitude I feel for all the people that accompanied me and contributed to the success of this thesis. Moreover, I am aware that I am very privileged to have all these people by my side and to have the freedom to actively determine the way of my life and my career.

I would like to express my deep gratitude to Prof. Daniel R. Engel. Daniel did not only give me the opportunity to make my phD thesis in his lab, but supported me also in the times before and after my phD. For me he was a great supervisor and mentor, always giving me the freedom to conduct my own research, but never been “too far away” thus always being a great partner for discussions and advice. I highly appreciate his open-door policy and his friendly and optimistic nature. I am looking forward to much cooperation in the future.

Next, I would like to thank Prof. Sven Brandau. He did not only agreed to being my second reviewer for this thesis but also accompanied during my phD in all the seminars and retreats of the graduate school.

Moreover, I thank Prof. Matthias Gunzer for having me after my phD at the ISAS e.V. and for his support for my future career development. I appreciate working with him.

Thanks to Dr. Oliver Hofnagel and Sabine Donglard for their great support and technical knowledge with the TEM.

My sincere gratitude also goes to all the past and present members of the AG Engel. All of them greatly contribute to the success of this thesis and it would not have been such an enjoyable time without you. You made me come every day with warm feelings to work and shared good and bad times with me. Thanks for the incredible support you all always provided to me and I really enjoyed the team spirit of prioritizing the others needs and always helping each other out.
Thanks to Judith for introducing me to the Stx-model and for helping me to structure my work during my Master thesis. Furthermore, I would like to thank Robin for being my student and performing good independent work in the lab. It was a pleasure to see how motivated and positive you were! My honest gratitude also goes to Steffi, who was always by my side working in long and laborious experiment. We always had nice conversations and the time flew by when we were working together. Moreover, Steffi never complained when the experiment schedule was spontaneously changed to weird working times or even weekend. Without her many of the experiments of this thesis would not have been feasible for me alone. Next, there is Niro who also deserves many Thanks. She answered patiently all my annoying questions, sang along with me in the office hours, recommended excellent podcasts for the train travels and has a natural talent in neutralizing my (disproportional) anger. Special mentions go to Jenny even though she denied to share a bed with me on conferences. Jenny enriched the lab days with her “Jinner-mentality” and spending time with her was always a pleasure to me. I owe her a special thanks for being the “Monk” to this thesis. Moreover, there was our honest soul Kristina- our “Gyro-Queen” and the walking whirlwind of the group. She always added some extra energy into everything and contributed a lot to the lab

seminars by being a bubbly source of ideas and information. Thanks a lot also to Elke, she always had an open ear for me and very valuable advice to all my problems. I highly appreciate your positive mindset and the energy you share with all of us. Also, thanks to Camille for being a member of the team and all the nice conversations we had.
We all shared uncountable laughs and even though there were not only positive days at work, I enjoyed every single with this team. I will definitely miss the annual “Sommerfest”, our Christmas market visits or our hiking days for “Betriebsausflug”. It was a great pleasure being part of this team and having the privilege to work with all of you. The vast majority of the members of our small Engel-Team became very important to me and I don’t want to miss you anymore.

But off course my gratitude is not only with the people from work but also with the people who supported me in my private life. I would like to express my deep gratitude to Andrea, my Australian friend, and Olga, my “black-sheep” buddy- both for their critical feedback on this thesis and their mental support whenever needed. Moreover, there are the famous “Hühner”, the bunch of my closest friend who always patiently listened to my work stories even though I am pretty sure they have till now not fully understood what I am precisely working on. I know that I can always count on them and I highly enjoy every second spend with them.

Moreover, I want to express my heartful thankfulness to my family- my parents, my grandma and my sister. They though me my values and to critically reflect myself. Without them I would not be the person I am today- a person that I am proud to be.

I still don’t know whether Molly and Grisú aimed at co-authoring my thesis or whether they purely wanted to express the boredom they felt when seeing me writing my thesis when sleeping on my keyboard. Nevertheless, I won’t hold their endless disturbances against my faithful furfriends as they have thus created numerous joyful distractions that have enlighten monotonous days of writing.

Last, but definitely not least, I want to express my deepest gratitude to my husband Pascal. Since our bachelor studies, we walked this path together- keeping each other’s back clear, studying, celebrating and being togethers. I could not have wished for a better study, but also life companion. Thanks for being the pillar of my support, the laugh on sad days, my shoulder to lean on but also my discussion partner for everything. You always helped me to reflect myself and my work. I feel unbelievable blessed to have you and no words can express how thankful I am.

VI. Appendix

Table 9: Results of MALDI-MS approach.

List of the 234 proteins that highly correlated with the expression of F4/80 and were differentially expressed in STEC-HUS over healthy controls (p<0.01).

Uniprot-ID	Protein name	p-value
F6YAT5	RIKEN cDNA 4932438A13 gene (Fragment)	0.00013
O70194	Eukaryotic translation initiation factor 3 subunit D (eIF3d) (Eukaryotic translation initiation factor 3 subunit 7) (eIF-3-zeta) (eIF3 p66)	0.00014
Q9DAW9	Calponin-3 (Calponin, acidic isoform)	0.00025
Q3UW53	Protein Niban 1 (Protein FAM129A) (Protein Niban)	0.00026
O35144	Telomeric repeat-binding factor 2 (TTAGGG repeat-binding factor 2) (Telomeric DNA-binding protein)	0.00034
Q925P2	Carcinoembryonic antigen-related cell adhesion molecule 2 (CEA-related cell adhesion molecule 2) (Biliary glycoprotein 2) (BGP-2)	0.00040
Q9JIF7	Coatomer subunit beta (Beta-coat protein) (Beta-COP)	0.00072
Q9QZ85	Interferon-inducible GTPase 1 (EC 3.6.5.-)	0.00074
P97461	40S ribosomal protein S5 [Cleaved into: 40S ribosomal protein S5, N-terminally processed]	0.00075
Q9DBG7	Signal recognition particle receptor subunit alpha (SR-alpha) (Docking protein alpha) (DP-alpha)	0.00078
Q3URZ6	AHNAK nucleoprotein 2	0.00080
P45376	Aldo-keto reductase family 1 member B1 (EC 1.1.1.300) (EC 1.1.1.372) (EC 1.1.1.54) (Aldehyde reductase) (Aldo-keto reductase family 1 member B3) (Aldose reductase) (AR) (EC 1.1.1.21)	0.00082
Q91ZE6	Spectrin beta chain	0.00082
Q99LM2	CDK5 regulatory subunit-associated protein 3	0.00082
Q9EQC5	N-terminal kinase-like protein (105 kDa kinase-like protein) (Mitosis-associated kinase-like protein NTKL) (SCY1-like protein 1)	0.00088
Q8CG03	cGMP-specific 3',5'-cyclic phosphodiesterase (EC 3.1.4.35) (cGMP-binding cGMP-specific phosphodiesterase) (CGB-PDE)	0.00091
Q4JIM5	Tyrosine-protein kinase ABL2 (EC 2.7.10.2) (Abelson murine leukemia viral oncogene homolog 2) (Abelson tyrosine-protein kinase 2) (Abelson-related gene protein) (Tyrosine-protein kinase ARG)	0.00093
O08553	Dihydropyrimidinase-related protein 2 (DRP-2) (Unc-33-like phosphoprotein 2) (ULIP-2)	0.00096
A0A286YD60	Kelch domain-containing 7B	0.00097
Q80ZA7	Fragile X mental retardation 1 neighbor protein (Protein mNY-SAR-35)	0.00105
Q3U276	Succinate dehydrogenase assembly factor 1, mitochondrial (SDH assembly factor 1) (SDHAF1) (LYR motif-containing protein 8)	0.00117
P07901	Heat shock protein HSP 90-alpha (Heat shock 86 kDa) (HSP 86) (HSP86) (Tumor-specific transplantation 86 kDa antigen) (TSTA)	0.00120
Q7TPH6	E3 ubiquitin-protein ligase MYCBP2 (EC 2.3.2.-) (Myc-binding protein 2) (Pam/highwire/rpm-1 protein) (Protein Magellan) (Protein associated with Myc)	0.00122
Q8CG72	ADP-ribose glycohydrolase ARH3 (ADP-ribosylhydrolase 3) (O-acetyl-ADP-ribose deacetylase ARH3) (EC 3.5.1.-) (Poly(ADP-ribose) glycohydrolase ARH3) (EC 3.2.1.143) ([Protein ADP-ribosylarginine] hydrolase-like protein 2) ([Protein ADP-ribosylserine] hydrolase) (EC 3.2.2.-)	0.00127
Q6P9Z1	SWI/SNF-related matrix-associated actin-dependent regulator of chromatin subfamily D member 3 (60 kDa BRG-1/Brm-associated factor subunit C) (BRG1-associated factor 60C) (BAF60C) (mBAF60c)	0.00130

Q69Z38	Inactive tyrosine-protein kinase PEAK1 (Pseudopodium-enriched atypical kinase 1) (Sugen kinase 269) (Tyrosine-protein kinase SgK269)	0.00134
P07724	Serum albumin	0.00140
P17427	AP-2 complex subunit alpha-2 (100 kDa coated vesicle protein C) (Adaptor protein complex AP-2 subunit alpha-2) (Adaptor-related protein complex 2 subunit alpha-2) (Alpha-adaptin C) (Alpha2-adaptin) (Clathrin assembly protein complex 2 alpha-C large chain) (Plasma membrane adaptor HA2/AP2 adaptin alpha C subunit)	0.00151
Q61554	Fibrillin-1 [Cleaved into: Asprosin]	0.00152
Q9WU40	Inner nuclear membrane protein Man1 (LEM domain-containing protein 3)	0.00153
Q8C050	Ribosomal protein S6 kinase alpha-5 (S6K-alpha-5) (EC 2.7.11.1) (90 kDa ribosomal protein S6 kinase 5) (Nuclear mitogen- and stress-activated protein kinase 1) (RSK-like protein kinase) (RLSK)	0.00154
Q8C5N5	Programmed cell death protein 2-like	0.00155
Q69ZK0	Phosphatidylinositol 3,4,5-trisphosphate-dependent Rac exchanger 1 protein (P-Rex1) (PtdIns(3,4,5)-dependent Rac exchanger 1)	0.00161
J3QQ16	Collagen, type VI, alpha 3	0.00161
Q8CAA7	Glucose 1,6-bisphosphate synthase (EC 2.7.1.106) (Phosphoglucomutase-2-like 1)	0.00176
Q5U4C3	Splicing factor, arginine/serine-rich 19 (SR-related and CTD-associated factor 1)	0.00179
Q9CR29	Coiled-coil domain-containing protein 43	0.00201
Q68FE7	Transmembrane protein 151B	0.00212
P13542	Myosin-8 (Myosin heavy chain 8) (Myosin heavy chain, skeletal muscle, perinatal) (MyHC-perinatal)	0.00212
Q91V76	Ester hydrolase C11orf54 homolog (EC 3.1.-.-)	0.00214
Q9QY80	Very-long-chain (3R)-3-hydroxyacyl-CoA dehydratase 1 (EC 4.2.1.134) (3-hydroxyacyl-CoA dehydratase 1) (HACD1) (Protein-tyrosine phosphatase-like member A)	0.00215
Q64442	Sorbitol dehydrogenase (SDH) (SORD) (EC 1.1.1.-) (L-iditol 2-dehydrogenase) (EC 1.1.1.14) (Polyol dehydrogenase) (Xylitol dehydrogenase) (XDH) (EC 1.1.1.9)	0.00240
Q0VF58	Collagen alpha-1(XIX) chain (Collagen alpha-1(Y) chain)	0.00241
P06745	Glucose-6-phosphate isomerase (GPI) (EC 5.3.1.9) (Autocrine motility factor) (AMF) (Neuroleukin) (NLK) (Phosphoglucose isomerase) (PGI) (Phosphohexose isomerase) (PHI)	0.00246
P26039	Talin-1	0.00259
Q9R1P4	Proteasome subunit alpha type-1 (EC 3.4.25.1) (Macropain subunit C2) (Multicatalytic endopeptidase complex subunit C2) (Proteasome component C2) (Proteasome nu chain)	0.00261
P14211	Calreticulin (CRP55) (Calregulin) (Endoplasmic reticulum resident protein 60) (ERp60) (HACBP)	0.00264
Q9D0F9	Phosphoglucomutase-1 (PGM 1) (EC 5.4.2.2) (Glucose phosphomutase 1) (Phosphoglucomutase-2)	0.00275
E9Q6E9	SUMO-interacting motifs-containing 1	0.00275
Q8C0S5	CAP-Gly domain-containing linker protein 1 (Fragment)	0.00287
Q29SA9	NCK-associated protein 5 (Peripheral clock protein 1)	0.00288
Q3UPL6	Membrane-spanning 4-domains subfamily A member 15	0.00299
Q8BYH8	Chromodomain-helicase-DNA-binding protein 9 (CHD-9) (EC 3.6.4.12) (ATP-dependent helicase CHD9) (PPAR-alpha-interacting complex protein 320 kDa) (Peroxisomal proliferator-activated receptor A-interacting complex 320 kDa protein)	0.00312
F6W2R3	TBC1 domain family member 2B	0.00315

Q8K183	Pyridoxal kinase (EC 2.7.1.35) (Pyridoxine kinase)	0.00318
Q791V5	Mitochondrial carrier homolog 2	0.00323
Q9WUZ7	SH3 domain-binding glutamic acid-rich protein (SH3BGR protein)	0.00323
Q8VBX6	Multiple PDZ domain protein (Multi-PDZ domain protein 1)	0.00332
P70697	Uroporphyrinogen decarboxylase (UPD) (URO-D) (EC 4.1.1.37)	0.00337
P11087	Collagen alpha-1(I) chain (Alpha-1 type I collagen)	0.00341
Q8K4L2	Archvillin (Supervillin)	0.00342
Q02788	Collagen alpha-2(VI) chain	0.00346
P08553	Neurofilament medium polypeptide (NF-M) (160 kDa neurofilament protein) (Neurofilament 3) (Neurofilament triplet M protein)	0.00355
Q8CAQ8	MICOS complex subunit Mic60 (Mitochondrial inner membrane protein) (Mitofilin)	0.00365
P50404	Pulmonary surfactant-associated protein D (PSP-D) (SP-D) (Lung surfactant protein D)	0.00372
O70435	Proteasome subunit alpha type-3 (EC 3.4.25.1) (Macropain subunit C8) (Multicatalytic endopeptidase complex subunit C8) (Proteasome component C8) (Proteasome subunit K)	0.00373
A0A0N4SVK8	[Protein ADP-ribosylarginine] hydrolase-like protein 1	0.00377
Q5RM08	Osterix (Transcription factor Sp7)	0.00387
Q6PDN3	Myosin light chain kinase, smooth muscle (MLCK) (smMLCK) (EC 2.7.11.18) (Kinase-related protein) (KRP) (Telokin) [Cleaved into: Myosin light chain kinase, smooth muscle, deglutamylated form]	0.00397
Q9ET47	Espin (Ectoplasmic specialization protein)	0.00398
Q6ZQ38	Cullin-associated NEDD8-dissociated protein 1 (Cullin-associated and neddylation-dissociated protein 1) (p120 CAND1)	0.00399
Q5FWK3	Rho GTPase-activating protein 1 (Rho-type GTPase-activating protein 1)	0.00399
Q8BVI4	Dihydropteridine reductase (EC 1.5.1.34) (HDHPR) (Quinoid dihydropteridine reductase)	0.00399
O35864	COP9 signalosome complex subunit 5 (SGN5) (Signalosome subunit 5) (EC 3.4.-.-) (Jun activation domain-binding protein 1) (Kip1 C-terminus-interacting protein 2)	0.00407
O08638	Myosin-11 (Myosin heavy chain 11) (Myosin heavy chain, smooth muscle isoform) (SMMHC)	0.00408
E9PVD3	Protocadherin-16 (Protein Dchs1) (Protein dachsous homolog 1)	0.00409
Q921G6	Leucine-rich repeat and calponin homology domain-containing protein 4	0.00411
Q9CX86	Heterogeneous nuclear ribonucleoprotein A0 (hnRNP A0)	0.00422
Q8CIB5	Fermitin family homolog 2 (Kindlin-2) (Pleckstrin homology domain-containing family C member 1)	0.00424
A0A2R8VI42	Poly(U)-binding-splicing factor PUF60	0.00427
Q8BH59	Calcium-binding mitochondrial carrier protein Aralar1 (Mitochondrial aspartate glutamate carrier 1) (Solute carrier family 25 member 12)	0.00427
O35491	Dual specificity protein kinase CLK2 (EC 2.7.12.1) (CDC-like kinase 2)	0.00427
Q62442	Vesicle-associated membrane protein 1 (VAMP-1) (Synaptobrevin-1)	0.00427
Q02566	Myosin-6 (Myosin heavy chain 6) (Myosin heavy chain, cardiac muscle alpha isoform) (MyHC-alpha)	0.00429
P62737	Actin, aortic smooth muscle (Alpha-actin-2) [Cleaved into: Actin, aortic smooth muscle, intermediate form]	0.00432
P26645	Myristoylated alanine-rich C-kinase substrate (MARCKS)	0.00432

Q8BZ47	Zinc finger protein 609	0.00435
Q9D2G5	Synaptojanin-2 (EC 3.1.3.36) (Synaptic inositol 1,4,5-trisphosphate 5-phosphatase 2)	0.00439
P45700	Mannosyl-oligosaccharide 1,2-alpha-mannosidase IA (EC 3.2.1.113) (Man(9)-alpha-mannosidase) (Man9-mannosidase) (Mannosidase alpha class 1A member 1) (Processing alpha-1,2-mannosidase IA) (Alpha-1,2-mannosidase IA)	0.00449
Q9D417	F-box only protein 24	0.00455
Q8K4P0	pre-mRNA 3' end processing protein WDR33 (WD repeat-containing protein 33) (WD repeat-containing protein of 146 kDa)	0.00456
Q9ER58	Testican-2 (SPARC/osteonectin, CWCV, and Kazal-like domains proteoglycan 2)	0.00459
Q8BFS6	Serine/threonine-protein phosphatase CPPED1 (EC 3.1.3.16) (Calcineurin-like phosphoesterase domain-containing protein 1)	0.00460
Q04857	Collagen alpha-1(VI) chain	0.00465
Q922P8	Transmembrane protein 132A (HSPA5-binding protein 1)	0.00466
Q63870	Collagen alpha-1(VII) chain (Long-chain collagen) (LC collagen)	0.00467
Q99KP3	Lambda-crystallin homolog (EC 1.1.1.45) (L-gulonate 3-dehydrogenase) (Gul3DH)	0.00474
A2A864	Integrin beta	0.00491
Q8VC57	BTB/POZ domain-containing protein KCTD5	0.00491
Q9QYY8	Spastin (EC 5.6.1.1)	0.00491
Q8BH69	Selenide, water dikinase 1 (EC 2.7.9.3) (Selenium donor protein 1) (Selenophosphate synthase 1)	0.00493
Q9D892	Inosine triphosphate pyrophosphatase (ITPase) (Inosine triphosphatase) (EC 3.6.1.9) (Non-canonical purine NTP pyrophosphatase) (Non-standard purine NTP pyrophosphatase) (Nucleoside-triphosphate diphosphatase) (Nucleoside-triphosphate pyrophosphatase) (NTPase)	0.00493
P56480	ATP synthase subunit beta, mitochondrial (EC 7.1.2.2) (ATP synthase F1 subunit beta)	0.00493
D3YX11	GTPase IMAP family member 1 (Fragment)	0.00498
Q8CC96	Protein BNIP5	0.00500
Q8K2P1	Leucine rich adaptor protein 1-like	0.00500
P09405	Nucleolin (Protein C23)	0.00517
O54910	NF-kappa-B inhibitor epsilon (NF-kappa-BIE) (I-kappa-B-epsilon) (IkB-E) (IkB-epsilon) (IkappaBepsilon)	0.00518
P26443	Glutamate dehydrogenase 1, mitochondrial (GDH 1) (EC 1.4.1.3)	0.00520
P35601	Replication factor C subunit 1 (A1-P145) (Activator 1 140 kDa subunit) (A1 140 kDa subunit) (Activator 1 large subunit) (Activator 1 subunit 1) (Differentiation-specific element-binding protein) (ISRE-binding protein) (Replication factor C 140 kDa subunit) (RF-C 140 kDa subunit) (RFC140) (Replication factor C large subunit)	0.00522
A2ALF0	DnaJ homolog subfamily C member 8	0.00527
P58771	Tropomyosin alpha-1 chain (Alpha-tropomyosin) (Tropomyosin-1)	0.00528
Q6PD29	Zinc finger protein 513	0.00529
O88569	Heterogeneous nuclear ribonucleoproteins A2/B1 (hnRNP A2/B1)	0.00534
E9Q616	AHNAK nucleoprotein (desmoyokin)	0.00534
Q62465	Synaptic vesicle membrane protein VAT-1 homolog (EC 1.-.-.-)	0.00536

Q9WTP7	GTP:AMP phosphotransferase AK3, mitochondrial (EC 2.7.4.10) (Adenylate kinase 3) (AK 3) (Adenylate kinase 3 alpha-like 1)	0.00553
Q60675	Laminin subunit alpha-2 (Laminin M chain) (Laminin-12 subunit alpha) (Laminin-2 subunit alpha) (Laminin-4 subunit alpha) (Merosin heavy chain)	0.00575
Q9QZ59	Doublesex- and mab-3-related transcription factor 1	0.00577
Q3UNH4	G protein-regulated inducer of neurite outgrowth 1 (GRIN1)	0.00577
Q80Y14	Glutaredoxin-related protein 5, mitochondrial (Monothiol glutaredoxin-5)	0.00578
Q6JHY2	Submandibular gland protein C	0.00590
Q3UMT1	Protein phosphatase 1 regulatory subunit 12C (Protein phosphatase 1 myosin-binding subunit of 85 kDa) (Protein phosphatase 1 myosin-binding subunit p85)	0.00596
Q8BGY7	Protein FAM210A	0.00596
Q9JHU4	Cytoplasmic dynein 1 heavy chain 1 (Cytoplasmic dynein heavy chain 1) (Dynein heavy chain, cytosolic)	0.00596
Q5QNR3	Ankyrin repeat domain 36 (Fragment)	0.00596
Q5XG71	Small subunit processome component 20 homolog (Down-regulated in metastasis protein)	0.00603
P62264	40S ribosomal protein S14	0.00603
Q7TPD0	Integrator complex subunit 3 (Int3) (SOSS complex subunit A) (Sensor of single-strand DNA complex subunit A) (SOSS-A) (Sensor of ssDNA subunit A)	0.00605
Q8CGZ0	Calcium homeostasis endoplasmic reticulum protein (SR-related CTD-associated factor 6)	0.00610
Q14AT5	Anoctamin-7 (New gene expressed in prostate homolog) (Transmembrane protein 16G)	0.00610
Q9QZZ4	Unconventional myosin-XV (Unconventional myosin-15)	0.00616
Q8BLX7	Collagen alpha-1(XVI) chain	0.00621
O35245	Polycystin-2 (Polycystic kidney disease 2 protein homolog) (Transient receptor potential cation channel subfamily P member 2)	0.00624
Q8BVE8	Histone-lysine N-methyltransferase NSD2 (EC 2.1.1.356) (Multiple myeloma SET domain-containing protein) (MMSET) (Nuclear SET domain-containing protein 2) (Wolf-Hirschhorn syndrome candidate 1 protein homolog)	0.00625
Q6URW6	Myosin-14 (Myosin heavy chain 14) (Myosin heavy chain, non-muscle IIc) (Non-muscle myosin heavy chain IIc) (NMHC II-C)	0.00627
O70423	Membrane primary amine oxidase (EC 1.4.3.21) (Copper amine oxidase) (Semicarbazide-sensitive amine oxidase) (SSAO) (Vascular adhesion protein 1) (VAP-1)	0.00629
O55042	Alpha-synuclein (Non-A beta component of AD amyloid) (Non-A4 component of amyloid precursor) (NACP)	0.00637
Q9DBG3	AP-2 complex subunit beta (AP105B) (Adaptor protein complex AP-2 subunit beta) (Adaptor-related protein complex 2 subunit beta) (Beta-2-adaptin) (Beta-adaptin) (Clathrin assembly protein complex 2 beta large chain) (Plasma membrane adaptor HA2/AP2 adaptin beta subunit)	0.00638
P17751	Triosephosphate isomerase (TIM) (EC 5.3.1.1) (Methylglyoxal synthase) (EC 4.2.3.3) (Triose-phosphate isomerase)	0.00640
A2AHJ4	Bromodomain and WD repeat-containing protein 3	0.00643
A0A0R4J0M1	Tubulin-specific chaperone C	0.00646
P16546	Spectrin alpha chain, non-erythrocytic 1 (Alpha-II spectrin) (Fodrin alpha chain)	0.00647
Q8BP27	Swi5-dependent recombination DNA repair protein 1 homolog (Meiosis protein 5 homolog)	0.00647
P62983	Ubiquitin-40S ribosomal protein S27a (Ubiquitin carboxyl extension protein 80) [Cleaved into: Ubiquitin; 40S ribosomal protein S27a]	0.00648

Q05793	Basement membrane-specific heparan sulfate proteoglycan core protein (HSPG) [Cleaved into: Endorepellin; LG3 peptide]	0.00650
Q01853	Transitional endoplasmic reticulum ATPase (TER ATPase) (EC 3.6.4.6) (15S Mg(2+)-ATPase p97 subunit) (Valosin-containing protein) (VCP)	0.00652
Q99JR8	SWI/SNF-related matrix-associated actin-dependent regulator of chromatin subfamily D member 2 (60 kDa BRG-1/Brm-associated factor subunit B) (BRG1-associated factor 60B) (BAF60B)	0.00658
E9PWW9	Remodeling and spacing factor 1	0.00665
P24270	Catalase (EC 1.11.1.6)	0.00667
O08648	Mitogen-activated protein kinase kinase kinase 4 (EC 2.7.11.25) (MAPK/ERK kinase kinase 4) (MEK kinase 4) (MEKK 4)	0.00673
Q9D8N0	Elongation factor 1-gamma (EF-1-gamma) (eEF-1B gamma)	0.00675
A2AHG0	Leucine zipper putative tumor suppressor 3 (ProSAP-interacting protein 1) (ProSAPiP1)	0.00677
P55194	SH3 domain-binding protein 1 (3BP-1)	0.00681
O88492	Perilipin-4 (Adipocyte protein S3-12)	0.00688
Q99JY4	TraB domain-containing protein	0.00705
Q99KK7	Dipeptidyl peptidase 3 (EC 3.4.14.4) (Dipeptidyl aminopeptidase III) (Dipeptidyl arylamidase III) (Dipeptidyl peptidase III) (DPP III) (Enkephalinase B)	0.00715
Q3UHJ0	AP2-associated protein kinase 1 (EC 2.7.11.1) (Adaptor-associated kinase 1)	0.00733
Q562E2	BTB/POZ domain-containing protein KCTD19	0.00736
P53995	Anaphase-promoting complex subunit 1 (APC1) (Cyclosome subunit 1) (Mitotic checkpoint regulator) (Testis-specific gene 24 protein)	0.00737
P60710	Actin, cytoplasmic 1 (Beta-actin) [Cleaved into: Actin, cytoplasmic 1, N-terminally processed]	0.00739
A0A140LHJ6	Oxygen-regulated protein 1	0.00744
Q04447	Creatine kinase B-type (EC 2.7.3.2) (B-CK) (Creatine kinase B chain) (Creatine phosphokinase B-type) (CPK-B)	0.00748
Q8CDM1	ATPase family AAA domain-containing protein 2 (EC 3.6.1.3)	0.00748
Q6IFZ6	Keratin, type II cytoskeletal 1b (Cytokeratin-1B) (CK-1B) (Embryonic type II keratin-1) (Keratin-77) (K77) (Type-II keratin Kb39)	0.00751
P14152	Malate dehydrogenase, cytoplasmic (EC 1.1.1.37) (Cytosolic malate dehydrogenase)	0.00753
Q8VDP4	Cell cycle and apoptosis regulator protein 2 (Cell division cycle and apoptosis regulator protein 2)	0.00754
P06909	Complement factor H (Protein beta-1-H)	0.00759
Q91YL7	PGAP2-interacting protein (Cell wall biogenesis protein 43 C-terminal homolog)	0.00759
Q78Y63	Phosducin-like protein 2 (MgcPhLP) (Phosducin-like protein similar 1)	0.00763
Q6P4T0	Autophagy-related protein 2 homolog A	0.00767
Q5MJS3	Extracellular serine/threonine protein kinase FAM20C (EC 2.7.11.1) (Dentin matrix protein 4) (DMP-4) (Golgi-enriched fraction casein kinase) (GEF-CK)	0.00776
A0A2I3BQ61	GDNF family receptor alpha-2	0.00781
Q6PFD5	Disks large-associated protein 3 (DAP-3) (PSD-95/SAP90-binding protein 3) (SAP90/PSD-95-associated protein 3) (SAPAP3)	0.00782
Q3TUQ5	Pinin	0.00786

P17182	Alpha-enolase (EC 4.2.1.11) (2-phospho-D-glycerate hydro-lyase) (Enolase 1) (Non-neural enolase) (NNE)	0.00789
Q91X20	Set1/Ash2 histone methyltransferase complex subunit ASH2 (ASH2-like protein)	0.00793
Q8BMK4	Cytoskeleton-associated protein 4 (63-kDa cytoskeleton-linking membrane protein) (Climp-63) (p63)	0.00794
Q9JK53	Prolargin (Proline-arginine-rich end leucine-rich repeat protein)	0.00798
Q9QXF8	Glycine N-methyltransferase (EC 2.1.1.20)	0.00798
Q8CC88	von Willebrand factor A domain-containing protein 8	0.00807
Q149F3	Eukaryotic peptide chain release factor GTP-binding subunit ERF3B (Eukaryotic peptide chain release factor subunit 3b) (eRF3b) (G1 to S phase transition protein 2 homolog)	0.00808
Q9CPQ3	Mitochondrial import receptor subunit TOM22 homolog (Translocase of outer membrane 22 kDa subunit homolog)	0.00811
P63276	40S ribosomal protein S17	0.00813
P02468	Laminin subunit gamma-1 (Laminin B2 chain) (Laminin-1 subunit gamma) (Laminin-10 subunit gamma) (Laminin-11 subunit gamma) (Laminin-2 subunit gamma) (Laminin-3 subunit gamma) (Laminin-4 subunit gamma) (Laminin-6 subunit gamma) (Laminin-7 subunit gamma) (Laminin-8 subunit gamma) (Laminin-9 subunit gamma) (S-laminin subunit gamma) (S-LAM gamma)	0.00815
P16125	L-lactate dehydrogenase B chain (LDH-B) (EC 1.1.1.27) (LDH heart subunit) (LDH-H)	0.00819
Q8VDK1	Deaminated glutathione amidase (dGSH amidase) (EC 3.5.1.128) (Nitrilase homolog 1)	0.00820
P59598	Polycomb group protein ASXL1 (Additional sex combs-like protein 1)	0.00821
Q8BFU4	GAIP/RGS19 short isoform (Regulator of G-protein-signaling 19)	0.00821
A0A1W2P6N4	Family with sequence similarity 184, member A (Fragment)	0.00829
Q69ZN7	Myoferlin (Fer-1-like protein 3)	0.00838
Q32KG4	Retrotransposon Gag-like protein 9 (Retrotransposon gag domain-containing protein 1) (Sushi-XF2)	0.00843
Q8BMA6	Signal recognition particle subunit SRP68 (SRP68) (Signal recognition particle 68 kDa protein)	0.00844
Q9QZQ3	Urotensin-2 (Urotensin II) (U-II) (UII)	0.00853
P97372	Proteasome activator complex subunit 2 (11S regulator complex subunit beta) (REG-beta) (Activator of multicatalytic protease subunit 2) (Proteasome activator 28 subunit beta) (PA28b) (PA28beta)	0.00855
P11679	Keratin, type II cytoskeletal 8 (Cytokeratin endo A) (Cytokeratin-8) (CK-8) (Keratin-8) (K8) (Type-II keratin Kb8)	0.00856
Q5F204	Putative malate dehydrogenase 1B (EC 1.1.1.-)	0.00857
Q9JI70	McKusick-Kaufman/Bardet-Biedl syndromes putative chaperonin (Protein Bbs6 homolog)	0.00869
Q9D051	Pyruvate dehydrogenase E1 component subunit beta, mitochondrial (PDHE1-B) (EC 1.2.4.1)	0.00876
J3QNX5	Protein shisa-8 (Cystine-knot AMPAR modulating protein of 39 kDa) (CKAMP39) (Shisa family member 8)	0.00883
Q62261	Spectrin beta chain, non-erythrocytic 1 (Beta-II spectrin) (Embryonic liver fodrin) (Fodrin beta chain)	0.00883
Q9QWF0	Chromatin assembly factor 1 subunit A (CAF-1 subunit A) (Chromatin assembly factor I p150 subunit) (CAF-I 150 kDa subunit) (CAF-I p150)	0.00884
Q9QZS0	Collagen alpha-3(IV) chain [Cleaved into: Tumstatin]	0.00884
Q9QXE2	DNA polymerase lambda (Pol Lambda) (EC 2.7.7.7) (EC 4.2.99.-) (DNA polymerase kappa)	0.00887
P63017	Heat shock cognate 71 kDa protein (Heat shock 70 kDa protein 8)	0.00890

Q64435	UDP-glucuronosyltransferase 1-6 (UDPGT 1-6) (UGT1*6) (UGT1-06) (UGT1.6) (EC 2.4.1.17) (Phenol UDP-glucuronosyltransferase) (UDP-glucuronosyltransferase 1A6) (UGT1A6) (UGP1A1) (UGT1A7)	0.00893
P08122	Collagen alpha-2(IV) chain [Cleaved into: Canstatin]	0.00898
Q61001	Laminin subunit alpha-5 (Laminin-10 subunit alpha) (Laminin-11 subunit alpha) (Laminin-15 subunit alpha)	0.00901
Q8BSA9	tRNA wybutosine-synthesizing protein 3 homolog (tRNA-yW-synthesizing protein 3) (EC 2.1.1.282) (tRNA(Phe) 7-((3-amino-3-carboxypropyl)-4-demethylwyosine(37)-N(4))-methyltransferase)	0.00906
P69525	Transmembrane protease serine 9 (EC 3.4.21.-) (Polyserase-I) (Polyserine protease 1) (Polyserase-1) [Cleaved into: Serase-1; Serase-2; Serase-3]	0.00910
Q8R151	NFX1-type zinc finger-containing protein 1	0.00911
Q32KG4	Retrotransposon Gag-like protein 9	0.00925
O88569	Heterogeneous nuclear ribonucleoproteins A2/B1	0.00925
Q8BMA6	Signal recognition particle subunit SRP68	0.00930
Q9QZQ3	Urotensin-2	0.00938
P97372	Proteasome activator complex subunit 2	0.00940
P11679	Keratin, type II cytoskeletal 8	0.00944
Q5F204	Putative malate dehydrogenase 1B	0.00946
Q9JI70	McKusick-Kaufman/Bardet-Biedl syndromes putative chaperonin	0.00946
Q9D051	Pyruvate dehydrogenase E1 component subunit beta, mitochondrial	0.00953
Q9DBG3	AP-2 complex subunit beta	0.00959
J3QNX5	Protein shisa-8	0.00962
Q62261	Spectrin beta chain, non-erythrocytic 1	0.00965
Q9QWF0	Chromatin assembly factor 1 subunit A	0.00966
Q9QZS0	Collagen alpha-3(IV) chain	0.00968
Q9QXE2	DNA polymerase lambda	0.00968
P63017	Heat shock cognate 71 kDa protein	0.00972
Q64435	UDP-glucuronosyltransferase 1-6	0.00973
P08122	Collagen alpha-2(IV) chain	0.00979
Q61001	Laminin subunit alpha-5	0.00979
Q8BSA9	tRNA wybutosine-synthesizing protein 3 homolog	0.00984
P69525	Transmembrane protease serine 9	0.00989
Q8R151	NFX1-type zinc finger-containing protein 1	0.00992

VII. List of Figures

VIII. List of tables

IX. References

Abrahamson, D.R. (1985). Origin of the glomerular basement membrane visualized after in vivo labeling of laminin in newborn rat kidneys. J Cell Biol *100*, 1988-2000.

Abtin, A., Jain, R., Mitchell, A.J., Roediger, B., Brzoska, A.J., Tikoo, S., Cheng, Q., Ng, L.G., Cavanagh, L.L., von Andrian, U.H.*, et al.* (2014). Perivascular macrophages mediate neutrophil recruitment during bacterial skin infection. Nat Immunol *15*, 45-53.

Acharya, V., and Olivero, J. (2018). The Kidney as an Endocrine Organ. Methodist Debakey Cardiovasc J *14*, 305-307.

Adrover, J.M., Aroca-Crevillen, A., Crainiciuc, G., Ostos, F., Rojas-Vega, Y., Rubio-Ponce, A., Cilloniz, C., Bonzon-Kulichenko, E., Calvo, E., Rico, D.*, et al.* (2020). Programmed 'disarming' of the neutrophil proteome reduces the magnitude of inflammation. Nat Immunol *21*, 135-144.

Aggarwal, B.B., Eessalu, T.E., and Hass, P.E. (1985). Characterization of receptors for human tumour necrosis factor and their regulation by gamma-interferon. Nature *318*, 665-667.

Alikhan, M.A., Jones, C.V., Williams, T.M., Beckhouse, A.G., Fletcher, A.L., Kett, M.M., Sakkal, S., Samuel, C.S., Ramsay, R.G., Deane, J.A.*, et al.* (2011). Colony-stimulating factor-1 promotes kidney growth and repair via alteration of macrophage responses. Am J Pathol *179*, 1243-1256.

Andreoli, S.P., Trachtman, H., Acheson, D.W., Siegler, R.L., and Obrig, T.G. (2002). Hemolytic uremic syndrome: epidemiology, pathophysiology, and therapy. Pediatr Nephrol *17*, 293-298.

Appel, D., Kershaw, D.B., Smeets, B., Yuan, G., Fuss, A., Frye, B., Elger, M., Kriz, W., Floege, J., and Moeller, M.J. (2009). Recruitment of podocytes from glomerular parietal epithelial cells. J Am Soc Nephrol *20*, 333-343.

Arlauckas, S.P., Garris, C.S., Kohler, R.H., Kitaoka, M., Cuccarese, M.F., Yang, K.S., Miller, M.A., Carlson, J.C., Freeman, G.J., Anthony, R.M.*, et al.* (2017). In vivo imaging reveals a tumor-associated macrophage-mediated resistance pathway in anti-PD-1 therapy. Sci Transl Med *9*.

Athens, J.W., Haab, O.P., Raab, S.O., Mauer, A.M., Ashenbrucker, H., Cartwright, G.E., and Wintrobe, M.M. (1961). Leukokinetic studies. IV. The total blood, circulating and marginal granulocyte pools and the granulocyte turnover rate in normal subjects. J Clin Invest *40*, 989-995.

Baek, J.H. (2019). The Impact of Versatile Macrophage Functions on Acute Kidney Injury and Its Outcomes. Front Physiol *10*, 1016.4

Baek, J.H., Zeng, R., Weinmann-Menke, J., Valerius, M.T., Wada, Y., Ajay, A.K., Colonna, M., and Kelley, V.R. (2015). IL-34 mediates acute kidney injury and worsens subsequent chronic kidney disease. J Clin Invest *125*, 3198-3214.

Bain, C.C., Bravo-Blas, A., Scott, C.L., Perdiguero, E.G., Geissmann, F., Henri, S., Malissen, B., Osborne, L.C., Artis, D., and Mowat, A.M. (2014). Constant replenishment from circulating monocytes maintains the macrophage pool in the intestine of adult mice. Nat Immunol *15*, 929-937.

Baranzoni, G.M., Fratamico, P.M., Gangiredla, J., Patel, I., Bagi, L.K., Delannoy, S., Fach, P., Boccia, F., Anastasio, A., and Pepe, T. (2016). Characterization of Shiga Toxin Subtypes and Virulence Genes in Porcine Shiga Toxin-Producing Escherichia coli. Front Microbiol *7*, 574.

Barry, K.C., Fontana, M.F., Portman, J.L., Dugan, A.S., and Vance, R.E. (2013). IL-1alpha signaling initiates the inflammatory response to virulent Legionella pneumophila in vivo. J Immunol *190*, 6329-6339.

Bartelmez, S.H., and Stanley, E.R. (1985). Synergism between hemopoietic growth factors (HGFs) detected by their effects on cells bearing receptors for a lineage specific HGF: assay of hemopoietin-1. J Cell Physiol *122*, 370-378.

Bathon, J.M., Martin, R.W., Fleischmann, R.M., Tesser, J.R., Schiff, M.H., Keystone, E.C., Genovese, M.C., Wasko, M.C., Moreland, L.W., Weaver, A.L.*, et al.* (2000). A comparison of etanercept and methotrexate in patients with early rheumatoid arthritis. N Engl J Med *343*, 1586-1593.

Bauwens, A., Kunsmann, L., Karch, H., Mellmann, A., and Bielaszewska, M. (2017). Antibiotic-Mediated Modulations of Outer Membrane Vesicles in Enterohemorrhagic Escherichia coli O104:H4 and O157:H7. Antimicrob Agents Chemother *61*.

Beck-Schimmer, B., Schwendener, R., Pasch, T., Reyes, L., Booy, C., and Schimmer, R.C. (2005). Alveolar macrophages regulate neutrophil recruitment in endotoxin-induced lung injury. Respir Res *6*, 61.

Bell, B.P., Goldoft, M., Griffin, P.M., Davis, M.A., Gordon, D.C., Tarr, P.I., Bartleson, C.A., Lewis, J.H., Barrett, T.J., Wells, J.G*., et al.* (1994). A multistate outbreak of Escherichia coli O157:H7-associated bloody diarrhea and hemolytic uremic syndrome from hamburgers. The Washington experience. JAMA *272*, 1349-1353.

Bell, B.P., Griffin, P.M., Lozano, P., Christie, D.L., Kobayashi, J.M., and Tarr, P.I. (1997). Predictors of hemolytic uremic syndrome in children during a large outbreak of Escherichia coli O157:H7 infections. Pediatrics *100*, E12.

Bell, D.R., Pinter, G.G., and Wilson, P.D. (1978). Albumin permeability of the peritubular capillaries in rat renal cortex. J Physiol *279*, 621-640.

Berman, M.E., and Muller, W.A. (1995). Ligation of platelet/endothelial cell adhesion molecule 1 (PECAM-1/CD31) on monocytes and neutrophils increases binding capacity of leukocyte CR3 (CD11b/CD18). J Immunol *154*, 299-307.

Bertrand, J.Y., Jalil, A., Klaine, M., Jung, S., Cumano, A., and Godin, I. (2005). Three pathways to mature macrophages in the early mouse yolk sac. Blood *106*, 3004-3011.

Bielaszewska, M., Mellmann, A., Zhang, W., Kock, R., Fruth, A., Bauwens, A., Peters, G., and Karch, H. (2011). Characterisation of the Escherichia coli strain associated with an outbreak of haemolytic uraemic syndrome in Germany, 2011: a microbiological study. Lancet Infect Dis *11*, 671-676.

Bindea, G., Mlecnik, B., Hackl, H., Charoentong, P., Tosolini, M., Kirilovsky, A., Fridman, W.H., Pages, F., Trajanoski, Z., and Galon, J. (2009). ClueGO: a Cytoscape plug-in to decipher functionally grouped gene ontology and pathway annotation networks. Bioinformatics *25*, 1091-1093.

Bisht, K., Sharma, K., Lacoste, B., and Tremblay, M.E. (2016a). Dark microglia: Why are they dark? Commun Integr Biol *9*, e1230575.

Bisht, K., Sharma, K.P., Lecours, C., Sanchez, M.G., El Hajj, H., Milior, G., Olmos-Alonso, A., Gomez-Nicola, D., Luheshi, G., Vallieres, L*., et al.* (2016b). Dark microglia: A new phenotype predominantly associated with pathological states. Glia *64*, 826-839.

Biswas, S.K., Gangi, L., Paul, S., Schioppa, T., Saccani, A., Sironi, M., Bottazzi, B., Doni, A., Vincenzo, B., Pasqualini, F*., et al.* (2006). A distinct and unique transcriptional program expressed by tumor-associated macrophages (defective NF-kappaB and enhanced IRF-3/STAT1 activation). Blood *107*, 2112-2122.

Black, R.A., Rauch, C.T., Kozlosky, C.J., Peschon, J.J., Slack, J.L., Wolfson, M.F., Castner, B.J., Stocking, K.L., Reddy, P., Srinivasan, S*., et al.* (1997). A metalloproteinase disintegrin that releases tumour-necrosis factor-alpha from cells. Nature *385*, 729-733.

Bolisetty, S., Zarjou, A., Hull, T.D., Traylor, A.M., Perianayagam, A., Joseph, R., Kamal, A.I., Arosio, P., Soares, M.P., Jeney, V*., et al.* (2015). Macrophage and epithelial cell H-ferritin expression regulates renal inflammation. Kidney Int *88*, 95-108.

Borges, E., Eytner, R., Moll, T., Steegmaier, M., Campbell, M.A., Ley, K., Mossmann, H., and Vestweber, D. (1997). The P-selectin glycoprotein ligand-1 is important for recruitment of neutrophils into inflamed mouse peritoneum. Blood *90*, 1934-1942.

Borregaard, N. (2010). Neutrophils, from marrow to microbes. Immunity *33*, 657-670.

Boulakirba, S., Pfeifer, A., Mhaidly, R., Obba, S., Goulard, M., Schmitt, T., Chaintreuil, P., Calleja, A., Furstoss, N., Orange, F*., et al.* (2018). IL-34 and CSF-1 display an equivalent macrophage differentiation ability but a different polarization potential. Sci Rep *8*, 256.

Bradley, J.R. (2008). TNF-mediated inflammatory disease. J Pathol *214*, 149-160.

Brigotti, M., Tazzari, P.L., Ravanelli, E., Carnicelli, D., Rocchi, L., Arfilli, V., Scavia, G., Minelli, F., Ricci, F., Pagliaro, P*., et al.* (2011). Clinical relevance of shiga toxin concentrations in the blood of patients with hemolytic uremic syndrome. Pediatr Infect Dis J *30*, 486-490.

Brinkmann, V., Reichard, U., Goosmann, C., Fauler, B., Uhlemann, Y., Weiss, D.S., Weinrauch, Y., and Zychlinsky, A. (2004). Neutrophil extracellular traps kill bacteria. Science *303*, 1532-1535.

Buteau, C., Proulx, F., Chaibou, M., Raymond, D., Clermont, M.J., Mariscalco, M.M., Lebel, M.H., and Seidman, E. (2000). Leukocytosis in children with Escherichia coli O157:H7 enteritis developing the hemolytic-uremic syndrome. Pediatr Infect Dis J *19*, 642-647.

Byrne, P.V., Guilbert, L.J., and Stanley, E.R. (1981). Distribution of cells bearing receptors for a colony-stimulating factor (CSF-1) in murine tissues. J Cell Biol *91*, 848-853.

Camp, V., and Martin, P. (1996). The role of macrophages in clearing programmed cell death in the developing kidney. Anat Embryol (Berl) *194*, 341-348.

Camussi, G., Cappio, F.C., Messina, M., Coppo, R., Stratta, P., and Vercellone, A. (1980). The polymorphonuclear neutrophil (PMN) immunohistological technique: detection of immune complexes bound to the PMN membrane in acute poststreptococcal and lupus nephritis. Clin Nephrol *14*, 280-287.

Cannarile, M.A., Weisser, M., Jacob, W., Jegg, A.M., Ries, C.H., and Ruttinger, D. (2017). Colony-stimulating factor 1 receptor (CSF1R) inhibitors in cancer therapy. J Immunother Cancer *5*, 53.

Cao, Q., Wang, Y., Wang, X.M., Lu, J., Lee, V.W., Ye, Q., Nguyen, H., Zheng, G., Zhao, Y., Alexander, S.I.*, et al.* (2015). Renal F4/80+ CD11c+ mononuclear phagocytes display phenotypic and functional characteristics of macrophages in health and in adriamycin nephropathy. J Am Soc Nephrol *26*, 349-363.

Carroll, M.C. (2008). Complement and humoral immunity. Vaccine *26 Suppl 8*, I28-33.

Carswell, E.A., Old, L.J., Kassel, R.L., Green, S., Fiore, N., and Williamson, B. (1975). An endotoxin-induced serum factor that causes necrosis of tumors. Proc Natl Acad Sci U S A *72*, 3666-3670.

Casanova-Acebes, M., Nicolas-Avila, J.A., Li, J.L., Garcia-Silva, S., Balachander, A., Rubio-Ponce, A., Weiss, L.A., Adrover, J.M., Burrows, K., N, A.G.*, et al.* (2018). Neutrophils instruct homeostatic and pathological states in naive tissues. J Exp Med *215*, 2778-2795.

Cassatella, M.A. (1999). Neutrophil-derived proteins: selling cytokines by the pound. Adv Immunol *73*, 369-509.

Cavaillon, J.M. (2011). The historical milestones in the understanding of leukocyte biology initiated by Elie Metchnikoff. J Leukoc Biol *90*, 413-424.4

Chalmers, S.A., Wen, J., Shum, J., Doerner, J., Herlitz, L., and Putterman, C. (2017). CSF-1R inhibition attenuates renal and neuropsychiatric disease in murine lupus. Clin Immunol *185*, 100-108.

Chen, M., and Geng, J.G. (2006). P-selectin mediates adhesion of leukocytes, platelets, and cancer cells in inflammation, thrombosis, and cancer growth and metastasis. Arch Immunol Ther Exp (Warsz) *54*, 75-84.

Chertov, O., Ueda, H., Xu, L.L., Tani, K., Murphy, W.J., Wang, J.M., Howard, O.M., Sayers, T.J., and Oppenheim, J.J. (1997). Identification of human neutrophil-derived cathepsin G and azurocidin/CAP37 as chemoattractants for mononuclear cells and neutrophils. J Exp Med *186*, 739-747.

Chihara, T., Suzu, S., Hassan, R., Chutiwitoonchai, N., Hiyoshi, M., Motoyoshi, K., Kimura, F., and Okada, S. (2010). IL-34 and M-CSF share the receptor Fms but are not identical in biological activity and signal activation. Cell Death Differ *17*, 1917-1927.

Chitu, V., and Stanley, E.R. (2006). Colony-stimulating factor-1 in immunity and inflammation. Curr Opin Immunol *18*, 39-48.

Chu, W.M. (2013). Tumor necrosis factor. Cancer Lett *328*, 222-225.

Coad, N.A., Marshall, T., Rowe, B., and Taylor, C.M. (1991). Changes in the postenteropathic form of the hemolytic uremic syndrome in children. Clin Nephrol *35*, 10-16.

Collins, A.J., Kasiske, B., Herzog, C., Chavers, B., Foley, R., Gilbertson, D., Grimm, R., Liu, J., Louis, T., Manning, W.*, et al.* (2005). Excerpts from the United States Renal Data System 2004 annual data report: atlas of end-stage renal disease in the United States. Am J Kidney Dis *45*, A5-7, S1-280.

Coppo, P., and Veyradier, A. (2009). Thrombotic microangiopathies: towards a pathophysiology-based classification. Cardiovasc Hematol Disord Drug Targets *9*, 36-50.

Dai, X.M., Ryan, G.R., Hapel, A.J., Dominguez, M.G., Russell, R.G., Kapp, S., Sylvestre, V., and Stanley, E.R. (2002). Targeted disruption of the mouse colony-stimulating factor 1 receptor gene results in osteopetrosis, mononuclear phagocyte deficiency, increased primitive progenitor cell frequencies, and reproductive defects. Blood *99*, 111-120.

Dancey, J.T., Deubelbeiss, K.A., Harker, L.A., and Finch, C.A. (1976). Neutrophil kinetics in man. J Clin Invest *58*, 705-715.

Davies, L.C., Jenkins, S.J., Allen, J.E., and Taylor, P.R. (2013). Tissue-resident macrophages. Nat Immunol *14*, 986-995.

de Boer, I.H., Bangalore, S., Benetos, A., Davis, A.M., Michos, E.D., Muntner, P., Rossing, P., Zoungas, S., and Bakris, G. (2017). Diabetes and Hypertension: A Position Statement by the American Diabetes Association. Diabetes Care *40*, 1273-1284.

De Clercq, E. (2019). Mozobil(R) (Plerixafor, AMD3100), 10 years after its approval by the US Food and Drug Administration. Antivir Chem Chemother *27*, 2040206619829382.

De Filippo, K., Henderson, R.B., Laschinger, M., and Hogg, N. (2008). Neutrophil chemokines KC and macrophage-inflammatory protein-2 are newly synthesized by tissue macrophages using distinct TLR signaling pathways. J Immunol *180*, 4308-4315.

deCathelineau, A.M., and Henson, P.M. (2003). The final step in programmed cell death: phagocytes carry apoptotic cells to the grave. Essays Biochem *39*, 105-117.

Dehnadi, A., Benedict Cosimi, A., Neal Smith, R., Li, X., Alonso, J.L., Means, T.K., and Arnaout, M.A. (2017). Prophylactic orthosteric inhibition of leukocyte integrin CD11b/CD18 prevents long-term fibrotic kidney failure in cynomolgus monkeys. Nat Commun *8*, 13899.

Delmas, Y., Vendrely, B., Clouzeau, B., Bachir, H., Bui, H.N., Lacraz, A., Helou, S., Bordes, C., Reffet, A., Llanas, B.*, et al.* (2014). Outbreak of Escherichia coli O104:H4 haemolytic uraemic syndrome in France: outcome with eculizumab. Nephrol Dial Transplant *29*, 565-572.

Deniset, J.F., Surewaard, B.G., Lee, W.Y., and Kubes, P. (2017). Splenic Ly6G(high) mature and Ly6G(int) immature neutrophils contribute to eradication of S. pneumoniae. J Exp Med *214*, 1333-1350.

Devi, S., Li, A., Westhorpe, C.L., Lo, C.Y., Abeynaike, L.D., Snelgrove, S.L., Hall, P., Ooi, J.D., Sobey, C.G., Kitching, A.R.*, et al.* (2013). Multiphoton imaging reveals a new leukocyte recruitment paradigm in the glomerulus. Nat Med *19*, 107-112.

Distler, U., Souady, J., Hulsewig, M., Drmic-Hofman, I., Haier, J., Friedrich, A.W., Karch, H., Senninger, N., Dreisewerd, K., Berkenkamp, S.*, et al.* (2009). Shiga toxin receptor Gb3Cer/CD77: tumor-association and promising therapeutic target in pancreas and colon cancer. PLoS One *4*, e6813.

Doerschuk, C.M., Allard, M.F., Martin, B.A., MacKenzie, A., Autor, A.P., and Hogg, J.C. (1987). Marginated pool of neutrophils in rabbit lungs. J Appl Physiol (1985) *63*, 1806-1815.

Don, B.R., Spin, G., Nestorov, I., Hutmacher, M., Rose, A., and Kaysen, G.A. (2005). The pharmacokinetics of etanercept in patients with end-stage renal disease on haemodialysis. J Pharm Pharmacol *57*, 1407-1413.

Donohue-Rolfe, A., Kondova, I., Mukherjee, J., Chios, K., Hutto, D., and Tzipori, S. (1999). Antibody-based protection of gnotobiotic piglets infected with Escherichia coli O157:H7 against systemic complications associated with Shiga toxin 2. Infect Immun *67*, 3645-3648.

Downey, C. (2016). Serious infection during etanercept, infliximab and adalimumab therapy for rheumatoid arthritis: A literature review. Int J Rheum Dis *19*, 536-550.

Dwyer, A.R., Greenland, E.L., and Pixley, F.J. (2017). Promotion of Tumor Invasion by Tumor-Associated Macrophages: The Role of CSF-1-Activated Phosphatidylinositol 3 Kinase and Src Family Kinase Motility Signaling. Cancers (Basel) *9*.

Eardley, K.S., Kubal, C., Zehnder, D., Quinkler, M., Lepenies, J., Savage, C.O., Howie, A.J., Kaur, K., Cooper, M.S., Adu, D.*, et al.* (2008). The role of capillary density, macrophage infiltration and interstitial scarring in the pathogenesis of human chronic kidney disease. Kidney Int *74*, 495-504.

Eastwood, J.B., Kerry, S.M., Plange-Rhule, J., Micah, F.B., Antwi, S., Boa, F.G., Banerjee, D., Emmett, L., Miller, M.A., and Cappuccio, F.P. (2010). Assessment of GFR by four methods in adults in Ashanti, Ghana: the need for an eGFR equation for lean African populations. Nephrol Dial Transplant *25*, 2178-2187.

Edwards, J.P., Zhang, X., Frauwirth, K.A., and Mosser, D.M. (2006). Biochemical and functional characterization of three activated macrophage populations. J Leukoc Biol *80*, 1298-1307.

Eisenhauer, P.B., Chaturvedi, P., Fine, R.E., Ritchie, A.J., Pober, J.S., Cleary, T.G., and Newburg, D.S. (2001). Tumor necrosis factor alpha increases human cerebral endothelial cell Gb3 and sensitivity to Shiga toxin. Infect Immun *69*, 1889-1894.

English, B.K., Weaver, W.M., and Wilson, C.B. (1991). Differential regulation of lymphotoxin and tumor necrosis factor genes in human T lymphocytes. J Biol Chem *266*, 7108-7113.

Epelman, S., Lavine, K.J., Beaudin, A.E., Sojka, D.K., Carrero, J.A., Calderon, B., Brija, T., Gautier, E.L., Ivanov, S., Satpathy, A.T.*, et al.* (2014). Embryonic and adult-derived resident cardiac macrophages are maintained through distinct mechanisms at steady state and during inflammation. Immunity *40*, 91-104.

Escamilla, J., Schokrpur, S., Liu, C., Priceman, S.J., Moughon, D., Jiang, Z., Pouliot, F., Magyar, C., Sung, J.L., Xu, J.*, et al.* (2015). CSF1 receptor targeting in prostate cancer reverses macrophage-mediated resistance to androgen blockade therapy. Cancer Res *75*, 950-962.

Exeni, R.A., Fernandez-Brando, R.J., Santiago, A.P., Fiorentino, G.A., Exeni, A.M., Ramos, M.V., and Palermo, M.S. (2018). Pathogenic role of inflammatory response during Shiga toxin-associated hemolytic uremic syndrome (HUS). Pediatr Nephrol *33*, 2057-2071.

Fakhouri, F., Zuber, J., Fremeaux-Bacchi, V., and Loirat, C. (2017). Haemolytic uraemic syndrome. Lancet *390*, 681-696.

Feng, L., Chen, S., Garcia, G.E., Xia, Y., Siani, M.A., Botti, P., Wilson, C.B., Harrison, J.K., and Bacon, K.B. (1999). Prevention of crescentic glomerulonephritis by immunoneutralization of the fractalkine receptor CX3CR1 rapid communication. Kidney Int *56*, 612-620.

Fenton, A., Montgomery, E., Nightingale, P., Peters, A.M., Sheerin, N., Wroe, A.C., and Lipkin, G.W. (2018). Glomerular filtration rate: new age- and gender- specific reference ranges and thresholds for living kidney donation. BMC Nephrol *19*, 336.

Fernandez, G.C., Gomez, S.A., Ramos, M.V., Bentancor, L.V., Fernandez-Brando, R.J., Landoni, V.I., Lopez, L., Ramirez, F., Diaz, M., Alduncin, M.*, et al.* (2007). The functional state of neutrophils correlates with the severity of renal dysfunction in children with hemolytic uremic syndrome. Pediatr Res *61*, 123-128.

Fernandez, G.C., Lopez, M.F., Gomez, S.A., Ramos, M.V., Bentancor, L.V., Fernandez-Brando, R.J., Landoni, V.I., Dran, G.I., Meiss, R., Isturiz, M.A.*, et al.* (2006). Relevance of neutrophils in the murine model of haemolytic uraemic syndrome: mechanisms involved in Shiga toxin type 2-induced neutrophilia. Clin Exp Immunol *146*, 76-84.

Fernandez, G.C., Rubel, C., Dran, G., Gomez, S., Isturiz, M.A., and Palermo, M.S. (2000). Shiga toxin-2 induces neutrophilia and neutrophil activation in a murine model of hemolytic uremic syndrome. Clin Immunol *95*, 227-234.

Floege, J., Eng, E., Young, B.A., and Johnson, R.J. (1993). Factors involved in the regulation of mesangial cell proliferation in vitro and in vivo. Kidney Int Suppl *39*, S47-54.

Fogg, D.K., Sibon, C., Miled, C., Jung, S., Aucouturier, P., Littman, D.R., Cumano, A., and Geissmann, F. (2006). A clonogenic bone marrow progenitor specific for macrophages and dendritic cells. Science *311*, 83-87.

Forsyth, K.D., Simpson, A.C., Fitzpatrick, M.M., Barratt, T.M., and Levinsky, R.J. (1989). Neutrophil-mediated endothelial injury in haemolytic uraemic syndrome. Lancet *2*, 411-414.

Foster, G.H., Armstrong, C.S., Sakiri, R., and Tesh, V.L. (2000). Shiga toxin-induced tumor necrosis factor alpha expression: requirement for toxin enzymatic activity and monocyte protein kinase C and protein tyrosine kinases. Infect Immun *68*, 5183-5189.

Frank, C., Faber, M.S., Askar, M., Bernard, H., Fruth, A., Gilsdorf, A., Hohle, M., Karch, H., Krause, G., Prager, R.*, et al.* (2011a). Large and ongoing outbreak of haemolytic uraemic syndrome, Germany, May 2011. Euro Surveill *16*.

Frank, C., Werber, D., Cramer, J.P., Askar, M., Faber, M., an der Heiden, M., Bernard, H., Fruth, A., Prager, R., Spode, A.*, et al.* (2011b). Epidemic profile of Shiga-toxin-producing Escherichia coli O104:H4 outbreak in Germany. N Engl J Med *365*, 1771-1780.

Garcia, S., Hartkamp, L.M., Malvar-Fernandez, B., van Es, I.E., Lin, H., Wong, J., Long, L., Zanghi, J.A., Rankin, A.L., Masteller, E.L.*, et al.* (2016). Colony-stimulating factor (CSF) 1 receptor blockade reduces inflammation in human and murine models of rheumatoid arthritis. Arthritis Res Ther *18*, 75.

Garg, A.X., Suri, R.S., Barrowman, N., Rehman, F., Matsell, D., Rosas-Arellano, M.P., Salvadori, M., Haynes, R.B., and Clark, W.F. (2003). Long-term renal prognosis of diarrhea-associated hemolytic uremic syndrome: a systematic review, meta-analysis, and meta-regression. JAMA *290*, 1360-1370.

Garrison, L., and McDonnell, N.D. (1999). Etanercept: therapeutic use in patients with rheumatoid arthritis. Ann Rheum Dis *58 Suppl 1*, I65-69.

Gasser, C., Gautier, E., Steck, A., Siebenmann, R.E., and Oechslin, R. (1955). [Hemolytic-uremic syndrome: bilateral necrosis of the renal cortex in acute acquired hemolytic anemia]. Schweiz Med Wochenschr *85*, 905-909.

Gautier, E.L., Shay, T., Miller, J., Greter, M., Jakubzick, C., Ivanov, S., Helft, J., Chow, A., Elpek, K.G., Gordonov, S.*, et al.* (2012). Gene-expression profiles and transcriptional regulatory pathways that underlie the identity and diversity of mouse tissue macrophages. Nat Immunol *13*, 1118-1128.

Geissmann, F., Manz, M.G., Jung, S., Sieweke, M.H., Merad, M., and Ley, K. (2010). Development of monocytes, macrophages, and dendritic cells. Science *327*, 656-661.

Gerrity, R.G. (1981). The role of the monocyte in atherogenesis: I. Transition of blood-borne monocytes into foam cells in fatty lesions. Am J Pathol *103*, 181-190.

Ginhoux, F., Greter, M., Leboeuf, M., Nandi, S., See, P., Gokhan, S., Mehler, M.F., Conway, S.J., Ng, L.G., Stanley, E.R.*, et al.* (2010). Fate mapping analysis reveals that adult microglia derive from primitive macrophages. Science *330*, 841-845.

Gisondi, P., Geat, D., Pizzolato, M., and Girolomoni, G. (2019). State of the art and pharmacological pipeline of biologics for chronic plaque psoriasis. Curr Opin Pharmacol *46*, 90-99.

Gomez, S.A., Abrey-Recalde, M.J., Panek, C.A., Ferrarotti, N.F., Repetto, M.G., Mejias, M.P., Fernandez, G.C., Vanzulli, S., Isturiz, M.A., and Palermo, M.S. (2013). The oxidative stress induced in vivo by Shiga toxin-2 contributes to the pathogenicity of haemolytic uraemic syndrome. Clin Exp Immunol *173*, 463-472.

Gordon, S. (2008). Elie Metchnikoff: father of natural immunity. Eur J Immunol *38*, 3257-3264.

Goswami, S., Sahai, E., Wyckoff, J.B., Cammer, M., Cox, D., Pixley, F.J., Stanley, E.R., Segall, J.E., and Condeelis, J.S. (2005). Macrophages promote the invasion of breast carcinoma cells via a colony-stimulating factor-1/epidermal growth factor paracrine loop. Cancer Res *65*, 5278-5283.

Gottschalk, C., and Kurts, C. (2015). The Debate about Dendritic Cells and Macrophages in the Kidney. Front Immunol *6*, 435.

Griffin, G.K., Newton, G., Tarrio, M.L., Bu, D.X., Maganto-Garcia, E., Azcutia, V., Alcaide, P., Grabie, N., Luscinskas, F.W., Croce, K.J.*, et al.* (2012). IL-17 and TNF-alpha sustain neutrophil recruitment during inflammation through synergistic effects on endothelial activation. J Immunol *188*, 6287-6299.

Gupta, S., and Kaplan, M.J. (2016). The role of neutrophils and NETosis in autoimmune and renal diseases. Nat Rev Nephrol *12*, 402-413.

Haack, J.P., Jelacic, S., Besser, T.E., Weinberger, E., Kirk, D.J., McKee, G.L., Harrison, S.M., Musgrave, K.J., Miller, G., Price, T.H.*, et al.* (2003). Escherichia coli O157 exposure in Wyoming and Seattle: serologic evidence of rural risk. Emerg Infect Dis *9*, 1226-1231.

Hamilton, J.A. (1993). Rheumatoid arthritis: opposing actions of haemopoietic growth factors and slow-acting anti-rheumatic drugs. Lancet *342*, 536-539.

Hamilton, J.A. (2008). Colony-stimulating factors in inflammation and autoimmunity. Nat Rev Immunol *8*, 533-544.

Haraldsson, B., Nystrom, J., and Deen, W.M. (2008). Properties of the glomerular barrier and mechanisms of proteinuria. Physiol Rev *88*, 451-487.

Harel, Y., Silva, M., Giroir, B., Weinberg, A., Cleary, T.B., and Beutler, B. (1993). A reporter transgene indicates renal-specific induction of tumor necrosis factor (TNF) by shiga-like toxin. Possible involvement of TNF in hemolytic uremic syndrome. J Clin Invest *92*, 2110-2116.

Harris, J., and Keane, J. (2010). How tumour necrosis factor blockers interfere with tuberculosis immunity. Clin Exp Immunol *161*, 1-9.

Hashimoto, D., Chow, A., Noizat, C., Teo, P., Beasley, M.B., Leboeuf, M., Becker, C.D., See, P., Price, J., Lucas, D.*, et al.* (2013). Tissue-resident macrophages self-maintain locally throughout adult life with minimal contribution from circulating monocytes. Immunity *38*, 792-804.

Hebert, L.A., Parikh, S., Prosek, J., Nadasdy, T., and Rovin, B.H. (2013). Differential diagnosis of glomerular disease: a systematic and inclusive approach. Am J Nephrol *38*, 253-266.

Herbert, D.R., Holscher, C., Mohrs, M., Arendse, B., Schwegmann, A., Radwanska, M., Leeto, M., Kirsch, R., Hall, P., Mossmann, H.*, et al.* (2004). Alternative macrophage activation is essential for survival during schistosomiasis and downmodulates T helper 1 responses and immunopathology. Immunity *20*, 623-635.

Hill, G.S., Delahousse, M., Nochy, D., Remy, P., Mignon, F., Mery, J.P., and Bariety, J. (2001). Predictive power of the second renal biopsy in lupus nephritis: significance of macrophages. Kidney Int *59*, 304-316.

Hinchliffe, S.A., Sargent, P.H., Howard, C.V., Chan, Y.F., and van Velzen, D. (1991). Human intrauterine renal growth expressed in absolute number of glomeruli assessed by the disector method and Cavalieri principle. Lab Invest *64*, 777-784.

Hoeffel, G., Chen, J., Lavin, Y., Low, D., Almeida, F.F., See, P., Beaudin, A.E., Lum, J., Low, I., Forsberg, E.C.*, et al.* (2015). C-Myb(+) erythro-myeloid progenitor-derived fetal monocytes give rise to adult tissue-resident macrophages. Immunity *42*, 665-678.

Hoeffel, G., and Ginhoux, F. (2015). Ontogeny of Tissue-Resident Macrophages. Front Immunol *6*, 486.

Honold, L., and Nahrendorf, M. (2018). Resident and Monocyte-Derived Macrophages in Cardiovascular Disease. Circ Res *122*, 113-127.

Hudson, B.G., Reeders, S.T., and Tryggvason, K. (1993). Type IV collagen: structure, gene organization, and role in human diseases. Molecular basis of Goodpasture and Alport syndromes and diffuse leiomyomatosis. J Biol Chem *268*, 26033-26036.

Hume, D.A. (2008). Macrophages as APC and the dendritic cell myth. J Immunol *181*, 5829-5835.

Hume, D.A. (2011). Applications of myeloid-specific promoters in transgenic mice support in vivo imaging and functional genomics but do not support the concept of distinct macrophage and dendritic cell lineages or roles in immunity. J Leukoc Biol *89*, 525-538.

Hume, D.A., and Gordon, S. (1983). Mononuclear phagocyte system of the mouse defined by immunohistochemical localization of antigen F4/80. Identification of resident macrophages in renal medullary and cortical interstitium and the juxtaglomerular complex. J Exp Med *157*, 1704-1709.

Hume, D.A., and MacDonald, K.P. (2012). Therapeutic applications of macrophage colony-stimulating factor-1 (CSF-1) and antagonists of CSF-1 receptor (CSF-1R) signaling. Blood *119*, 1810-1820.

Hume, D.A., Ross, I.L., Himes, S.R., Sasmono, R.T., Wells, C.A., and Ravasi, T. (2002). The mononuclear phagocyte system revisited. J Leukoc Biol *72*, 621-627.

Humphreys, B.D., and Bonventre, J.V. (2007). The contribution of adult stem cells to renal repair. Nephrol Ther *3*, 3-10.

Hurley, B.P., Jacewicz, M., Thorpe, C.M., Lincicome, L.L., King, A.J., Keusch, G.T., and Acheson, D.W. (1999). Shiga toxins 1 and 2 translocate differently across polarized intestinal epithelial cells. Infect Immun *67*, 6670-6677.

Hyun, Y.M., Lefort, C.T., and Kim, M. (2009). Leukocyte integrins and their ligand interactions. Immunol Res *45*, 195-208.

Ikezumi, Y., Hurst, L.A., Masaki, T., Atkins, R.C., and Nikolic-Paterson, D.J. (2003). Adoptive transfer studies demonstrate that macrophages can induce proteinuria and mesangial cell proliferation. Kidney Int *63*, 83-95.

Inker, L.A., Schmid, C.H., Tighiouart, H., Eckfeldt, J.H., Feldman, H.I., Greene, T., Kusek, J.W., Manzi, J., Van Lente, F., Zhang, Y.L.*, et al.* (2012). Estimating glomerular filtration rate from serum creatinine and cystatin C. N Engl J Med *367*, 20-29.

Inward, C.D., Howie, A.J., Fitzpatrick, M.M., Rafaat, F., Milford, D.V., and Taylor, C.M. (1997). Renal histopathology in fatal cases of diarrhoea-associated haemolytic uraemic syndrome. British Association for Paediatric Nephrology. Pediatr Nephrol *11*, 556-559.

Isbel, N.M., Nikolic-Paterson, D.J., Hill, P.A., Dowling, J., and Atkins, R.C. (2001). Local macrophage proliferation correlates with increased renal M-CSF expression in human glomerulonephritis. Nephrol Dial Transplant *16*, 1638-1647.

Isogai, E., Isogai, H., Kimura, K., Hayashi, S., Kubota, T., Fujii, N., and Takeshi, K. (1998). Role of tumor necrosis factor alpha in gnotobiotic mice infected with an Escherichia coli O157:H7 strain. Infect Immun *66*, 197-202.

Jacquel, A., Obba, S., Solary, E., and Auberger, P. (2012). Proper macrophagic differentiation requires both autophagy and caspase activation. Autophagy *8*, 1141-1143.

Janeway's immunobiology, K.P. Murphy, C.Weaver, C. Janeway, 9th edition, 2017, Garland Science

Jing, C., Castro-Dopico, T., Richoz, N., Tuong, Z.K., Ferdinand, J.R., Lok, L.S.C., Loudon, K.W., Banham, G.D., Mathews, R.J., Cader, Z.*, et al.* (2020). Macrophage metabolic reprogramming presents a therapeutic target in lupus nephritis. Proc Natl Acad Sci U S A *117*, 15160-15171.

Jo, S.K., Sung, S.A., Cho, W.Y., Go, K.J., and Kim, H.K. (2006). Macrophages contribute to the initiation of ischaemic acute renal failure in rats. Nephrol Dial Transplant *21*, 1231-1239.

Jung, S., Aliberti, J., Graemmel, P., Sunshine, M.J., Kreutzberg, G.W., Sher, A., and Littman, D.R. (2000). Analysis of fractalkine receptor CX(3)CR1 function by targeted deletion and green fluorescent protein reporter gene insertion. Mol Cell Biol *20*, 4106-4114.

Kaplan, B.S., Cleary, T.G., and Obrig, T.G. (1990). Recent advances in understanding the pathogenesis of the hemolytic uremic syndromes. Pediatr Nephrol *4*, 276-283.

Karmali, M.A. (2009). Host and pathogen determinants of verocytotoxin-producing Escherichia coli-associated hemolytic uremic syndrome. Kidney Int Suppl, S4-7.

Karmali, M.A., Steele, B.T., Petric, M., and Lim, C. (1983). Sporadic cases of haemolytic-uraemic syndrome associated with faecal cytotoxin and cytotoxin-producing Escherichia coli in stools. Lancet *1*, 619-620.

Karpman, D., Andreasson, A., Thysell, H., Kaplan, B.S., and Svanborg, C. (1995). Cytokines in childhood hemolytic uremic syndrome and thrombotic thrombocytopenic purpura. Pediatr Nephrol *9*, 694-699.

Kavaliauskiene, S., Dyve Lingelem, A.B., Skotland, T., and Sandvig, K. (2017). Protection against Shiga Toxins. Toxins (Basel) *9*.

Kavi, J., Chant, I., Maris, M., and Rose, P.E. (1987). Cytopathic effect of verotoxin on endothelial cells. Lancet *2*, 1035.

Kawakami, T., Lichtnekert, J., Thompson, L.J., Karna, P., Bouabe, H., Hohl, T.M., Heinecke, J.W., Ziegler, S.F., Nelson, P.J., and Duffield, J.S. (2013). Resident renal mononuclear phagocytes comprise five discrete populations with distinct phenotypes and functions. J Immunol *191*, 3358-3372.

Keepers, T.R., Psotka, M.A., Gross, L.K., and Obrig, T.G. (2006). A murine model of HUS: Shiga toxin with lipopolysaccharide mimics the renal damage and physiologic response of human disease. J Am Soc Nephrol *17*, 3404-3414.

Kelker, H.C., Oppenheim, J.D., Stone-Wolff, D., Henriksen-DeStefano, D., Aggarwal, B.B., Stevenson, H.C., and Vilcek, J. (1985). Characterization of human tumor necrosis factor produced by peripheral blood monocytes and its separation from lymphotoxin. Int J Cancer *36*, 69-73.

Kerjaschki, D. (2005). The crucial role of macrophages in lymphangiogenesis. J Clin Invest *115*, 2316-2319.

Kessenbrock, K., Krumbholz, M., Schonermarck, U., Back, W., Gross, W.L., Werb, Z., Grone, H.J., Brinkmann, V., and Jenne, D.E. (2009). Netting neutrophils in autoimmune small-vessel vasculitis. Nat Med *15*, 623-625.

Kieusseian, A., Brunet de la Grange, P., Burlen-Defranoux, O., Godin, I., and Cumano, A. (2012). Immature hematopoietic stem cells undergo maturation in the fetal liver. Development *139*, 3521-3530.

Kim, M.G., Boo, C.S., Ko, Y.S., Lee, H.Y., Cho, W.Y., Kim, H.K., and Jo, S.K. (2010). Depletion of kidney CD11c+ F4/80+ cells impairs the recovery process in ischaemia/reperfusion-induced acute kidney injury. Nephrol Dial Transplant *25*, 2908-2921.

Kim, N.D., and Luster, A.D. (2015). The role of tissue resident cells in neutrophil recruitment. Trends Immunol *36*, 547-555.

Kitamoto, K., Machida, Y., Uchida, J., Izumi, Y., Shiota, M., Nakao, T., Iwao, H., Yukimura, T., Nakatani, T., and Miura, K. (2009). Effects of liposome clodronate on renal leukocyte populations and renal fibrosis in murine obstructive nephropathy. J Pharmacol Sci *111*, 285-292.

Kitching, A.R., Holdsworth, S.R., and Hickey, M.J. (2008). Targeting leukocytes in immune glomerular diseases. Curr Med Chem *15*, 448-458.

Kitching, A.R., and Hutton, H.L. (2016). The Players: Cells Involved in Glomerular Disease. Clinical journal of the American Society of Nephrology : CJASN *11*, 1664-1674.

Kitic, M., See, P., Bruttger, J., Ginhoux, F., and Waisman, A. (2019). Novel Microglia Depletion Systems: A Genetic Approach Utilizing Conditional Diphtheria Toxin Receptor Expression and a Pharmacological Model Based on the Blocking of Macrophage Colony-Stimulating Factor 1 Receptor. Methods Mol Biol *2034*, 217-230.

Kivelevitch, D., Mansouri, B., and Menter, A. (2014). Long term efficacy and safety of etanercept in the treatment of psoriasis and psoriatic arthritis. Biologics *8*, 169-182.

Klareskog, L., van der Heijde, D., de Jager, J.P., Gough, A., Kalden, J., Malaise, M., Martin Mola, E., Pavelka, K., Sany, J., Settas, L.*, et al.* (2004). Therapeutic effect of the combination of etanercept and methotrexate compared with each treatment alone in patients with rheumatoid arthritis: double-blind randomised controlled trial. Lancet *363*, 675-681.

Klingberg, A., Hasenberg, A., Ludwig-Portugall, I., Medyukhina, A., Mann, L., Brenzel, A., Engel, D.R., Figge, M.T., Kurts, C., and Gunzer, M. (2017). Fully Automated Evaluation of Total Glomerular Number and Capillary Tuft Size in Nephritic Kidneys Using Lightsheet Microscopy. J Am Soc Nephrol *28*, 452-459.

Kobayashi, S.D., Voyich, J.M., Whitney, A.R., and DeLeo, F.R. (2005). Spontaneous neutrophil apoptosis and regulation of cell survival by granulocyte macrophage-colony stimulating factor. J Leukoc Biol *78*, 1408-1418.

Kolaczkowska, E., and Kubes, P. (2013). Neutrophil recruitment and function in health and inflammation. Nat Rev Immunol *13*, 159-175.

Komohara, Y., Jinushi, M., and Takeya, M. (2014). Clinical significance of macrophage heterogeneity in human malignant tumors. Cancer Sci *105*, 1-8.

Koopman, M.G., Koomen, G.C., Krediet, R.T., de Moor, E.A., Hoek, F.J., and Arisz, L. (1989). Circadian rhythm of glomerular filtration rate in normal individuals. Clin Sci (Lond) *77*, 105-111.

Korkosz, M., Bukowska-Strakova, K., Sadis, S., Grodzicki, T., and Siedlar, M. (2012). Monoclonal antibodies against macrophage colony-stimulating factor diminish the number of circulating intermediate and nonclassical (CD14(++)CD16(+)/CD14(+)CD16(++)) monocytes in rheumatoid arthritis patient. Blood *119*, 5329-5330.

Koster, F., Levin, J., Walker, L., Tung, K.S., Gilman, R.H., Rahaman, M.M., Majid, M.A., Islam, S., and Williams, R.C., Jr. (1978). Hemolytic-uremic syndrome after shigellosis. Relation to endotoxemia and circulating immune complexes. N Engl J Med *298*, 927-933.

Kotloff, K.L., Riddle, M.S., Platts-Mills, J.A., Pavlinac, P., and Zaidi, A.K.M. (2018). Shigellosis. Lancet *391*, 801-812.

Kuligowski, M.P., Kitching, A.R., and Hickey, M.J. (2006). Leukocyte recruitment to the inflamed glomerulus: a critical role for platelet-derived P-selectin in the absence of rolling. J Immunol *176*, 6991-6999.

Kunsmann, L., Ruter, C., Bauwens, A., Greune, L., Gluder, M., Kemper, B., Fruth, A., Wai, S.N., He, X., Lloubes, R.*, et al.* (2015). Virulence from vesicles: Novel mechanisms of host cell injury by Escherichia coli O104:H4 outbreak strain. Sci Rep *5*, 13252.

Kusaba, T., and Humphreys, B.D. (2014). Controversies on the origin of proliferating epithelial cells after kidney injury. Pediatr Nephrol *29*, 673-679.

Kwiatkowski, D., Hill, A.V., Sambou, I., Twumasi, P., Castracane, J., Manogue, K.R., Cerami, A., Brewster, D.R., and Greenwood, B.M. (1990). TNF concentration in fatal cerebral, non-fatal cerebral, and uncomplicated Plasmodium falciparum malaria. Lancet *336*, 1201-1204.

Lamb, Y.N. (2019). Pexidartinib: First Approval. Drugs.

Lan, H.Y., Paterson, D.J., and Atkins, R.C. (1991). Initiation and evolution of interstitial leukocytic infiltration in experimental glomerulonephritis. Kidney Int *40*, 425-433.

Lapeyraque, A.L., Malina, M., Fremeaux-Bacchi, V., Boppel, T., Kirschfink, M., Oualha, M., Proulx, F., Clermont, M.J., Le Deist, F., Niaudet, P.*, et al.* (2011). Eculizumab in severe Shiga-toxin-associated HUS. N Engl J Med *364*, 2561-2563.

Lavin, Y., Winter, D., Blecher-Gonen, R., David, E., Keren-Shaul, H., Merad, M., Jung, S., and Amit, I. (2014). Tissue-resident macrophage enhancer landscapes are shaped by the local microenvironment. Cell *159*, 1312-1326.

Lee, H.W., Qin, Y.X., Kim, Y.M., Park, E.Y., Hwang, J.S., Huo, G.H., Yang, C.W., Kim, W.Y., and Kim, J. (2011a). Expression of lymphatic endothelium-specific hyaluronan receptor LYVE-1 in the developing mouse kidney. Cell Tissue Res *343*, 429-444.

Lee, M.S., and Tesh, V.L. (2019). Roles of Shiga Toxins in Immunopathology. Toxins (Basel) *11*.

Lee, S., Huen, S., Nishio, H., Nishio, S., Lee, H.K., Choi, B.S., Ruhrberg, C., and Cantley, L.G. (2011b). Distinct macrophage phenotypes contribute to kidney injury and repair. J Am Soc Nephrol *22*, 317-326.

Lenzo, J.C., Turner, A.L., Cook, A.D., Vlahos, R., Anderson, G.P., Reynolds, E.C., and Hamilton, J.A. (2012). Control of macrophage lineage populations by CSF-1 receptor and GM-CSF in homeostasis and inflammation. Immunol Cell Biol *90*, 429-440.

Lever, J.M., Hull, T.D., Boddu, R., Pepin, M.E., Black, L.M., Adedoyin, O.O., Yang, Z., Traylor, A.M., Jiang, Y., Li, Z.*, et al.* (2019). Resident macrophages reprogram toward a developmental state after acute kidney injury. JCI Insight *4*.

Levine, M.M., DuPont, H.L., Formal, S.B., Hornick, R.B., Takeuchi, A., Gangarosa, E.J., Snyder, M.J., and Libonati, J.P. (1973). Pathogenesis of Shigella dysenteriae 1 (Shiga) dysentery. J Infect Dis *127*, 261-270.

Ley, K., Hoffman, H.M., Kubes, P., Cassatella, M.A., Zychlinsky, A., Hedrick, C.C., and Catz, S.D. (2018). Neutrophils: New insights and open questions. Sci Immunol *3*.

Ley, K., Laudanna, C., Cybulsky, M.I., and Nourshargh, S. (2007). Getting to the site of inflammation: the leukocyte adhesion cascade updated. Nat Rev Immunol *7*, 678-689.

Liew, P.X., and Kubes, P. (2019). The Neutrophil's Role During Health and Disease. Physiol Rev *99*, 1223-1248.

Lin, E.Y., Nguyen, A.V., Russell, R.G., and Pollard, J.W. (2001). Colony-stimulating factor 1 promotes progression of mammary tumors to malignancy. J Exp Med *193*, 727-740.

Lingwood, C.A. (1994). Verotoxin-binding in human renal sections. Nephron *66*, 21-28.

Liu, K., Victora, G.D., Schwickert, T.A., Guermonprez, P., Meredith, M.M., Yao, K., Chu, F.F., Randolph, G.J., Rudensky, A.Y., and Nussenzweig, M. (2009). In vivo analysis of dendritic cell development and homeostasis. Science *324*, 392-397.

Lloyd, S.A., Yuan, Y.Y., Simske, S.J., Riffle, S.E., Ferguson, V.L., and Bateman, T.A. (2009). Administration of high-dose macrophage colony-stimulating factor increases bone turnover and trabecular volume fraction. J Bone Miner Metab *27*, 546-554.

Lloyd-Jones, D., Adams, R.J., Brown, T.M., Carnethon, M., Dai, S., De Simone, G., Ferguson, T.B., Ford, E., Furie, K., Gillespie, C.*, et al.* (2010). Executive summary: heart disease and stroke statistics--2010 update: a report from the American Heart Association. Circulation *121*, 948-954.

Loirat, C., and Fremeaux-Bacchi, V. (2011). Atypical hemolytic uremic syndrome. Orphanet J Rare Dis *6*, 60.

Lopez, E.L., Contrini, M.M., Glatstein, E., Gonzalez Ayala, S., Santoro, R., Allende, D., Ezcurra, G., Teplitz, E., Koyama, T., Matsumoto, Y.*, et al.* (2010). Safety and pharmacokinetics of urtoxazumab, a humanized monoclonal antibody, against Shiga-like toxin 2 in healthy adults and in pediatric patients infected with Shiga-like toxin-producing Escherichia coli. Antimicrob Agents Chemother *54*, 239-243.

Louise, C.B., and Obrig, T.G. (1992). Shiga toxin-associated hemolytic uremic syndrome: combined cytotoxic effects of shiga toxin and lipopolysaccharide (endotoxin) on human vascular endothelial cells in vitro. Infect Immun *60*, 1536-1543.

Ma, F.Y., Ikezumi, Y., and Nikolic-Paterson, D.J. (2010). Macrophage signaling pathways: a novel target in renal disease. Semin Nephrol *30*, 334-344.

MacDonald, K.P., Palmer, J.S., Cronau, S., Seppanen, E., Olver, S., Raffelt, N.C., Kuns, R., Pettit, A.R., Clouston, A., Wainwright, B.*, et al.* (2010). An antibody against the colony-stimulating factor 1 receptor depletes the resident subset of monocytes and tissue- and tumor-associated macrophages but does not inhibit inflammation. Blood *116*, 3955-3963.

MacDonald, K.P., Rowe, V., Bofinger, H.M., Thomas, R., Sasmono, T., Hume, D.A., and Hill, G.R. (2005). The colony-stimulating factor 1 receptor is expressed on dendritic cells during differentiation and regulates their expansion. J Immunol *175*, 1399-1405.

Martinez, F.O., and Gordon, S. (2014). The M1 and M2 paradigm of macrophage activation: time for reassessment. F1000Prime Rep *6*, 13.

Masek-Hammerman, K., Peeva, E., Ahmad, A., Menon, S., Afsharvand, M., Peng Qu, R., Cheng, J.B., Syed, J., Zhan, Y., O'Neil, S.P.*, et al.* (2016). Monoclonal antibody against macrophage colony-stimulating factor suppresses circulating monocytes and tissue macrophage function but does not alter cell infiltration/activation in cutaneous lesions or clinical outcomes in patients with cutaneous lupus erythematosus. Clin Exp Immunol *183*, 258-270.

Mass, E., Ballesteros, I., Farlik, M., Halbritter, F., Gunther, P., Crozet, L., Jacome-Galarza, C.E., Handler, K., Klughammer, J., Kobayashi, Y.*, et al.* (2016). Specification of tissue-resident macrophages during organogenesis. Science *353*.

Mauer, A.M., Athens, J.W., Ashenbrucker, H., Cartwright, G.E., and Wintrobe, M.M. (1960). Leukokinetic Studies. Ii. A Method for Labeling Granulocytes in Vitro with Radioactive Diisopropylfluorophosphate (Dfp). J Clin Invest *39*, 1481-1486.

Mayadas, T.N., Rosetti, F., Ernandez, T., and Sethi, S. (2010). Neutrophils: game changers in glomerulonephritis? Trends Mol Med *16*, 368-378.

McCullough, K.P., Morgenstern, H., Saran, R., Herman, W.H., and Robinson, B.M. (2019). Projecting ESRD Incidence and Prevalence in the United States through 2030. J Am Soc Nephrol *30*, 127-135.

McGrath, K.E., Koniski, A.D., Malik, J., and Palis, J. (2003). Circulation is established in a stepwise pattern in the mammalian embryo. Blood *101*, 1669-1676.

Melton-Celsa, A.R. (2014). Shiga Toxin (Stx) Classification, Structure, and Function. Microbiol Spectr *2*, EHEC-0024-2013.

Mene, P., Simonson, M.S., and Dunn, M.J. (1989). Physiology of the mesangial cell. Physiol Rev *69*, 1347-1424.

Merad, M., Manz, M.G., Karsunky, H., Wagers, A., Peters, W., Charo, I., Weissman, I.L., Cyster, J.G., and Engleman, E.G. (2002). Langerhans cells renew in the skin throughout life under steady-state conditions. Nat Immunol *3*, 1135-1141.

Merten, M., and Thiagarajan, P. (2000). P-selectin expression on platelets determines size and stability of platelet aggregates. Circulation *102*, 1931-1936.

Merten, M., and Thiagarajan, P. (2004). P-selectin in arterial thrombosis. Z Kardiol *93*, 855-863.

Mestas, J., and Ley, K. (2008). Monocyte-endothelial cell interactions in the development of atherosclerosis. Trends Cardiovasc Med *18*, 228-232.

Meyers, K.E., and Kaplan, B.S. (2000). Many cell types are Shiga toxin targets. Kidney Int *57*, 2650-2651.

Mian, A.N., and Schwartz, G.J. (2017). Measurement and Estimation of Glomerular Filtration Rate in Children. Adv Chronic Kidney Dis *24*, 348-356.

Michino, H., Araki, K., Minami, S., Takaya, S., Sakai, N., Miyazaki, M., Ono, A., and Yanagawa, H. (1999). Massive outbreak of Escherichia coli O157:H7 infection in schoolchildren in Sakai City, Japan, associated with consumption of white radish sprouts. Am J Epidemiol *150*, 787-796.

Milford, D., Taylor, C.M., Rafaat, F., Halloran, E., and Dawes, J. (1989). Neutrophil elastases and haemolytic uraemic syndrome. Lancet *2*, 1153.

Mills, C.D., Kincaid, K., Alt, J.M., Heilman, M.J., and Hill, A.M. (2000). M-1/M-2 macrophages and the Th1/Th2 paradigm. J Immunol *164*, 6166-6173.

Miner, J.H. (2011). Glomerular basement membrane composition and the filtration barrier. Pediatr Nephrol *26*, 1413-1417.

Mitchem, J.B., Brennan, D.J., Knolhoff, B.L., Belt, B.A., Zhu, Y., Sanford, D.E., Belaygorod, L., Carpenter, D., Collins, L., Piwnica-Worms, D*., et al.* (2013). Targeting tumor-infiltrating macrophages decreases tumor-initiating cells, relieves immunosuppression, and improves chemotherapeutic responses. Cancer Res *73*, 1128-1141.

Miyabe, Y., Miyabe, C., Murooka, T.T., Kim, E.Y., Newton, G.A., Kim, N.D., Haribabu, B., Luscinskas, F.W., Mempel, T.R., and Luster, A.D. (2017). Complement C5a Receptor is the Key Initiator of Neutrophil Adhesion Igniting Immune Complex-induced Arthritis. Sci Immunol *2*.

Mohawk, K.L., and O'Brien, A.D. (2011). Mouse models of Escherichia coli O157:H7 infection and shiga toxin injection. J Biomed Biotechnol *2011*, 258185.

Molawi, K., Wolf, Y., Kandalla, P.K., Favret, J., Hagemeyer, N., Frenzel, K., Pinto, A.R., Klapproth, K., Henri, S., Malissen, B*., et al.* (2014). Progressive replacement of embryo-derived cardiac macrophages with age. J Exp Med *211*, 2151-2158.

Montecucco, F., Steffens, S., Burger, F., Da Costa, A., Bianchi, G., Bertolotto, M., Mach, F., Dallegri, F., and Ottonello, L. (2008). Tumor necrosis factor-alpha (TNF-alpha) induces integrin CD11b/CD18 (Mac-1) up-regulation and migration to the CC chemokine CCL3 (MIP-1alpha) on human neutrophils through defined signalling pathways. Cell Signal *20*, 557-568.

Moon, H.W., Whipp, S.C., Argenzio, R.A., Levine, M.M., and Giannella, R.A. (1983). Attaching and effacing activities of rabbit and human enteropathogenic Escherichia coli in pig and rabbit intestines. Infect Immun *41*, 1340-1351.

Moore, K.J., and Tabas, I. (2011). Macrophages in the pathogenesis of atherosclerosis. Cell *145*, 341-355.

Mora-Bau, G., Platt, A.M., van Rooijen, N., Randolph, G.J., Albert, M.L., and Ingersoll, M.A. (2015). Macrophages Subvert Adaptive Immunity to Urinary Tract Infection. PLoS Pathog *11*, e1005044.

Moreland, L.W. (1998). Soluble tumor necrosis factor receptor (p75) fusion protein (ENBREL) as a therapy for rheumatoid arthritis. Rheum Dis Clin North Am *24*, 579-591.

Morigi, M., Micheletti, G., Figliuzzi, M., Imberti, B., Karmali, M.A., Remuzzi, A., Remuzzi, G., and Zoja, C. (1995). Verotoxin-1 promotes leukocyte adhesion to cultured endothelial cells under physiologic flow conditions. Blood *86*, 4553-4558.

Mowat, A.M., Scott, C.L., and Bain, C.C. (2017). Barrier-tissue macrophages: functional adaptation to environmental challenges. Nat Med *23*, 1258-1270.

Mucenski, M.L., McLain, K., Kier, A.B., Swerdlow, S.H., Schreiner, C.M., Miller, T.A., Pietryga, D.W., Scott, W.J., Jr., and Potter, S.S. (1991). A functional c-myb gene is required for normal murine fetal hepatic hematopoiesis. Cell *65*, 677-689.

Munro, D.A.D., and Hughes, J. (2017). The Origins and Functions of Tissue-Resident Macrophages in Kidney Development. Front Physiol *8*, 837.

Murata, A., Shimazu, T., Yamamoto, T., Taenaka, N., Nagayama, K., Honda, T., Sugimoto, H., Monden, M., Matsuura, N., and Okada, S. (1998). Profiles of circulating inflammatory- and anti-inflammatory cytokines in patients with hemolytic uremic syndrome due to E. coli O157 infection. Cytokine *10*, 544-548.

Murdoch, C., Muthana, M., Coffelt, S.B., and Lewis, C.E. (2008). The role of myeloid cells in the promotion of tumour angiogenesis. Nat Rev Cancer *8*, 618-631.

Murray, P.J., Allen, J.E., Biswas, S.K., Fisher, E.A., Gilroy, D.W., Goerdt, S., Gordon, S., Hamilton, J.A., Ivashkiv, L.B., Lawrence, T.*, et al.* (2014). Macrophage activation and polarization: nomenclature and experimental guidelines. Immunity *41*, 14-20.

Nahrendorf, M., and Swirski, F.K. (2016). Abandoning M1/M2 for a Network Model of Macrophage Function. Circ Res *119*, 414-417.

Naito, M., Takahashi, K., and Nishikawa, S. (1990). Development, differentiation, and maturation of macrophages in the fetal mouse liver. J Leukoc Biol *48*, 27-37.

Nakatsuka, M., Asagiri, K., Noguchi, S., Habara, T., and Kudo, T. (2000). Nafamostat mesilate, a serine protease inhibitor, suppresses lipopolysaccharide-induced nitric oxide synthesis and apoptosis in cultured human trophoblasts. Life Sci *67*, 1243-1250.

Nandi, S., Gokhan, S., Dai, X.M., Wei, S., Enikolopov, G., Lin, H., Mehler, M.F., and Stanley, E.R. (2012). The CSF-1 receptor ligands IL-34 and CSF-1 exhibit distinct developmental brain expression patterns and regulate neural progenitor cell maintenance and maturation. Dev Biol *367*, 100-113.

Nathan, C., Srimal, S., Farber, C., Sanchez, E., Kabbash, L., Asch, A., Gailit, J., and Wright, S.D. (1989). Cytokine-induced respiratory burst of human neutrophils: dependence on extracellular matrix proteins and CD11/CD18 integrins. J Cell Biol *109*, 1341-1349.

Nikolic-Paterson, D.J., and Atkins, R.C. (2001). The role of macrophages in glomerulonephritis. Nephrol Dial Transplant *16 Suppl 5*, 3-7.

Nikolic-Paterson, D.J., Wang, S., and Lan, H.Y. (2014). Macrophages promote renal fibrosis through direct and indirect mechanisms. Kidney Int Suppl (2011) *4*, 34-38.

Niu, S., Paluszynski, J., Bian, Z., Shi, L., Kidder, K., and Liu, Y. (2018). LPS-primed CD11b(+) leukocytes serve as an effective carrier of Shiga toxin 2 to cause hemolytic uremic syndrome in mice. Sci Rep *8*, 3994.

Noda, M., Yutsudo, T., Nakabayashi, N., Hirayama, T., and Takeda, Y. (1987). Purification and some properties of Shiga-like toxin from Escherichia coli O157:H7 that is immunologically identical to Shiga toxin. Microb Pathog *2*, 339-349.

Noy, R., and Pollard, J.W. (2014). Tumor-associated macrophages: from mechanisms to therapy. Immunity *41*, 49-61.

O'Brien, C.D., Lim, P., Sun, J., and Albelda, S.M. (2003). PECAM-1-dependent neutrophil transmigration is independent of monolayer PECAM-1 signaling or localization. Blood *101*, 2816-2825.

Odaka, C., Mizuochi, T., Yang, J., and Ding, A. (2003). Murine macrophages produce secretory leukocyte protease inhibitor during clearance of apoptotic cells: implications for resolution of the inflammatory response. J Immunol *171*, 1507-1514.

Okabe, Y., and Medzhitov, R. (2014). Tissue-specific signals control reversible program of localization and functional polarization of macrophages. Cell *157*, 832-844.

Orecchioni, M., Ghosheh, Y., Pramod, A.B., and Ley, K. (2019). Macrophage Polarization: Different Gene Signatures in M1(LPS+) vs. Classically and M2(LPS-) vs. Alternatively Activated Macrophages. Front Immunol *10*, 1084.

Palermo, M.S., Alves Rosa, M.F., Van Rooijen, N., and Isturiz, M.A. (1999). Depletion of liver and splenic macrophages reduces the lethality of Shiga toxin-2 in a mouse model. Clin Exp Immunol *116*, 462-467.

Palis, J., Robertson, S., Kennedy, M., Wall, C., and Keller, G. (1999). Development of erythroid and myeloid progenitors in the yolk sac and embryo proper of the mouse. Development *126*, 5073-5084.

Parnaik, R., Raff, M.C., and Scholes, J. (2000). Differences between the clearance of apoptotic cells by professional and non-professional phagocytes. Curr Biol *10*, 857-860.

Paulus, P., Stanley, E.R., Schafer, R., Abraham, D., and Aharinejad, S. (2006). Colony-stimulating factor-1 antibody reverses chemoresistance in human MCF-7 breast cancer xenografts. Cancer Res *66*, 4349-4356.

Petruzziello-Pellegrini, T.N., Moslemi-Naeini, M., and Marsden, P.A. (2013). New insights into Shiga toxin-mediated endothelial dysfunction in hemolytic uremic syndrome. Virulence *4*, 556-563.

Petruzziello-Pellegrini, T.N., Yuen, D.A., Page, A.V., Patel, S., Soltyk, A.M., Matouk, C.C., Wong, D.K., Turgeon, P.J., Fish, J.E., Ho, J.J.*, et al.* (2012). The CXCR4/CXCR7/SDF-1 pathway contributes to the pathogenesis of Shiga toxin-associated hemolytic uremic syndrome in humans and mice. J Clin Invest *122*, 759-776.

Pillay, J., den Braber, I., Vrisekoop, N., Kwast, L.M., de Boer, R.J., Borghans, J.A., Tesselaar, K., and Koenderman, L. (2010). In vivo labeling with 2H2O reveals a human neutrophil lifespan of 5.4 days. Blood *116*, 625-627.

Pober, J.S., and Sessa, W.C. (2007). Evolving functions of endothelial cells in inflammation. Nat Rev Immunol *7*, 803-815.

Pohl, J.M., Volke, J.K., Thiebes, S., Brenzel, A., Fuchs, K., Beziere, N., Ehrlichmann, W., Pichler, B.J., Squire, A., Gueler, F.*, et al.* (2018). CCR2-dependent Gr1(high) monocytes promote kidney injury in shiga toxin-induced hemolytic uremic syndrome in mice. Eur J Immunol *48*, 990-1000.

Pollak, M.R., Quaggin, S.E., Hoenig, M.P., and Dworkin, L.D. (2014). The glomerulus: the sphere of influence. Clinical journal of the American Society of Nephrology : CJASN *9*, 1461-1469.

Pollard, J.W. (2009). Trophic macrophages in development and disease. Nat Rev Immunol *9*, 259-270.

Ponzoni, M., Pastorino, F., Di Paolo, D., Perri, P., and Brignole, C. (2018). Targeting Macrophages as a Potential Therapeutic Intervention: Impact on Inflammatory Diseases and Cancer. Int J Mol Sci *19*.

Potter, A.A., Klashinsky, S., Li, Y., Frey, E., Townsend, H., Rogan, D., Erickson, G., Hinkley, S., Klopfenstein, T., Moxley, R.A.*, et al.* (2004). Decreased shedding of Escherichia coli O157:H7 by cattle following vaccination with type III secreted proteins. Vaccine *22*, 362-369.

Puga, I., Cols, M., Barra, C.M., He, B., Cassis, L., Gentile, M., Comerma, L., Chorny, A., Shan, M., Xu, W.*, et al.* (2011). B cell-helper neutrophils stimulate the diversification and production of immunoglobulin in the marginal zone of the spleen. Nat Immunol *13*, 170-180.

Puranik, A.S., Leaf, I.A., Jensen, M.A., Hedayat, A.F., Saad, A., Kim, K.W., Saadalla, A.M., Woollard, J.R., Kashyap, S., Textor, S.C.*, et al.* (2018). Kidney-resident macrophages promote a proangiogenic environment in the normal and chronically ischemic mouse kidney. Sci Rep *8*, 13948.

Pyonteck, S.M., Akkari, L., Schuhmacher, A.J., Bowman, R.L., Sevenich, L., Quail, D.F., Olson, O.C., Quick, M.L., Huse, J.T., Teijeiro, V.*, et al.* (2013). CSF-1R inhibition alters macrophage polarization and blocks glioma progression. Nat Med *19*, 1264-1272.

Rabinovitch, M. (1995). Professional and non-professional phagocytes: an introduction. Trends Cell Biol *5*, 85-87.

Rae, F., Woods, K., Sasmono, T., Campanale, N., Taylor, D., Ovchinnikov, D.A., Grimmond, S.M., Hume, D.A., Ricardo, S.D., and Little, M.H. (2007). Characterisation and trophic functions of murine embryonic macrophages based upon the use of a Csf1r-EGFP transgene reporter. Dev Biol *308*, 232-246.

Rafat, C., Coppo, P., Fakhouri, F., Fremeaux-Bacchi, V., Loirat, C., Zuber, J., and Rondeau, E. (2017). [Hemolytic and uremic syndrome and related thrombotic microangiopathies: Treatment and prognosis]. Rev Med Interne *38*, 833-839.

Ramos, M.V., Auvynet, C., Poupel, L., Rodero, M., Mejias, M.P., Panek, C.A., Vanzulli, S., Combadiere, C., and Palermo, M. (2012). Chemokine receptor CCR1 disruption limits renal damage in a murine model of hemolytic uremic syndrome. Am J Pathol *180*, 1040-1048.

Ramos, M.V., Mejias, M.P., Sabbione, F., Fernandez-Brando, R.J., Santiago, A.P., Amaral, M.M., Exeni, R., Trevani, A.S., and Palermo, M.S. (2016). Induction of Neutrophil Extracellular Traps in Shiga Toxin-Associated Hemolytic Uremic Syndrome. J Innate Immun *8*, 400-411.

Ricardo, S.D., van Goor, H., and Eddy, A.A. (2008). Macrophage diversity in renal injury and repair. J Clin Invest *118*, 3522-3530.

Ries, C.H., Cannarile, M.A., Hoves, S., Benz, J., Wartha, K., Runza, V., Rey-Giraud, F., Pradel, L.P., Feuerhake, F., Klaman, I.*, et al.* (2014). Targeting tumor-associated macrophages with anti-CSF-1R antibody reveals a strategy for cancer therapy. Cancer Cell *25*, 846-859.

Riley, L.W., Remis, R.S., Helgerson, S.D., McGee, H.B., Wells, J.G., Davis, B.R., Hebert, R.J., Olcott, E.S., Johnson, L.M., Hargrett, N.T*., et al.* (1983). Hemorrhagic colitis associated with a rare Escherichia coli serotype. N Engl J Med *308*, 681-685.

Robak, T., Gladalska, A., and Stepien, H. (1998). The tumour necrosis factor family of receptors/ligands in the serum of patients with rheumatoid arthritis. Eur Cytokine Netw *9*, 145-154.

Robson, W.L., Fick, G.H., and Wilson, P.C. (1988). Prognostic factors in typical postdiarrhea hemolytic-uremic syndrome. Child Nephrol Urol *9*, 203-207.

Roche, J.K., Keepers, T.R., Gross, L.K., Seaner, R.M., and Obrig, T.G. (2007). CXCL1/KC and CXCL2/MIP-2 are critical effectors and potential targets for therapy of Escherichia coli O157:H7-associated renal inflammation. Am J Pathol *170*, 526-537.

Rowley, W.R., Bezold, C., Arikan, Y., Byrne, E., and Krohe, S. (2017). Diabetes 2030: Insights from Yesterday, Today, and Future Trends. Popul Health Manag *20*, 6-12.

Ruggenenti, P., Noris, M., and Remuzzi, G. (2001). Thrombotic microangiopathy, hemolytic uremic syndrome, and thrombotic thrombocytopenic purpura. Kidney Int *60*, 831-846.

Ruggenenti, P., and Remuzzi, G. (1991). Thrombotic microangiopathies. Crit Rev Oncol Hematol *11*, 243-265.

Sadik, C.D., Kim, N.D., and Luster, A.D. (2011). Neutrophils cascading their way to inflammation. Trends Immunol *32*, 452-460.

Salvadori, M., and Bertoni, E. (2013). Update on hemolytic uremic syndrome: Diagnostic and therapeutic recommendations. World J Nephrol *2*, 56-76.

Sandvig, K., and van Deurs, B. (1996). Endocytosis, intracellular transport, and cytotoxic action of Shiga toxin and ricin. Physiol Rev *76*, 949-966.

Sarrazin, S., Mossadegh-Keller, N., Fukao, T., Aziz, A., Mourcin, F., Vanhille, L., Kelly Modis, L., Kastner, P., Chan, S., Duprez, E*., et al.* (2009). MafB restricts M-CSF-dependent myeloid commitment divisions of hematopoietic stem cells. Cell *138*, 300-313.

Sasaki, S., Omoe, K., Tagawa, Y., Iwakura, Y., Sekikawa, K., Shinagawa, K., and Nakane, A. (2002). Roles of gamma interferon and tumor necrosis factor-alpha in shiga toxin lethality. Microb Pathog *33*, 43-47.

Sasmono, R.T., Oceandy, D., Pollard, J.W., Tong, W., Pavli, P., Wainwright, B.J., Ostrowski, M.C., Himes, S.R., and Hume, D.A. (2003). A macrophage colony-stimulating factor receptor-green fluorescent protein transgene is expressed throughout the mononuclear phagocyte system of the mouse. Blood *101*, 1155-1163.

Sauter, K.A., Melton-Celsa, A.R., Larkin, K., Troxell, M.L., O'Brien, A.D., and Magun, B.E. (2008). Mouse model of hemolytic-uremic syndrome caused by endotoxin-free Shiga toxin 2 (Stx2) and protection from lethal outcome by anti-Stx2 antibody. Infect Immun *76*, 4469-4478.

Schindelin, J., Arganda-Carreras, I., Frise, E., Kaynig, V., Longair, M., Pietzsch, T., Preibisch, S., Rueden, C., Saalfeld, S., Schmid, B*., et al.* (2012). Fiji: an open-source platform for biological-image analysis. Nat Methods *9*, 676-682.

Schiwon, M., Weisheit, C., Franken, L., Gutweiler, S., Dixit, A., Meyer-Schwesinger, C., Pohl, J.M., Maurice, N.J., Thiebes, S., Lorenz, K*., et al.* (2014). Crosstalk between sentinel and helper macrophages permits neutrophil migration into infected uroepithelium. Cell *156*, 456-468.

Schultze, J.L. (2016). Reprogramming of macrophages--new opportunities for therapeutic targeting. Curr Opin Pharmacol *26*, 10-15.

Schulz, C., Gomez Perdiguero, E., Chorro, L., Szabo-Rogers, H., Cagnard, N., Kierdorf, K., Prinz, M., Wu, B., Jacobsen, S.E., Pollard, J.W*., et al.* (2012). A lineage of myeloid cells independent of Myb and hematopoietic stem cells. Science *336*, 86-90.

Schulz, C., Lai, X., Bertrams, W., Jung, A.L., Sittka-Stark, A., Herkt, C.E., Janga, H., Zscheppang, K., Stielow, C., Schulte, L*., et al.* (2017). THP-1-derived macrophages render lung epithelial cells hypo-responsive to Legionella pneumophila - a systems biology study. Sci Rep *7*, 11988.

Scott, C.L., Zheng, F., De Baetselier, P., Martens, L., Saeys, Y., De Prijck, S., Lippens, S., Abels, C., Schoonooghe, S., Raes, G*., et al.* (2016). Bone marrow-derived monocytes give rise to self-renewing and fully differentiated Kupffer cells. Nat Commun *7*, 10321.

Sedger, L.M., and McDermott, M.F. (2014). TNF and TNF-receptors: From mediators of cell death and inflammation to therapeutic giants - past, present and future. Cytokine Growth Factor Rev *25*, 453-472.

Segerer, S., Henger, A., Schmid, H., Kretzler, M., Draganovici, D., Brandt, U., Noessner, E., Nelson, P.J., Kerjaschki, D., Schlondorff, D.*, et al.* (2006). Expression of the chemokine receptor CXCR1 in human glomerular diseases. Kidney Int *69*, 1765-1773.

Serna, A.t., and Boedeker, E.C. (2008). Pathogenesis and treatment of Shiga toxin-producing Escherichia coli infections. Curr Opin Gastroenterol *24*, 38-47.

Sethi, S., Haas, M., Markowitz, G.S., D'Agati, V.D., Rennke, H.G., Jennette, J.C., Bajema, I.M., Alpers, C.E., Chang, A., Cornell, L.D.*, et al.* (2016). Mayo Clinic/Renal Pathology Society Consensus Report on Pathologic Classification, Diagnosis, and Reporting of GN. J Am Soc Nephrol *27*, 1278-1287.

Shankland, S.J., Smeets, B., Pippin, J.W., and Moeller, M.J. (2014). The emergence of the glomerular parietal epithelial cell. Nat Rev Nephrol *10*, 158-173.

Sheng, J., Ruedl, C., and Karjalainen, K. (2015). Most Tissue-Resident Macrophages Except Microglia Are Derived from Fetal Hematopoietic Stem Cells. Immunity *43*, 382-393.

Soehnlein, O., Zernecke, A., Eriksson, E.E., Rothfuchs, A.G., Pham, C.T., Herwald, H., Bidzhekov, K., Rottenberg, M.E., Weber, C., and Lindbom, L. (2008). Neutrophil secretion products pave the way for inflammatory monocytes. Blood *112*, 1461-1471.

Sola, A., Weigert, A., Jung, M., Vinuesa, E., Brecht, K., Weis, N., Brune, B., Borregaard, N., and Hotter, G. (2011). Sphingosine-1-phosphate signalling induces the production of Lcn-2 by macrophages to promote kidney regeneration. J Pathol *225*, 597-608.

Soos, T.J., Sims, T.N., Barisoni, L., Lin, K., Littman, D.R., Dustin, M.L., and Nelson, P.J. (2006). CX3CR1+ interstitial dendritic cells form a contiguous network throughout the entire kidney. Kidney Int *70*, 591-596.

Speeckaert, M.M., Speeckaert, R., Laute, M., Vanholder, R., and Delanghe, J.R. (2012). Tumor necrosis factor receptors: biology and therapeutic potential in kidney diseases. Am J Nephrol *36*, 261-270.

Sridharan, M., Go, R.S., and Willrich, M.A.V. (2018). Atypical hemolytic uremic syndrome: Review of clinical presentation, diagnosis and management. J Immunol Methods *461*, 15-22.

Stamatiades, E.G., Tremblay, M.E., Bohm, M., Crozet, L., Bisht, K., Kao, D., Coelho, C., Fan, X., Yewdell, W.T., Davidson, A.*, et al.* (2016). Immune Monitoring of Trans-endothelial Transport by Kidney-Resident Macrophages. Cell *166*, 991-1003.

Stanley, E.R., Chen, D.M., and Lin, H.S. (1978). Induction of macrophage production and proliferation by a purified colony stimulating factor. Nature *274*, 168-170.

Stanley, E.R., and Chitu, V. (2014). CSF-1 receptor signaling in myeloid cells. Cold Spring Harb Perspect Biol *6*.

Stanley, E.R., Cifone, M., Heard, P.M., and Defendi, V. (1976). Factors regulating macrophage production and growth: identity of colony-stimulating factor and macrophage growth factor. J Exp Med *143*, 631-647.

Stein, M., Keshav, S., Harris, N., and Gordon, S. (1992). Interleukin 4 potently enhances murine macrophage mannose receptor activity: a marker of alternative immunologic macrophage activation. J Exp Med *176*, 287-292.

Stout, R.D., Jiang, C., Matta, B., Tietzel, I., Watkins, S.K., and Suttles, J. (2005). Macrophages sequentially change their functional phenotype in response to changes in microenvironmental influences. J Immunol *175*, 342-349.

Sugioka, Y., Inui, K., and Koike, T. (2008). Use of etanercept in a patient with rheumatoid arthritis on hemodialysis. Mod Rheumatol *18*, 293-295.

Suh, J.H., and Miner, J.H. (2013). The glomerular basement membrane as a barrier to albumin. Nat Rev Nephrol *9*, 470-477.

Summers, C., Rankin, S.M., Condliffe, A.M., Singh, N., Peters, A.M., and Chilvers, E.R. (2010). Neutrophil kinetics in health and disease. Trends Immunol *31*, 318-324.

Takano, T., Azuma, N., Satoh, M., Toda, A., Hashida, Y., Satoh, R., and Hohdatsu, T. (2009). Neutrophil survival factors (TNF-alpha, GM-CSF, and G-CSF) produced by macrophages in cats infected with feline infectious peritonitis virus contribute to the pathogenesis of granulomatous lesions. Arch Virol *154*, 775-781.

Tamoutounour, S., Guilliams, M., Montanana Sanchis, F., Liu, H., Terhorst, D., Malosse, C., Pollet, E., Ardouin, L., Luche, H., Sanchez, C.*, et al.* (2013). Origins and functional specialization of macrophages and of conventional and monocyte-derived dendritic cells in mouse skin. Immunity *39*, 925-938.

Taschenatlas Physiologie, S. Silbernagl, A. Despopoulos, W.-R. Gay, 7. Auflage, 2007, Thieme

Tarr, P.I., Gordon, C.A., and Chandler, W.L. (2005). Shiga-toxin-producing Escherichia coli and haemolytic uraemic syndrome. Lancet *365*, 1073-1086.

Tartaglia, L.A., Rothe, M., Hu, Y.F., and Goeddel, D.V. (1993). Tumor necrosis factor's cytotoxic activity is signaled by the p55 TNF receptor. Cell *73*, 213-216.

Tavian, M., Robin, C., Coulombel, L., and Peault, B. (2001). The human embryo, but not its yolk sac, generates lympho-myeloid stem cells: mapping multipotent hematopoietic cell fate in intraembryonic mesoderm. Immunity *15*, 487-495.

Tesh, V.L., Ramegowda, B., and Samuel, J.E. (1994). Purified Shiga-like toxins induce expression of proinflammatory cytokines from murine peritoneal macrophages. Infect Immun *62*, 5085-5094.

Tipping, P.G., Leong, T.W., and Holdsworth, S.R. (1991). Tumor necrosis factor production by glomerular macrophages in anti-glomerular basement membrane glomerulonephritis in rabbits. Lab Invest *65*, 272-279.

Tomita, N., Morishita, R., Lan, H.Y., Yamamoto, K., Hashizume, M., Notake, M., Toyosawa, K., Fujitani, B., Mu, W., Nikolic-Paterson, D.J.*, et al.* (2000). In vivo administration of a nuclear transcription factor-kappaB decoy suppresses experimental crescentic glomerulonephritis. J Am Soc Nephrol *11*, 1244-1252.

Trachtman, H., Austin, C., Lewinski, M., and Stahl, R.A. (2012). Renal and neurological involvement in typical Shiga toxin-associated HUS. Nat Rev Nephrol *8*, 658-669.

Trachtman, H., Cnaan, A., Christen, E., Gibbs, K., Zhao, S., Acheson, D.W., Weiss, R., Kaskel, F.J., Spitzer, A., Hirschman, G.H.*, et al.* (2003). Effect of an oral Shiga toxin-binding agent on diarrhea-associated hemolytic uremic syndrome in children: a randomized controlled trial. JAMA *290*, 1337-1344.

Tumer, N.E., and Li, X.P. (2012). Interaction of ricin and Shiga toxins with ribosomes. Curr Top Microbiol Immunol *357*, 1-18.

Tushinski, R.J., Oliver, I.T., Guilbert, L.J., Tynan, P.W., Warner, J.R., and Stanley, E.R. (1982). Survival of mononuclear phagocytes depends on a lineage-specific growth factor that the differentiated cells selectively destroy. Cell *28*, 71-81.

Tzipori, S., Sheoran, A., Akiyoshi, D., Donohue-Rolfe, A., and Trachtman, H. (2004). Antibody therapy in the management of shiga toxin-induced hemolytic uremic syndrome. Clin Microbiol Rev *17*, 926-941, table of contents.

van de Kar, N.C., Monnens, L.A., Karmali, M.A., and van Hinsbergh, V.W. (1992). Tumor necrosis factor and interleukin-1 induce expression of the verocytotoxin receptor globotriaosylceramide on human endothelial cells: implications for the pathogenesis of the hemolytic uremic syndrome. Blood *80*, 2755-2764.

van Furth, R., Cohn, Z.A., Hirsch, J.G., Humphrey, J.H., Spector, W.G., and Langevoort, H.L. (1972). The mononuclear phagocyte system: a new classification of macrophages, monocytes, and their precursor cells. Bull World Health Organ *46*, 845-852.

van Goor, H., van der Horst, M.L., Fidler, V., and Grond, J. (1992). Glomerular macrophage modulation affects mesangial expansion in the rat after renal ablation. Lab Invest *66*, 564-571.

van Luijn, J.C., Danz, M., Bijlsma, J.W., Gribnau, F.W., and Leufkens, H.G. (2011). Post-approval trials of new medicines: widening use or deepening knowledge? Analysis of 10 years of etanercept. Scand J Rheumatol *40*, 183-191.

Van Rooijen, N., and Sanders, A. (1994). Liposome mediated depletion of macrophages: mechanism of action, preparation of liposomes and applications. J Immunol Methods *174*, 83-93.

Venkatachalam, M.A., and Rennke, H.G. (1978). The structural and molecular basis of glomerular filtration. Circ Res *43*, 337-347.

Vieira, S.M., Lemos, H.P., Grespan, R., Napimoga, M.H., Dal-Secco, D., Freitas, A., Cunha, T.M., Verri, W.A., Jr., Souza-Junior, D.A., Jamur, M.C.*, et al.* (2009). A crucial role for TNF-alpha in mediating neutrophil influx induced by endogenously generated or exogenous chemokines, KC/CXCL1 and LIX/CXCL5. Br J Pharmacol *158*, 779-789.

Vielhauer, V., and Mayadas, T.N. (2007). Functions of TNF and its receptors in renal disease: distinct roles in inflammatory tissue injury and immune regulation. Semin Nephrol *27*, 286-308.

Waage, A., Halstensen, A., and Espevik, T. (1987). Association between tumour necrosis factor in serum and fatal outcome in patients with meningococcal disease. Lancet *1*, 355-357.

Walters, M.D., Matthei, I.U., Kay, R., Dillon, M.J., and Barratt, T.M. (1989). The polymorphonuclear leucocyte count in childhood haemolytic uraemic syndrome. Pediatr Nephrol *3*, 130-134.

Wang, J., Hossain, M., Thanabalasuriar, A., Gunzer, M., Meininger, C., and Kubes, P. (2017). Visualizing the function and fate of neutrophils in sterile injury and repair. Science *358*, 111-116.

Wang, Y., Szretter, K.J., Vermi, W., Gilfillan, S., Rossini, C., Cella, M., Barrow, A.D., Diamond, M.S., and Colonna, M. (2012). IL-34 is a tissue-restricted ligand of CSF1R required for the development of Langerhans cells and microglia. Nat Immunol *13*, 753-760.

Watanabe, M., Matsuoka, K., Kita, E., Igai, K., Higashi, N., Miyagawa, A., Watanabe, T., Yanoshita, R., Samejima, Y., Terunuma, D.*, et al.* (2004). Oral therapeutic agents with highly clustered globotriose for treatment of Shiga toxigenic Escherichia coli infections. J Infect Dis *189*, 360-368.

Wei, S., Nandi, S., Chitu, V., Yeung, Y.G., Yu, W., Huang, M., Williams, L.T., Lin, H., and Stanley, E.R. (2010). Functional overlap but differential expression of CSF-1 and IL-34 in their CSF-1 receptor-mediated regulation of myeloid cells. J Leukoc Biol *88*, 495-505.

Weinblatt, M.E., Kremer, J.M., Bankhurst, A.D., Bulpitt, K.J., Fleischmann, R.M., Fox, R.I., Jackson, C.G., Lange, M., and Burge, D.J. (1999). A trial of etanercept, a recombinant tumor necrosis factor receptor:Fc fusion protein, in patients with rheumatoid arthritis receiving methotrexate. N Engl J Med *340*, 253-259.

Weisheit, C.K., Engel, D.R., and Kurts, C. (2015). Dendritic Cells and Macrophages: Sentinels in the Kidney. Clinical journal of the American Society of Nephrology : CJASN *10*, 1841-1851.

Wells, J.M., Rossi, O., Meijerink, M., and van Baarlen, P. (2011). Epithelial crosstalk at the microbiota-mucosal interface. Proc Natl Acad Sci U S A *108 Suppl 1*, 4607-4614.

Westhorpe, C.L., Bayard, J.E., O'Sullivan, K.M., Hall, P., Cheng, Q., Kitching, A.R., and Hickey, M.J. (2017). In Vivo Imaging of Inflamed Glomeruli Reveals Dynamics of Neutrophil Extracellular Trap Formation in Glomerular Capillaries. Am J Pathol *187*, 318-331.

Wiktor-Jedrzejczak, W., Bartocci, A., Ferrante, A.W., Jr., Ahmed-Ansari, A., Sell, K.W., Pollard, J.W., and Stanley, E.R. (1990). Total absence of colony-stimulating factor 1 in the macrophage-deficient osteopetrotic (op/op) mouse. Proc Natl Acad Sci U S A *87*, 4828-4832.

Wiktor-Jedrzejczak, W., Ratajczak, M.Z., Ptasznik, A., Sell, K.W., Ahmed-Ansari, A., and Ostertag, W. (1992). CSF-1 deficiency in the op/op mouse has differential effects on macrophage populations and differentiation stages. Exp Hematol *20*, 1004-1010.

Winthrop, K.L. (2006). Risk and prevention of tuberculosis and other serious opportunistic infections associated with the inhibition of tumor necrosis factor. Nat Clin Pract Rheumatol *2*, 602-610.

Wong, C.S., Jelacic, S., Habeeb, R.L., Watkins, S.L., and Tarr, P.I. (2000). The risk of the hemolytic-uremic syndrome after antibiotic treatment of Escherichia coli O157:H7 infections. N Engl J Med *342*, 1930-1936.

World Health Organization. Zoonotic non-O157 shiga toxin-producing Escherichia coli (STEC), 23–26 June 1998, Berlin, Germany

Wynn, T.A., and Vannella, K.M. (2016). Macrophages in Tissue Repair, Regeneration, and Fibrosis. Immunity *44*, 450-462.

Xu, J., Escamilla, J., Mok, S., David, J., Priceman, S., West, B., Bollag, G., McBride, W., and Wu, L. (2013). CSF1R signaling blockade stanches tumor-infiltrating myeloid cells and improves the efficacy of radiotherapy in prostate cancer. Cancer Res *73*, 2782-2794.

Xue, J., Schmidt, S.V., Sander, J., Draffehn, A., Krebs, W., Quester, I., De Nardo, D., Gohel, T.D., Emde, M., Schmidleithner, L.*, et al.* (2014). Transcriptome-based network analysis reveals a spectrum model of human macrophage activation. Immunity *40*, 274-288.

Yamagami, S., Motoki, M., Kimura, T., Izumi, H., Takeda, T., Katsuura, Y., and Matsumoto, Y. (2001). Efficacy of postinfection treatment with anti-Shiga toxin (Stx) 2 humanized monoclonal antibody TMA-15 in mice lethally challenged with Stx-producing Escherichia coli. J Infect Dis *184*, 738-742.

Yang, L., and Zhang, Y. (2017). Tumor-associated macrophages: from basic research to clinical application. J Hematol Oncol *10*, 58.

Yeung, Y.G., Jubinsky, P.T., Sengupta, A., Yeung, D.C., and Stanley, E.R. (1987). Purification of the colony-stimulating factor 1 receptor and demonstration of its tyrosine kinase activity. Proc Natl Acad Sci U S A *84*, 1268-1271.

Yipp, B.G., Kim, J.H., Lima, R., Zbytnuik, L.D., Petri, B., Swanlund, N., Ho, M., Szeto, V.G., Tak, T., Koenderman, L.*, et al.* (2017). The Lung is a Host Defense Niche for Immediate Neutrophil-Mediated Vascular Protection. Sci Immunol *2*.

Yona, S., Kim, K.W., Wolf, Y., Mildner, A., Varol, D., Breker, M., Strauss-Ayali, D., Viukov, S., Guilliams, M., Misharin, A.*, et al.* (2013). Fate mapping reveals origins and dynamics of monocytes and tissue macrophages under homeostasis. Immunity *38*, 79-91.

Zhang, H., Schaff, U.Y., Green, C.E., Chen, H., Sarantos, M.R., Hu, Y., Wara, D., Simon, S.I., and Lowell, C.A. (2006). Impaired integrin-dependent function in Wiskott-Aldrich syndrome protein-deficient murine and human neutrophils. Immunity *25*, 285-295.

Zhu, Y., Knolhoff, B.L., Meyer, M.A., Nywening, T.M., West, B.L., Luo, J., Wang-Gillam, A., Goedegebuure, S.P., Linehan, D.C., and DeNardo, D.G. (2014). CSF1/CSF1R blockade reprograms tumor-infiltrating macrophages and improves response to T-cell checkpoint immunotherapy in pancreatic cancer models. Cancer Res *74*, 5057-5069.

Der Lebenslauf ist aus datenschutzrechtlichen Gründen nicht in der Online-Version enthalten.

PUBLICATIONS

1. **Lill JK**, Pohl JM, Thiebes S, Vijitha N, Bottek J, Soun S, Vijitha N, Gueler F, Hoffmann F, von Eggeling F, Bracht T, Sitek B, Hickey MJ, Hofnagel O, Engel DR. Tissue resident macrophages mediate neutrophil recruitment and kidney injury in Shiga toxin-induced Hemolytic Uremic Syndrome. *Currently in review at Kidney International*
2. Fleig S, Kapanadze T, Bernier-Latmani J, **Lill JK**, Kijas D, Halle S, Gamrekelashvili J, Ricke-Hoch M, Hilfiker-Kleiner D, von Vietinghoff S, Förster R, Adams R, Engel DR, Haller H, Petrova TV, Limbourg F. Loss of Vascular Notch Signaling Induces Spontaneous Formation of Tertiary Lymphoid Structures in the Kidney. *Currently in revision at Nature Communications*
3. Bottek J, Soun C, **Lill JK**, Dixit A, Thiebes S, Beerlage AL, Horstmann M, Urbanek A, Uszkoreit J, Eisenacher M, Bracht Th, Sitek B, Hoffmann F, Vijitha N, Eggeling F, Engel DR. Spatial proteomics revealed CX_3CL1-dependent crosstalk between the urothelium and relocated macrophages through IL-6 during an acute bacterial infection in the urinary bladder. *Mucosal Immunol.,* (2020)
4. Pohl JM, **Volke JK**, Thiebes S, Brenzel A, Fuchs K, Beziere N, Ehrlichmann W, Pichler BJ, Squire A, Gueler F, Engel DR. CCR2-dependent $Gr1^{high}$ monocytes promote kidney injury in shiga toxin-induced hemolytic uremic syndrome in mice. *Eur J Immunol* 2018, *48*, 990-1000 (2018)
5. Pohl JM, Gutweiler S, Thiebes S, **Volke JK**, Klein-Hitpass L, Zwanziger D, Gunzer M, Jung S, Agace WW, Kurts C, Engel DR. *Irf4*-dependent $CD103^{+}CD11b^{+}$ dendritic cells and the intestinal microbiome regulate monocyte and macrophage activation and intestinal peristalsis in postoperative ileus. *Gut 66*, 2110-2120 (2017)
6. Zec K, **Volke J**, Vijitha N, Thiebes S, Gunzer M, Kurts C, Engel DR. Neutrophil migration into the infected uroepithelium is regulated by the crosstalk between resident and helper macrophages *Pathogens* 5 (2016)

AWARDS, COMMITMENTS, INTERNATIONAL CONFERENCES

November 2019	Poster award, BIOME Retreat, University Hospital Essen
2019	Organization of the annual Retreat (BIOME) of the Graduate School
July 2019	Scientific writing course
July 2019	International project management course
November 2018	Poster award, Medical Research Day, University Hospital Essen
November 2018:	International symposium on regulatory myeloid cells, Essen
October 2018	International conference: Repair and regeneration of renal tissue, Maine, USA
October 2017	International conference: Seeing is believing, EMBL, Heidelberg
Since 2012	Student representative in the animal ethics commission
2012 – 2014	Student representative
2009 – 2012	Volunteering at AFS, international students exchange organization

Julia K. Lill

Eidesstattliche Erklärungen

Hiermit erkläre ich, gem. § 7 Abs. 2, d und f der Promotionsordnung der Fakultät für Biologie zur Erlangung des Dr. rer. nat., dass ich die vorliegende Dissertation selbständig verfasst und mich keiner anderen als der angegebenen Hilfsmittel bedient habe und alle wörtlich oder inhaltlich übernommenen Stellen als solche gekennzeichnet habe.

Essen, den _____ _____

(Unterschrift des/r Doktoranden/in)

Hiermit erkläre ich, gem. § 7 Abs. 2, e und g der Promotionsordnung der Fakultät für Biologie zur Erlangung des Dr. rer. nat., dass ich keine anderen Promotionen bzw. Promotionsversuche in der Vergangenheit durchgeführt habe, dass diese Arbeit von keiner anderen Fakultät abgelehnt worden ist, und dass ich die Dissertation nur in diesem Verfahren einreiche.

Essen, den _____ _____

(Unterschrift des/r Doktoranden/in)

Hiermit erkläre ich, gem. § 6 Abs. 2, g der Promotionsordnung der Fakultät für Biologie zur Erlangung des Dr. rer. nat., dass ich das Arbeitsgebiet, dem das Thema „ Renal macrophages promote Shiga toxin-induced Hemolytic Uremic Syndrome through TNFα and CXCR2-dependent neutrophil recruitment“ “ zuzuordnen ist, in Forschung und Lehre vertrete und den Antrag von Julia Klara Katharina Lill (geborene Volke) befürworte.

Essen, den _____ _____

(Name d. wissenschaftlichen Betreuers/Mitglieds der Universität Duisburg-Essen)

_____

(Unterschrift d. wissenschaftlichen Betreuers/Mitglieds der Universität Duisburg-Essen)